

OVERDUE FINES: 25¢ per day per item

RETURNING LIBRARY MATERIALS:

Place in book return to remove charge from circulation records

ELECTROCHEMICAL INVESTIGATION OF SOLVENT EFFECTS ON THE ELECTRODE KINETICS AND THERMODYNAMICS OF SOME TRANSITION-METAL REDOX COUPLES

Ву

Saeed Sahami

A DISSERTATION

Submitted to

Michigan State University

in partial fulfillment of the requirements

for the degree of

DOCTOR OF PHILOSOPHY

Department of Chemistry

ABSTRACT

ELECTROCHEMICAL INVESTIGATION OF SOLVENT EFFECTS
ON THE ELECTRODE KINETICS AND THERMODYNAMICS
OF SOME TRANSITION-METAL REDOX COUPLES

Ву

Saeed Sahami

Electrochemical methods were used in order to explore the influences of the solvent upon the electrode kinetics and thermodynamics of some transition-metal redox couples. For the following redox couples: (i) couples containing aromatic ligands; $Cr(bpy)_3^{3+/2+}$, $Fe(bpy)_3^{3+/2+}$, $Co(bpy)_3^{3+/2+}$ and $Co(phen)_3^{3+/2+}$ (where bpy = 2,2'-bipyridine, phen = 1,10-phenanthroline), (ii) couples containing ammine and ethylenediamine ligands; $Ru(NH_3)_6^{3+/2+}$, $Ru(NH_3)_5^{NCS}^{2+/+}$, $Ru(en)_3^{3+/2+}$, $Co(en)_3^{3+/2+}$ and $Co(sep)_3^{3+/2+}$ (where en = ethylenediamine, sep = sepulchrate), and (iii) anionic redox couples such as $Fe(EDTA)_{-/2-}^{-/2-}$ and $Co(EDTA)_{-/2-}^{-/2-}$ (where EDTA = ethylenediaminetetraacetato), formal potential E_f were evaluated using cyclic voltammetry as a function of temperature in eight solvents (water, dimethylsulfoxide, N,N-dimethylformamide, N-methylformamide, formamide,

propylene carbonate, acetonitrile, and nitromethane). The reaction entropies $\Delta S_{\text{rc}}^{\circ}$ for each redox couple in each solvent were obtained from the temperature dependence of E_{f} using a nonisothermal cell arrangement. These measurements were done in order to understand the various structural influences of the solvent upon the redox thermodynamics of such simple redox couples where the oxidized and the reduced forms have identical structures and the composition of the coordination shell remains unchanged when the solvent is varied. These measurements coupled with extrathermodynamic methods such as the "ferrocene", and "tetraphenylarsonium-tetraphenylborate" assumptions, yield estimates of the free energy $\Delta(\Delta G_{\text{rc}}^{\circ})^{\text{S-W}}$, entropy $\Delta(\Delta S_{\text{rc}}^{\circ})^{\text{S-W}}$, and enthalpy $\Delta(\Delta H_{\text{rc}}^{\circ})^{\text{S-W}}$ of transfer for the redox couple of interest from water to other solvents.

It has been found that the values of ΔS_{rc}° for all redox couples investigated here are substantially (up to ~40 cal. deg⁻¹ mol⁻¹) larger in nonaqueous solvents compared with water. These entropic variations appear to correlate well with the empirical "a" parameter as a measure of the degree of "internal order" of the solvent, but fail to correlate with the solvent "donor number". Small negative values of $\Delta(\Delta G_{rc}^{\circ})^{S-W}$ for couples containing aromatic ligand were typically obtained as a result of partial compensation of the entropic terms by the corresponding enthalpic components. On the other hand, the large variations in free energy, and enthalpy of transfer for

amine couples and anionic complexes correlate broadly with the "donor number" for the former system and with the "acceptor number" for the latter system.

Normal pulse and d.c. polarography were employed to investigate the one-electron reduction kinetics of Co-(en)₃³⁺, $Co^{III}(NH_3)_5X$ and $Cr^{III}(NH_3)_5X$ (where $X = F^-$, NO_3 , NCS^- , N_3^- , SO_4^{2-} , Cl^- , Br^- and NH_3) in various solvents at mercury electrodes. Substantial variations in the experimental rate parameters were observed as the solvent was altered. The substantial decreases in corrected rate constants k_{corr} seen when substituting several nonaqueous solvents for water were traced to increases in the outershell component of the intrinsic free energy barrier $(\Delta G_1^{\neq})_{\alpha}$. A roughly linear correlation between the observed solvent dependence of ΔG_1^{\neq} for $Co(en)_3^{3+/2+}$ and the corresponding values of $\Delta S_{\mathbf{rc}}^{o}$ were found. This suggests that there is a significant contribution to $(\Delta G_{i}^{\neq})_{os}$ from extensive short-range reorientation of solvent molecules. In addition, it was found that the outer-sphere reaction mechanism provides the usual pathway for the reduction of these complexes at mercury/nonaqueous interfaces.

ACKNOWLEDGMENTS

I wish to express sincere thanks to Dr. Michael Weaver for his invaluable advice, guidance, encouragement, friendship, and enthusiasm during the course of this study.

Thanks are given to Professor S. R. Crouch for his helpful suggestions as second reader.

Financial support by Michigan State University, Department of Chemistry and the Office of Naval Research is gratefully acknowledged. In addition, partial financial aids
of the people of Iran, as administered by the Ministry of
Science and Higher Education is acknowledged.

I would like to thank my colleagues in the research group of Dr. Weaver for their friendship, and assistance during our association. I especially thank Dr. Ed Yee, Dr. Paul Tyma, Ken Guyer, Steve Barr and Ed Schindler.

I wish to thank my parents and sisters for their understanding and constant support. Finally, I would like to thank my wife, Jila, for her love, her patience and her encouragement.

TABLE OF CONTENTS

Chapter								Page
LIST OF	TABLES	•	•	•	•	•	•	vii
LIST OF	FIGURES	•	•		•	•	•	xii
CHAPTER	I - INTRODUCTION AND BACKGROUND	•	•	•	•	•	•	1
Α.	Introduction	•		•	•		•	2
В.	Mechanisms of Electron Transfer						•	4
С.	Redox Thermodynamics	•	•			•		6
D.	Ionic and Reaction Entropies	•	•	•	•	•	•	8
CHAPTER	II - EXPERIMENTAL	•	•	•	•	•	•	12
Α.	Materials	•	•	•	•			13
	1. Reagents	•	•	•	•			13
	2. Solvents		•		•			13
	3. Transition Metal Complexes and Compounds	•	•	•	•	•	•	14
В.	Apparatus		•		•	•		17
С.	Electrochemical Techniques	•	•	•	•		•	18
	1. Sample Preparation and Reference Electrodes	•	•	•	•	•	•	18
	2. Cyclic Voltammetry	•	•		•			19
	3. Polarography							19
	4. Preparative Electrolyses	•						20
	5. Potential of Zero Charge (PZC) Measurement		•	•	•	•	•	20

Chapter		Page
CHAPTER	III - SOLVENT TREATMENTS OF THERMODYNAMIC AND ELECTRODE KINETIC DATA FOR REDOX COUPLES	21
Α.	Solvent Dependence of Redox Thermodynamics	22
	1. The Reaction Free Energy and Transfer Free Energy Concepts	22
	2. Some Extra Thermodynamic Methods for Estimation of Transfer Free Energies	24
	a. The "Ferrocene Assumption"	24
	b. The "Zero Liquid Junction Potential Potential" Procedure	26
	<pre>c. The "tetraphenylarsonium- tetraphenyl borate" (TATB) Assumption</pre>	27
	3. Estimation of Transfer Free Energies for Redox Couples	28
	4. Determination of Reaction Entropies for Redox Couples	30
	5. Electrostatic Born Model For Calculating Transfer Free Energies and Reaction Entropies of Redox Couples	35
В.	Solvent Dependence of Redox Electrode	
	Kinetics	37
	1. Evaluation of Activation Free Energies and Other Electrode Kinetic Parameters	37
	2. Solvent Dependence of Intrinsic	51
	Barriers	41
CHAPTER	IV - SOLVENT PROPERTIES	44
Α.	Classification	45
В.	The Dipole Moments and Dielectric Constant	45
С.	The Donor- and Acceptor-Numbers	47

Chapte	r	Page
D.	Solvent "Internal Order", "a" Parameter	49
E.	Potential Range in Nonaqueous Solvents	50
F.	Choice of Solvent	50
CHAPTE	R V - SOLVENT EFFECTS UPON THE THERMO- DYNAMICS OF M(III)/(II) TRANSITION- METAL REDOX COUPLES	55
Α.	Introduction	56
В.	Results	57
2.		71
	<pre>l. Ferricinium-Ferrocene Redox Couple</pre>	57
	 Couples Containing Polypyridine Ligands	64
	3. Couples Containing Ammine and	7.5
	Ethylenediamine Ligands	75 84
•		
C.	Discussion	88
	1. Ferricinium-Ferrocene Couple	88
	2. Polypyridine Redox Couples	96
	3. Ammine and Ethylenediamine	110
	Couples	113
	4. Anionic Couples	129
CHAPTE	R VI - SOLVENT EFFECTS ON THE KINETICS OF SIMPLE ELECTROCHEMICAL REACTIONS: COMPARISON OF THE BEHAVIOR OF Co(III)/(II) - TRISETHYLENEDIAMINE AND AMINE COUPLES WITH THE PREDICTIONS OF DIELECTRIC CONTINUUM THEORY	138
Α.	Introduction	139
В.	Experimental	140
C.	Results	141
ח	Discussion	7 117

.

Chapter		Page
CHAPTER	VII - DETERMINATION OF REACTION MECHANISMS FOR Co(III)- AND Cr(III)-AMINE COMPLEXES AT Hg/NONAQUEOUS INTERFACES	166
Α.	Introduction	167
В.	Method for Distinction Between I.S. and O.S. Mechanisms	168
С.	Results	169
	 Co(III)-Amine Reactants Cr(III)-Amine Reactants 	169 176
D.	Discussion	176
CHAPTER	VIII - CONCLUSIONS AND SUGGESTIONS FOR FURTHER WORK	185
Α.	Conclusions	186
в.	Suggestions for Further Work	191
LIST OF	REFERENCES	194

LIST OF TABLES

Table		Page
1	Voltage Range on Mercury and	
	Platinum in Selected Solvents	
	and Supporting Electrolytes	51
2	Some Properties of Various Solvents	53
3	Reaction Entropies for Ferricinium-	
	Ferrocene Couple in Various Sol-	
	vents	60
4	ΔS_{rc}° (= S_{Fc}° - S_{Fc}°) for the	
	Ferricinium-Ferrocene Redox	
	Couple in Various Solvents.	
	Comparison with Predictions	
	from Born Model	63
5	Temperature Derivatives of Di-	
	electric Constants for Various	
	Solvents	65
6	Formal Potentials and Reaction	
	Entropies for M(III)/(II) Poly-	
	pyridine Redox Couples in Various	
	Solvents	68
7	Free Energies, Enthalpies and	
	Entropies of Transfer of	

Table		Page
	M(III)/(II) Polypyridine Redox	
	Couples from Water to Various	
	Solvents	. 71
8	Formal Potentials and Reaction	
	Entropies for M(III)/(II) Amine	
	and Ethylenediamine Redox Couples	
	in Various Solvents	. 77
9	Free Energies, Enthalpies, and	
	Entropies of Transfer of M(III)/	
	(II) Amine and Ethylenediamine	
	Redox Couples from Water to	
	Various Solvents	. 81
10	Formal Potentials and Reaction	
	Entropies for M(III)/(II) Amine	
	and Ethylenediamine Redox Couples	
	in Different Ionic Strength	. 85
11	Formal Potentials and Reaction	
	Entropies for $Fe(EDTA)^{-/2}$ and	
	$Co(EDTA)^{-/2}$ Redox Couples in	
	Various Solvents	. 86
12	Free Energies, Enthalpies, and	
	Entropies of Transfer of Fe(EDTA) -/2-	
	and $Co(EDTA)^{-/2}$ Redox Couples from	
	Water to Various Solvents	. 89

Table		Page
13	Estimates of Transfer Free Energies	
	for Ferricinium-ferrocene Redox	
	Couple from Water to Various Other	
	Solvents $\Delta(\overline{G}_{Fc}^{\circ} - \overline{G}_{Fc}^{\circ})^{s-w}$ Obtained	
	Using Equation (5), Compared with	
	Corresponding Transfer Entropies	
	$T(\overline{S_{FC}^{\circ}} - \overline{S_{FC}^{\circ}})^{S-W}$ for $T=25^{\circ}C$. 94
14	Solvent Dependence of Electro-	
	chemical Kinetic Parameters for	
	the $Co(en)_3^{3+/2+}$ Couple at	
	Mercury Electrodes at 25°C	. 142
15	Solvent Dependence of Electro-	
	chemical Kinetic Parameters for	
	the One-electron Reduction of	
	$Co(NH_3)_6^{3+}$ and $Co(NH_3)_5^{2+}$ at	
	Mercury Electrodes at 25°C	. 148
16	Estimates of the Variations in	
	the Potential-independent Free	
	Energy of Activation $\Delta(\Delta G_{corr}^{\neq})_{c}^{s-w}$	
	for $Co(en)_3^{3+}$ and $Co(NH_3)_6^{3+}$	
	Reduction Resulting from Sub-	
	stituting Various Nonaqueous	
	Solvents for Water	. 151
17	Experimental Estimates of the	
	Variations in the Intrinsic	

Table		Page
	Barrier $\Delta(\Delta G_1^{\neq})^{S-W}$ for Co(en) $_3^{3+/2+}$	
	Resulting from Substituting Various	
	Nonaqueous Solvents for Water. Com-	
	parison with Predicted Variations	
	$\Delta(\Delta G_i^{\neq})_{calc}^{s-w}$ from Dielectric Continuum	
	Theory	153
18	Calculated Values of the Outer-	
	shell Intrinsic Barrier for	
	$Co(en)_3^{3+/2+}$ from Dielectric	
	Continuum Theory	156
19	Experimental Rate Constants and	
	Transfer Coefficients for Electro-	
	reduction of Various Co(III)-amine	
	Complexes at Hg/DMSO at 25°C	171
20	Experimental Rate Constants and	
	Transfer Coefficients for Electro-	
	reduction of Various Co(III)-amine	
	Complexes at Hg/DMF at 25°C	172
21	Experimental Rate Constants and	
	Transfer Coefficients for Electro-	
	reduction of Various Co(III)-Amine	
	Complexes at Hg/Formamide at 25°C	173
22	Experimental Rate Constants and	
	Transfer Coefficients for Electro-	
	reduction of Various Co(III)-amine	
	Complexes at Hg/PC at 25°C	175

٧.

Table			Page
23	Experimental Rate Constants and		
	Transfer Coefficients for Electro-		
	reduction of Various Cr(III)-amine		
	Complexes at Hg/DMSO, Hg/DMF and		
	Hg/Formamide Interfaces at 25°C	•	177

LIST OF FIGURES

Figure		Page
1.	Plots of $\Delta(\Delta S_{rc}^{\circ})^{S-W}$ for each	
	polypyridine redox couple against	
	the corresponding Born estimates	
	$\Delta(\Delta S_{rc}^{o})^{s-w}$ obtained from the	
	values of $(\Delta S_{rc}^{\circ})_{Born}$ calculated	
	from water and appropriate non-	
	aqueous solvent	. 100
2	Plots of $\Delta(\Delta S_{rc}^{o})^{S-W}$ for a given	
	polypyridine redox couple against	
	-a for each solvent	. 105
3	Plots of $\Delta(\Delta S_{rc}^{\circ})^{S-W}$ for each poly-	
	pyridine redox couple against the	
	"Donor Number" for the various non-	
	aqueous solvents	. 107
4	Plots of $\Delta(\Delta G_{rc}^{\circ})^{S-W}$ and $\Delta(\Delta H_{rc}^{\circ})^{S-W}$	
	for $Co(en)_3^{3+/2+}$ and $Ru(NH_3)_6^{3+/2+}$	
	against the "Donor Number" for	
	each solvent	. 117
5	Plots of $\Delta(\Delta S_{rc}^{\circ})^{S-W}$ for a given	
	amine redox couple against the	
	corresponding Born estimates	

Figure		Page
	$\Delta(\Delta S_{rc}^{o})_{Born}^{s-w}$ obtained from the values	
	of (ΔS_{rc}°) _{Born} calculated for water	
	and appropriate nonaqueous solvent	121
6	Plots of $\Delta(\Delta S_{rc}^{o})^{s-w}$ for each amine	
	redox couple against the "Donor	
	Number" for various nonaqueous	
	solvents	124
7	Plots of $\Delta(\Delta S_{rc}^{o})^{S-W}$ for each amine	
	redox couple against -a for the	
	various solvents	127
8	Plots of $\Delta(\Delta G_{rc}^{o})^{s-w}$ and $\Delta(\Delta H_{rc}^{o})^{s-w}$	
	for $Fe(EDTA)^{-/2}$ against the "Ac-	
	ceptor Number" for each solvent	132
9	Plots of ΔS_{rc}^{o} for Fe(EDTA) ^{-/2-}	
	against -a for the various	
	solvents	137
10	Plots of the variation in the	
	intrinsic free energy of activa-	
	tion for $Co(en)_3^{3+/2+}$ resulting	
	from substituting various non-	
	aqueous solvents for water,	
	$\Delta(\Delta G_1^{\neq})^{s-w}$, against the correspond-	
	ing reaction entropies ΔS_{rc}^{o}	163
11	Comparison of the effect of specific	
	iodide adsorption upon rate-potentials	

Figure		Page
	plots for the electroreduction of	
	$Co(NH_3)_5F^{2+}$ in mixed LiClO ₄ + LiI	
	supporting electrolytes in DMSO	180
12	Comparison of the effect of	
	specific NCS adsorption upon	
	rate-potential plots for the	
	electroreduction of $Co(NH_3)_5NCS^{2+}$	
	in mixed LiClO $_{\mbox{\scriptsize \downarrow}}$ + NaNCS supporting	
	electrolytes in DMSO	182

CHAPTER I

INTRODUCTION AND BACKGROUND

A. INTRODUCTION

Along with other types of solution reactions, most fundamental studies of the rates and mechanisms of electrode processes have been conducted in aqueous solution. There are several factors responsible for this situation, including the availability of numerous bulk and surface thermodynamic data for aqueous systems and the relative lack of such data in other solvents. However, there are a number of important limitations to the use of aqueous media for electrochemical reactions, both from theoretical and practical points of view. For example, the available range of electrode potentials in aqueous media is usually limited by cathodic hydrogen and anodic oxygen evolution. In addition many electrode reactions are complicated in water or do not even occur because of hydrolysis reactions. In contrast, the large potential range that is available at a number of electrodes in nonaqueous, particularly aprotic, solvents allows a wider variety of electrode processes to be examined than in water. These features also make aprotic and other nonaqueous solvents especially attractive for use in high-energy battery systems. Moreover, water is a decidedly atypical solvent from a physical point of view, so that large influences upon the thermodynamics

and kinetics of electrode reactions could generally be expected when substituting nonaqueous solvents for water. Nevertheless, surprisingly little progress has been made in gaining a fundamental understanding of redox processes especially for inorganic complexes in solvents other than water, either in homogeneous solutions or at electrode surfaces.

The nature of the solvent is expected to have profound influences upon the kinetics of electron transfer re-The observed effects arise from a variety of sources, such as changes in the relative stability of oxidation states caused by reactant-solvent bonding, electrostatic interactions, shifts in complexation equilibria, alterations in reaction mechanism, etc. Indeed, the major difficulty in interpreting solvent effects on electrode kinetics, as well as on other types of chemical processes including homogeneous electron transfer, has been that a number of separate factors may be responsible for the observed changes in the kinetic parameters as the solvent composition is altered. The majority of studies of solvent substitution on the kinetics of electrochemical reactions have employed substitutionally labile cations. For these systems the observed effects can arise from changes in the composition of the coordination shell (inner-shell effect), as well as from reactant-solvent interactions (outer-shell contribution). Moreover, a number of the

reactions studied up to now involve multi-electron and atom transfer [e.g., $Cd^{2+} + 2e^{-} + Cd(Hg)$] so that the charge and structure of the transition state is usually ill-defined (1-7).

We have chosen to focus attention on transitionmetal complexes because this class of reactant provides
a large number of simple redox couples of related structure. They often involve the transfer of a single
electron for which both halves of the redox couple are
stable in solution. Most importantly, the use of substitutionally inert octahedral complexes allows the solvent
to be varied while keeping the composition of the reactant's
coordination sphere constant. This approach therefore
allows the "inner-shell" (coordination sphere) and "outershell" (longer-range solvation) effects to be investigated
separately.

B. MECHANISMS OF ELECTRON TRANSFER

A unique feature of redox reactions compared with other chemical processes is that in many cases efficient electron transfer probably occurs without any significant specific interaction between the two reacting centers (8). Reactions proceeding via such pathways in which the primary coordination spheres of both reactants remain intact in the transition state have been termed "outer-sphere" (0.S.). However, when strong specific interactions occur

between the reacting centers a more favorable pathway for electron transfer is usually expected to result. Not surprisingly, the rates of these "inner-sphere" (I.S.) reactions are sensitive not only to the structure of the reactants, but also to the nature and extent of their mutual interactions within the transition state. For redox reactions between metal ions, the I.S. and O.S. reaction mechanisms usually correspond to cases where a ligand coordinated to a reactant does, or does not penetrate the inner coordination sphere of the other reactant during electron transfer. These basic notions and definitions, originally developed for homogeneous redox reactions (8), can be directly employed to the analogous heterogeneous (i.e., electrochemical) systems by noting that the electrode surface and the adjacent layer ("inner-layer") of the solvent molecules play the role of the co-reactant (9).

It is obvious that O.S. electron-transfer reactions are much easier to treat theoretically than I.S. processes since no chemical bonds are formed or broken in the former type (10). On the other hand, electrochemical I.S. reactions are of particular interest because they correspond to cases where the interactions between the reactant and electrode surface act to lower the activation energy for electron transfer.

In order to select appropriate theoretical models and interpret electrochemical kinetic parameters, it is

necessary to distinguish between outer-sphere and innersphere pathways. No direct method is available for the determination of electrode reaction mechanisms (except that chronocoulometry can be used for reactants having sufficiently stable adsorbed intermediates (11)). Recently, indirect methods for distinguishing between O.S. and I.S. (anion-bridged) mechanisms have been developed for substitutionally inert cationic complexes (12). These tactics have successfully been used in aqueous solution for mechanism diagnosis of the reduction of Co^{III} and Cr^{III} complexes at mercury (9,13) and solid electrode surfaces (14). These methods were employed in the present work for determination of electroreduction mechanisms of various $Co^{III}(NH_3)_5X$ and $Cr^{III}(NH_3)_5X$ complexes (where X = F⁻, C1, Br, N_3 , NCS, NO_3 , SO_4^2 and NH_3) at mercury/nonaqueous interfaces and are presented in Chapter VII.

C. REDOX THERMODYNAMICS

The thermodynamics of redox couples in different solvents can provide significant information about the influences of the solvent structure upon the electrochemical reactivity. Thermodynamic parameters for redox couples in a given solvent are expected to be sensitive to the chemical nature of the coordinated ligands, the metal center and the charge on the reactant. Thermodynamic

parameters can be obtained by measurements of the standard or formal electrode potentials $E_{\rm f}$ for the redox couple of interest. This is due to the fact that in a given solvent, the difference between the partial molal free energies of the reduced and oxidized halves of a redox couple ("reaction free energy") is related to the measured $E_{\rm f}$ by Equation (1).

$$(\overline{G}_{red}^{\circ} - \overline{G}_{ox}^{\circ}) = \Delta G_{rc}^{\circ} \approx -nF E_{f}$$
 (1)

In addition, the dependence of E_f upon temperature and the solvent composition can provide valuable information on the factors influencing ionic solvation, in particular the structural changes in the surrounding solvent that accompany electron transfer.

In general, analyzing the free energies in terms of enthalpic and entropic components can provide more information than could be obtained from free energies alone. One effective method for evaluating such entropic and enthalpic data is through the employment of ionic entropies and particularly reaction entropies (for redox couples) as is now discussed.

D. IONIC AND REACTION ENTROPIES

Partial molal entropies can provide useful information about the thermodynamic properties of a species in solution. By definition (15) the partial molal entropy of the ith component of a system $\overline{S}_{\bf i}$ is the temperature dependence (under constant pressure and composition) of $\mu_{\bf i}$, the chemical potential of component i

$$\left(\frac{\partial \mu_{1}}{\partial T}\right)_{p} = \overline{S}_{1} \tag{2}$$

Determination of partial molal entropies of single ions has been an important goal of thermodynamic studies in solution. Strictly speaking, it is not possible to determine the ionic entropies of single ions, since only the partial molal entropy of an electrolyte (i.e., the sum of the ionic entropies for the cation and anion) is experimentally accessible (16). However, different methods are available for estimating single ion entropies. One may arbitrarily assign an entropy value to some ion and thus obtain a relative scale of single ion partial molal entropies. It is conventional for aqueous solution to use the scale based on the assumption that $\overline{S}_{H+}^{\circ}(aq) = 0$ (16). All other techniques involve some sort of extrathermodynamic assumption. Fortunately, most of these methods have yielded similar

values of $\overline{S}_{H^+}^{\circ}(aq)$ (17), which are not far from the conventional value of $\overline{S}_{H^+}^{\circ}(aq) = 0$ (16). An approximate value of $\overline{S}_{H^+}^{\circ}(aq) = -5$ e.u. (e.u. \equiv cal deg⁻¹ mol⁻¹) was obtained by each of these methods (17).

Similar treatments have been employed for solvents other than water. The total entropies of solvated electrolytes were divided into their ionic components by assigning a value for ionic entropy for the hydrogen ion (18). The division was made in such a manner that the ionic entropies for both cations and anions in a given solvent, when plotted vs. the ionic entropies of the corresponding ions in water fell on the same curve (17,19). It has been shown that the ionic entropies in any given solvent x, can be represented by

$$\overline{S}_{ion}^{\circ}(x) = a + b \overline{S}_{ion}^{\circ}(H_{2}O)$$
 (3)

where a and b are empirical constants characteristic of solvent x and $\overline{S}_{100}^{\circ}(H_2O)$ is the absolute entropy of the corresponding ions in water (17,20).

Although the ionic entropies of single ions can provide useful information on the interaction between an ion and the solvent molecules surrounding it, a variation of this concept is particularly appropriate when dealing with redox systems. One can consider ΔS_{rc}^{o} (the so-called reaction entropy), as the difference between the ionic entropies of

the reduced and oxidized forms of the redox couple $\overline{S}_{red}^{\circ}$ - $\overline{S}_{ox}^{\circ}$ (= ΔS_{rc}°) (21,22). Under this definition ΔS_{rc}° is the reaction entropy for one-half of a complete electrochemical reaction. The values of ΔS_{rc}° in a given solvent are expected to be sensitive to the relative extent of solvent polarization induced by the reduced \underline{vs} , the oxidized forms of the redox couple. They are also of particular significance in redox kinetics because they provide a unique opportunity to monitor solvent structural changes in the vicinity of the solute as a result of adding an electron to convert the oxidized form into the corresponding reduced species (22,23).

The utility of reaction entropies has been recognized recently by Weaver and coworkers (21). They have conducted a study of reaction entropies for a number of transition-metal redox couples containing aquo, simple monodentate and chelating ligands in aqueous media (21,24). The values of ΔS_{rc}^{o} for redox couples containing aquo and monodentate ligands were found to be affected by electrostatic factors and the hydrogen bonding between the solvent and bound ligands, but were relatively insensitive to the nature of the metal ion (21). However, the values of reaction entropies for couples containing chelating ligands were found to depend on the electronic structure of the oxidized and reduced metal cations as well as their charge and the nature of the coordinating ligands (21). In addition reaction

entropies for a series of copper(III/II)- and nickel (III/II)-peptide redox couples have also been determined in various media (25).

Essentially no information is available on the solvent dependence of ΔS_{rc}^{o} for any redox couple (especially octahedral transition-metal complexes with fixed coordination sphere) except for Fe(phen) $_{3}^{3+/2+}$ (phen = 1,10-phenanthroline) and its related derivatives in water and acetonitrile (26).

Determination of reaction entropies for a given redox couple as a function of solvent should also help to understand the solvent structural factors influencing transfer free energies. Although appropriate redox couples are not abundant, it was found that a number of transition-metal redox couples such as Ru(III)/(II), Cr(III)/(II), Co(III)/(II), and Fe(III)/(II) containing ammonia, ethylenediamine and polypyridine ligands are suitable. These redox couples are substitutionally inert, sufficiently stable and electrochemically reversible or quasi-reversible. Therefore, their formal potentials and reaction entropies can be obtained using cyclic voltammetry. In Chapter V values of reaction entropy are presented for these redox couples measured in different solvents.

CHAPTER II

EXPERIMENTAL

A. MATERIALS

1. Reagents

The reagents used in this work were analytical grade and used without further purification, except when otherwise noted. Anhydrous lithium perchlorate (from K & K or G. F. Smith), lithium bromide (Matheson Coleman and Bell) and lithium chloride (Fisher) were dried at ~180°C for several days. Lithium iodide (K & K) was dried over CaSO₄ at ambient temperature. Tetraethylammonium perchlorate (TEAP, Eastman) was recrystallized from water and dried in a vacuum oven at 80°C. KPF₆ (P & B) was twice recrystallized from water and dried in a vacuum oven at 110°C for several days. Sodium thiocyanate (Matheson Coleman and Bell), nickelous nitrate (Fisher) and zinc perchlorate (G. F. Smith) were dried in a vacuum oven at 60°, 40° and 60°C, respectively. Mercury which had been triply distilled under vacuum was purchased from Bethlehem Apparatus Co.

2. Solvents

Dimethylsulfoxide (DMSO), N,N-dimethylformamide (DMF), methanol (MeOH), acetonitrile (AN) and nitromethane (NM) all were Aldrich "Gold Label" grade. Formamide (F) was purchased from Eastman. Propylene carbonate (PC),

N-methylformamide (NMF), and hexamethylphosphoramide (HMPA) obtained from Aldrich. Propylene carbonate was further refluxed over calcium hydride (Fisher) under reduced pressure overnight, then fractionally distilled; only the middle 70% fraction was collected. Most of the solvents used were kept over freshly activated molecular sieves (Lind type 3A). The water content of most of these solvents was <0.05% as determined by an automatic Karl Fischer These solvents were kept in a dry box under titrator. nitrogen atmosphere. Water was purified by distillation from alkaline permanganate followed by "pyrodistillation", which consisted of cycling a mixture of steam and oxygen through a silica tube network held at 800°C for two days before collecting the distillate. Water for synthesis and cleaning the glassware was purified by the use of a "Milli-Q" purification system (Millipore Corp.).

3. Transition Metal Complexes and Compounds

 ${\rm Cr(bpy)_3(ClO_4)_3~complex~(where bpy = 2,2'-bipyridine)}$ was prepared by electrolyzing (25 ml) an aqueous solution containing 50 mM ${\rm Cr^{3+}}$ and 50 mM ${\rm HClO_4}$ in 100 mM ${\rm NaClO_4}$ over a stirred mercury pool held at -1100 mV ${\rm vs.}$ a saturated calomel electrode (SCE), while continuously passing prepurified argon to form ${\rm Cr^{2+}}$. This solution was then transferred using a gas-tight syringe to a deoxygenated suspension of (1.0 g) of 2,2'-bipyridine in (45 ml) aqueous 10 mM ${\rm HClO_4}$.

The resulting black suspension of $Cr(bpy)_3(ClO_4)_2$ was bubbled with oxygen for one hour to yield a yellow precipitate of $Cr(bpy)_3(ClO_4)_3$ which was filtered, washed with ethanol and water, and dried in a vacuum desicator (27).

 ${\rm Co(bpy)_3(ClO_4)_3}$ was synthesized using the procedure of Burstall and Nyholm (28). ${\rm CoCl_2\cdot 6H_2O}$ (2.4 g) and 2,2'-bipyridine (4.7 g) were heated with 50 ml of water until complete solution had occurred. To this yellow solution 10 ml ${\rm H_2O_2}$ and 10 ml HCl was added, and the mixture evaporated to a syrupy consistency. Then 50 ml of water was added, and the solution was treated with 10 ml HClO₄. The yellow precipitate was recrystallized from hot water and air-dried.

The salt of Na[Fe^{III}(EDTA)] (where EDTA = ethylenediamine-NNN'N'-tetraacetic acid) was prepared according to Reference (29) by treating freshly prepared Fe(OH)₃ with a stoichiometric amount of the disodium salt of EDTA. Heating at about 80-90°C with regular stirring produced a yellow solution. Slow evaporation of the resulting solution (vacuum aspirator) yielded yellow-brown crystals of Na[Fe^{III}(EDTA)]·3H₂O which is very soluble in water.

The salt of $Na[Co^{III}(EDTA)]\cdot 4H_2O$ was prepared according to the method of Dwyer et al (30).

The compound $Co(phen)_3(ClO_4)_2$ (where phen = 1,10-phenanthroline) was prepared by the method of Pfeiffer and Werdelmann (31).

The salt of $Fe(bpy)_3(ClO_4)_2$ was obtained from G. F. Smith

and used without further purification.

The $Co(pby)_3^{2+}$ was prepared (in situ) by adding an excess of ligand to a solution of anhydrous $CoCl_2$.

Ferrocene (Fc) was purchased from Aldrich and used without further purification. Ferricinium picrate (Fc $^+$) was prepared as described in Reference (32).

The compound $Ru(NH_3)_6(ClO_4)_3$ was prepared by dissolving the $Ru(NH_3)_6\cdot Cl_3$ (Matthey Bishop Inc.) in hot water; addition of $1.0\underline{M}$ solution of sodium perchlorate gave a white precipitate of perchlorate which was filtered, washed and dried.

The salt of $Ru(NH_3)_5NCS(ClO_4)_2$ was synthesized according to References (22,33).

Co(III)ammine complexes were prepared according to the following procedures. $[\text{Co(NH}_3)_5\text{CO}_3]\text{NO}_3\cdot\frac{1}{2}\text{H}_2\text{O}$ (34) was used as the starting material for the preparation of $\text{Co(NH}_3)_5\text{F}^{2+}$ (34) and $\text{Co(NH}_3)_5\text{OSO}_3^+$ (35). The remaining cobalt-ammine complexes were synthesized by oxidation of CoCl_2 : $\text{Co(NH}_3)_5^{3+}$ (36), $\text{Co(NH}_3)_5\text{NO}_3^{2+}$ (37), $\text{Co(NH}_3)_5\text{NCS}^{2+}$ (38), $\text{Co(NH}_3)_5\text{N}_3^{2+}$ (39), and Co(en)_3^{3+} (40) (where en = ethylenediamine). These solid complexes were prepared as perchlorate salts.

Synthesis of the Cr(III) ammine complexes followed standard published procedures. The double salt aquopenta-aminechromium(III)ammonium nitrate (41) was used as the starting point for the preparation of $\text{Cr}(\text{NH}_3)_5\text{Br}^{2+}$ (41), $\text{Cr}(\text{NH}_3)_5\text{Cl}^{2+}$ (41), $\text{Cr}(\text{NH}_3)_5\text{NO}_3^{2+}$ (41), $\text{Cr}(\text{NH}_3)_5\text{F}^{2+}$ (42),

 ${\rm Cr(NH_3)_5NCS}^{2+}$ (43), and ${\rm Cr(NH_3)_5N_3^{2+}}$ (44). All solid complexes were recrystallized from acidified water by precipitation as the perchlorate or chloride salts.

Samples of Ru(en)₃Br₃ were kindly supplied by Dr. Gilbert Brown of Brookhaven National Laboratory, and Co(sep)Cl₃ (where sep=sepulchrate, see Reference (45) for further details) was kindly provided by Professor John Endicott of Wayne State University.

B. APPARATUS

Conventional two-compartment glass cells were employed for the electrochemical measurements. The working compartment which had a volume capacity of 10-15 ml was separated from the reference compartment by a frit of "very fine" or "ultrafine" grade manufactured by Corning, Inc. The average porosity of these frits was 1-3 µm which prevented significant mixing of the two solutions on the time scale of 2-3 hrs required for most experiments. For most measurements, the working and reference compartments were filled with the same solution (except when otherwise noted) so that the solvent junction was formed between the aqueous reference electrode and the solvent of interest at the fiber tip separating the reference compartment and the reference electrode itself. The working compartment, the liquid junction formed in the frit, and part of the salt bridge between the working compartment and the reference electrode were surrounded by a

common jacket through which water from a Braun Melsungen circulating thermostat could be circulated. The temperature of the cell solution could be controlled within ±0.05°C.

C. ELECTROCHEMICAL TECHNIQUES

1. Sample Preparation and Reference Electrodes

All non-aqueous solutions were prepared in a dry box under nitrogen atmosphere. These solutions were deoxygenated by bubbling with prepurified nitrogen or argon which had passed through a wash bottle containing concentrated H2SO4 and finally through a bottle containing the non-aqueous solvent of interest for that experiment. For aqueous solutions, prepurified nitrogen or argon which had been passed through a V(II) solution was employed. Commercial saturated aqueous calomel reference electrodes (Sargent-Welch), either filled with saturated KCl (KSCE) or with saturated NaCl (NaSCE), were used for most thermodynamic measurements. In some cases a normal calomel reference electrode (NCE) filled with 1.0 normal aqueous KCl was used. For measurements in aqueous perchlorate media a NaSCE was employed instead of the KSCE because of the low solubility of KClO, which might precipitate in the liquid junction of the electrode and cause spurious potentials.

A platinum wire placed in the working compartment served as the counter (auxiliary) electrode for most experiments.

2. Cyclic Voltammetry

Cyclic voltammograms were obtained using a PAR 174A polarographic analyzer (Princeton Applied Research Corp.) coupled with a Hewlett-Packard Model 7044A X-Y recorder. Sweep rates in the 50-500 mV/sec range were used in this work. This arrangement allowed peak potentials to be measured with a precision of ±1-2 mV.

Several working electrodes were used in cyclic voltammetric studies. For redox couples that exhibit formal potentials that are sufficiently negative to be examined at mercury electrodes, a commercial (Metrohm Model E410, Brinkmann Instruments) hanging mercury drop electrode (HMDE) was used. Platinum "flag" or glassy carbon electrodes were used for work at positive potentials (E > 0 mV vs. KSCE). The platinum "flag" electrode consisted of a 2 mm² sheet of platinum spot-welded to a fine platinum wire. This electrode was pretreated by immersion in warm 1:1 HNO3 and activation by passage over a Bunsen burner flame. The use of a Pt electrode in formamide and N-methylformamide solutions was not possible; instead, a glassy carbon electrode was employed whenever necessary.

3. Polarography

The same instruments that were used for cyclic voltammetry were also employed to obtain dc, and normal pulse polarograms. Sweep rates in the 1-5 mV/sec range were used. A dropping mercury electrode (DME) was used as the working electrode. Mercury flow rates of 1.5 mg/sec and column heights of 50 cm were used. The drop time could be mechanically controlled by means of a PAR 174/70 drop timer to be 0.5, 1 or 2 sec.

4. Preparative Electrolyses

In preparing ${\rm Cr}^{2+}$ for the synthesis of ${\rm Cr(bpy)}_3({\rm ClO}_4)_3$, constant potential electrolyses were performed with a PAR 173 potentiostat. A stirred mercury pool and a Pt gauze were used as working and counter electrodes respectively. The electrolyzed solution was bubbled with deoxygenated argon to prevent any reaction with atmospheric ${\rm O}_2$.

5. Potential of Zero Charge (PZC) Measurement

The PZC values for mercury in contact with various non-aqueous electrolytes were determined using a streaming mercury electrode and a digital voltmeter. Solutions were deoxygenated by bubbling with prepurified nitrogen prior to measurements. Then the potential differences between a streaming mercury electrode and a SCE reference electrode were measured while changing the height of mercury reservoir. Beyond a certain height the potential became constant. This was taken as the potential of zero charge.

CHAPTER III

SOLVENT TREATMENTS OF THERMODYNAMIC AND ELECTRODE KINETIC DATA FOR REDOX COUPLES

A. SOLVENT DEPENDENCE OF REDOX THERMODYNAMICS

1. The Reaction Free Energy and Transfer Free Energy Concepts

In order to evaluate solvent effects upon thermodynamics of redox couples, it is useful to obtain estimates of the solvation energies and standard free energies of transfer.

Consider the generalized electrochemical reaction proceeding at a Galvani potential $\varphi_{\text{m}}\colon$

$$ox + e^{-}(\phi_m) \neq red$$
 (1)

The free energies of the ground states I and II that are prior to, and following, electron transfer, can be expressed as (46,47):

$$G_{I}^{\circ} = \overline{G}_{OX}^{\circ} + \mu_{P}^{\circ} - F\phi_{m}$$
 (2)

$$G_{II}^{\circ} = \overline{G}_{red}^{\circ}$$
 (3)

where $\overline{G}_{\text{ox}}^{\circ}$ and $\overline{G}_{\text{red}}^{\circ}$ are the partial molal free energies of the oxidized and reduced species, respectively, and μ_{e}° is the chemical potential of the reacting electron. Since the overall free energy of reaction ΔG° (= G_{II}° - G_{I}°) for

Equation (1) will by definition equal zero when $\phi_m = \phi_m^o$ (the standard Galvani metal-solution potential difference), then,

$$-F\phi_{m}^{\circ} = \overline{G}_{red}^{\circ} - \overline{G}_{ox}^{\circ} = \Delta G_{rc}^{\circ}$$
 (4)

For convenience, we shall term $(\overline{G}_{red}^{\circ} - \overline{G}_{ox}^{\circ})$ the "reaction free energy" of the redox couple ΔG_{rc}° . The change in free energies of the ions forming the redox couple resulting from changing from water (W) (as a reference solvent) to a nonaqueous solvent (s), $\Delta (\overline{G}_{red}^{\circ} - \overline{G}_{ox}^{\circ})^{S-W}$ [= $\Delta (\Delta G_{rc}^{\circ})^{S-W}$], will therefore be related to the corresponding variation in ϕ_m° , $\Delta (\phi_m^{\circ})^{S-W}$, by

$$-F_{\Delta}(\phi_{m}^{\circ})^{s-w} = \Delta(\Delta G_{rc}^{\circ})^{s-w}$$
 (5)

Since the changes in the standard Galvani metal-solution potential difference $\Delta(\phi_m^o)^{S-W}$ correspond to the measured changes in formal potential, ΔE_f^{S-W} , for a given redox couple between pairs of solvents s and water, Equation (5) can be written as

$$\Delta(\Delta G_{rc}^{\circ})^{s-w} = -F[\Delta E_{f}^{s-w} - \Delta \phi_{\ell,j}^{s-w}]. \tag{6}$$

In this equation, $\Delta \phi_{\ell,j}^{s-w}$ is the change in the liquid junction potential between the working and reference compartments which is brought about by substituting solvent s

for water. Although the estimation of $\Delta \phi_{\ell,j}^{S-W}$ and hence $\Delta (\Delta G_{rc}^{o})^{S-W}$ (free energy of transfer for redox couple) requires an extrathermodynamic assumption, there are a number of routes available by which such transfer free energies can be obtained to a reasonable approximation (probably within 1-2 Kcal mole⁻¹ (48)). Some of these methods are now discussed.

2. <u>Some Extrathermodynamic Methods for Estimation of</u> Transfer Free Energies

Although different direct methods are available for determination of the free energy of transfer of an uncharged solute or an electrolyte as a whole, estimation of the thermodynamics of transfer of single ions between various solvents requires some sort of extrathermodynamic assumption (48). In recent years there has been a great deal of interest in developing methods by which to formulate a solvent-independent series for standard electrode potentials as well as to evaluate the liquid junction potentials at the interfaces of different solvents. The most widely accepted approaches are:

a. The "Ferrocene Assumption"

This model, which was originally introduced by Strehlow and his co-workers (49), involves the assumption that the

absolute standard potential ϕ_m° of the ferricinium-ferrocene $(F_c^+-F_c)$ redox couple is independent of the solvent. This means that the difference in the solvation energy between ferricinium and ferrocene is solvent independent; i.e., $\Delta G_t(F_c^+) = \Delta G_t(F_c)$. Strehlow and his co-workers have indicated that ferricinium and ferrocene are large and essentially equal in size and symmetrical in structure with the active atom situated in the center of an effectively spherical molecule insulated from solvent by the cyclopentadienyl rings. Thus they would be expected to have minimal specific interactions with solvents and a small electrostatic energy of solvation.

The Fc⁺/Fc redox couple has been used extensively in determining free energies of transfer of ions from water to other solvents. The method is particularly convenient for electrochemical determinations of the free energy of single ion transfer, ΔG_{t}° , since ΔG_{t}° can be estimated simply from the solvent effect upon the measured standard electrode potential for the appropriate cell reaction relative to the corresponding potentials for Fc⁺/Fc under the same conditions. However, the use of the ferrocene assumption has been shown to yield significantly different estimates of ΔG_{t}° compared with those obtained by using other extrathermodynamic approaches, particularly when one of the solvents is water (48,50-53). Several reasons are given in the literature indicating the inadequacy of Fc⁺/Fc for estimating

the thermodynamics of transfer of single ions. Among them are: the small radius of the ferricinium (Fc⁺) ion, which can give rise to ion-dipole interaction and cause solvent dipoles to orient toward the ion (53); the quadropole-dipole interaction between the ferrocene (Fc) molecule and the solvent dipoles (54); and variations in the specific solvation of the ferricinium cation, between solvents which are not entirely compensated by corresponding changes in the solvation of the ferrocene molecule (50,53). Some results presented in Chapter V for Fc⁺/Fc couple further indicate the inadequacy of the ferrocene assumption.

b. The "Zero Liquid Junction Potential" Procedure

This procedure, which is recommended by Parker and his associates (55,56), involves using the following cell

Ag
$$|0.01\underline{M}|$$
 Ag $|0.01\underline{M}|$ Et₄NPic $|0.01\underline{M}|$ Ag $|0.01\underline{M}|$

where reference solvent (s_1) is either acetonitrile or methanol and the bridge solution of 0.1 $\underline{\text{M}}$ tetraethylammonium picrate is contained either in the reference solvent (s_1) or in solvent of interest (s_2) , whichever is the weaker solvator for the silver ions. This procedure assumes that the net liquid junction potential between a pair of solvents is negligible (when 0.1 $\underline{\text{M}}$ Et₄NPicrate dissolved in either

solvent is used as the salt bridge). Therefore, the measured cell potential is directly proportional to the free energy of transfer of ${\rm Ag}^+$ from $({\rm s}_1)$ to $({\rm s}_2)$. This model has been shown to give similar values of ${\rm AG}_{\rm t}^{\circ}$ when compared with other assumptions (55). Particularly the agreement between the zero liquid junction assumption and the more reliable "TATB" assumption (see below) have been shown to be usually within \approx 1 Kcal mole⁻¹ (48,55).

c. The "tetraphenylarsonium-tetraphenylborate" (TATB) Assumption

Among different extrathermodynamic assumptions, this method has been preferred by many authors (48,52,55-57). The cation $Ph_{\mu}As^{+}$ and the anion $Ph_{\mu}B^{-}$ are very large and essentially equal in size, so the short-range electrostatic interactions are expected to be negligible. This model is based on the assumption that the transfer free energies of such counterions are very similar, <u>1.e.</u>, $\Delta G_{t}^{\circ}(Ph_{\mu}As^{+})$ = $\Delta G_{t}^{\circ}(Ph_{\mu}B^{-}) = \frac{1}{2}\Delta G_{t}^{\circ}(Ph_{\mu}AsPh_{\mu}B)$. Values of $\Delta G_{t}^{\circ}(TATB)$ can easily be obtained from their solubility products in a pair of solvents of interest.

Other reference electrolyte assumptions which have been shown to yield values of free energy of transfer similar to those of TATB assumption (± 1 Kcal mole⁻¹) are: tetraphenylphosphonium-tetraphenylborate ($Ph_{ll}PBPh_{ll}$),

introduced by Grunwald et al. (58), and triisoamyl-n-butylammoniumtetraphenylborate (TABBPh $_{\mu}$), introduced by Popovych (59).

The TATB assumption appears to be a more reliable extrathermodynamic method, and has been employed by a number of investigators (52,55-57,59-61) for estimation of transfer free energies of single ions. In addition, further support for the TATB procedure comes from theoretical calculations (62,63). It should be mentioned that the values of transfer free energy obtained by this procedure are probably trustworthy only to within cal Kcal mole⁻¹. However, when the objective is to interpret or predict large solvent effects, an error or uncertainty of 1-2 Kcal mole⁻¹ in the transfer free energy may well be acceptable (48).

3. Estimation of Transfer Free Energies for Redox Couples

The quantity $\Delta(\Delta G_{rc}^{\circ})^{S_1-S_2}$ is of fundamental interest for simple redox couples since it provides a measure of the relative changes in solvation energy of the reduced versus the oxidized forms as the solvent is varied: the correlation of values of $\Delta(\Delta G_{rc}^{\circ})^{S_1-S_2}$ for a series of solvents S with their physical properties should provide valuable information about the variations in the reactant-solvent interactions.

In the present work, estimates of the change in

 $(\overline{G}_{red}^{\circ} - \overline{G}_{ox}^{\circ})$ for the redox couples resulting from substituting the various nonaqueous solvents for water. $\Delta(\Delta G_{\mathbf{rc}}^{\mathbf{o}})^{\mathbf{S}-\mathbf{W}}$, were obtained from the corresponding values of $\Delta E_{\mathbf{f}}^{\mathbf{S}-\mathbf{W}}$ using Equation (6). As mentioned before, a common extrathermodynamic approach for obtaining the required values of $\Delta \phi_{0,i}^{S-W}$ (change in liquid junction potential difference between aqueous reference electrode and nonaqueous working compartment) has been to assume that $\Delta \phi_{\ell,i}^{s-w}$ equals the measured values of $\Delta E_{\rm f}^{\rm S-W}$ for the Fc⁺/Fc couple, $(\Delta E_f)_{Fc}^{s-w}$; i.e., that $\Delta (\Delta G_{rc}^{\circ})^{s-w}$ for the Fc⁺/Fc couple, $\Delta(\Delta G_{rc}^{\circ})_{Fc}^{s-w}$, equals zero (48). It was discussed in the previous section that the validity of the "ferrocene assumption" is questionable; on the balance of the evidence presently available (48) it appears that the so-called "tetraphenylarsonium-tetraphenylborate" (TATB) assumption is a more reliable extrathermodynamic method. Nevertheless, the values of $(\Delta E_f)_{Fc}^{S-W}$ can still provide a straightforward route to the evaluation of $\Delta \phi_{2j}^{S-W}$ and hence $\Delta (\Delta G_{rc}^{o})^{S-W}$ on the TATB scale if the appropriate values of $\Delta(\Delta G_{rc}^{\circ})_{Fc}^{s-w}$ on this scale are known. Fortunately, the required values of $\Delta(\Delta G_{rc}^{\circ})_{Fc}^{s-w}$ for most solvents can be easily obtained from the differences in the apparent values of $\Delta G_{\mbox{\it t}}^{\mbox{\it o}}$ for a given ion that have been obtained using the ferrocene and TATB assumptions. Since from Equation (6) one can write

$$F\Delta\phi_{\ell,j}^{s-w} = F(\Delta E_f)_{Fc}^{s-w} + \Delta(\Delta G_{rc}^{\circ})_{Fc}^{s-w}$$
 (7)

the required values of $\Delta(\Delta G_{rc}^o)^{S-W}$ for a given redox couple can be obtained from

$$\Delta(\Delta G_{rc}^{\circ})^{s-w} = F(\Delta E_{f})_{Fc}^{s-w} - F_{\Delta} E_{f}^{s-w} + \Delta(\Delta G_{rc}^{\circ})_{Fc}^{s-w}$$

$$= -F\Delta(E_{f}^{Fc})^{s-w} + \Delta(\Delta G_{rc}^{\circ})_{Fc}^{s-w}$$
(8)

where $\Delta(E_{\mathbf{f}}^{\mathbf{Fc}})^{\mathbf{S-W}}$ is the change in the formal potential for the redox couple of interest (versus those for the Fc⁺/Fc couple), and $\Delta(\Delta G_{\mathbf{rc}}^{\mathbf{o}})_{\mathbf{Fc}}^{\mathbf{S-W}}$ is the estimate of free energy of transfer for the Fc⁺/Fc itself obtained from Ag⁺ transfer data (48) resulting from substituting another solvent for water (see notes to Table 7 for details).

4. <u>Determination of Reaction Entropies for Redox Couples</u>

Although the reaction entropy has been defined in Chapter I, it is useful to present this definition in the following form. One can consider the general reaction

$$M^{III}L_{m}L_{n}^{"} + e^{-(metal electrode)} \stackrel{?}{\downarrow} M^{II}L_{m}^{"}L_{n}^{"}$$
 (9)

in which M is a metal which has trivalent and divalent oxidation states, L' and L" are neutral or anionic ligands and the number of L' and L" coordinated to M is given by

m and n, respectively. The reaction entropy ΔS_{rc}^{o} of the $M^{III}L_{m}^{i}L_{n}^{i}/M^{II}L_{m}^{i}L_{n}^{i}$ redox couple following reaction (9) can be written as

$$\Delta S_{rc}^{\circ} = \overline{S}_{red}^{\circ} - \overline{S}_{OX}^{\circ} = \overline{S}_{II}^{\circ} - \overline{S}_{III}^{\circ}$$
 (10)

where $\overline{S}^{\circ}_{II}$ and $\overline{S}^{\circ}_{III}$ are the absolute ionic entropies of $M^{II}_{m}L_{n}^{"}$ (reduced) and $M^{III}_{m}L_{n}^{"}$ (oxidized), respectively.

Since reaction (9) is only one-half of a complete electrochemical cell reaction, its equilibrium properties cannot be determined without resort to extrathermodynamic assumptions. However, there are a number of reliable methods for the quantitative estimation of individual ionic entropies, and especially ΔS_{rc}^{o} . A sueful summary of these methods has been given by Criss and Salomon (17). the present purposes, the most convenient method involves the use of nonisothermal electrochemical cells (64,65). In this arrangement, the temperature of the working compartment (the half-cell containing the redox couple of interest) is varied while the temperature of the other half-cell consisting of some convenient reference electrode is held constant. In the present work values of ΔS_{rc}^{o} for each redox couple in various solvents were determined using either nonisothermal electrochemical cells "a" or "b"

"a"

SCE(aq)||0.1M LiClO4(solvent s)|0.1M LiClO4(s),M^{III}-M^{II}
|Pt,Hg or Carbon
A
B
C

"b"

SCE(aq) | 0.1M TEAP(aq) | | 0.1M TEAP(solvent s) | 0.1M TEAP(s),
A

B

(where TEAP = tetraethylammonium perchlorate)

In the above arrangements, the reference electrode (SCE) was held at room temperature and the temperature of the working compartment BC was varied over as wide a range as practicable (usually 30-60 deg. C); the thermal liquid junction (21) was formed within the region AB so that the unknown solvent liquid junction potential at A did not affect the temperature dependence of formal potential. The formal potential E_f across nonisothermal cells "a" and "b" was determined as a function of temperature. The temperature dependence of the formal potential measured here can be separated into three components (21)

$$\frac{dE_{f}}{dT} = \frac{d\phi_{tlj}}{dT} + \frac{d\phi_{tc}}{dT} + \frac{d\phi_{f}}{dT}$$
 (11)

where ϕ_{tlj} is the Galvani potential difference across the thermal liquid junction within the region AB, ϕ_{tc} is the "thermocouple" potential difference between the hot and cold regions of the working electrode, and ϕ_f^m is the Galvani metal-solution potential difference at the working electrode. Since

$$\Delta S_{rc}^{o} = F(\frac{d\phi_{f}^{m}}{dT})$$
 (12)

then if $d\phi_{tc}/dT$ and $d\phi_{tlj}/dT$ are known or can be estimated, ΔS_{rc}° can be obtained from measurements of dE_f/dT . Following the arguments given or quoted in Reference (21) for aqueous media, it is very likely that the temperature derivative of the thermal junction potential is negligible in comparison with (dE_f/dT) . Since the thermocouple potential difference generated between the hot and cold regions of the mercury, platinum or carbon working electrode (or copper connecting leads) is also negligible (21), then to a very good approximation $(dE_f/dT) = (d\phi_f^m/dT)$ so that

$$\Delta S_{rc}^{\circ} = F(\frac{dE_{f}}{dT})$$
 (13)

It is seen in Tables 3, 6 and 10 (Chapter V) that the values of ΔS_{rc}^{o} are essentially independent (within the experimental reproducibility of ± 1 e.u.) of the ionic strength μ and composition of the supporting electrolyte in the thermal junction region for $0.025 \le \mu \le 0.02\underline{M}$. This supports the assumption used here for the determination of reaction entropy.

The formal potential E_f which is required for determination of ΔS_{rc}^{o} was obtained from measurement of $E_{1/2}$, the (polarographic) half-wave potential using cyclic voltammetry. For a reversible cyclic voltammogram, $E_{1/2}$ was obtained by bisecting the cathodic- and anodic-going peak potentials (66). There is a relation between E_f and $E_{1/2}$ (67,68) as shown in Equation (14)

$$E_{1/2} = E_f + \frac{RT}{nF} \ln \left(\frac{D_{II}}{D_{III}} \right)^{1/2}$$
 (14)

where D_{II} and $\mathrm{D}_{\mathrm{III}}$ are the diffusion coefficients of the reduced and oxidized species, respectively. It is obvious from Equation (14) that the actual values of E_{f} will differ slightly from the experimental estimates due to the

inequality of the diffusion coefficients. However, the $D_{\rm II}/D_{\rm III}$ ratio is usually close to unity so that the $E_{1/2}$ differs from $E_{\rm f}$ by only 2-3 mV. Therefore $dE_{1/2}/dT$ can be equated to $dE_{\rm f}/dT$ and from that one can write

$$\Delta S_{rc}^{\circ} = F(\frac{dE_{1/2}}{dT}) \tag{15}$$

(where $F = 23.06 \text{ cal mV}^{-1} \text{ mol}^{-1}$)

5. <u>Electrostatic Born Model for Calculating Transfer Free</u> Energies and Reaction Entropies of Redox Couples

There has been considerable effort to calculate the thermodynamics of transfer of single ions between various solvents. The simplest theoretical model is the Born dielectric continuum (69). This is an electrostatic model which treats the surrounding solvent as a structureless medium of uniform dielectric constant. It also assumes the ion to be a rigid sphere with crystallographic radius r. For the transfer of 1 mole of single ion from water to a given nonaqueous solvent, the Born free energy is given by (48)

$$\Delta G_{t}^{o}(Born) = \frac{NZ^{2}e^{2}}{2r} \cdot (\frac{1}{\varepsilon_{s}} - \frac{1}{\varepsilon_{w}})$$
 (16)

This equation can be written in the following form when we are dealing with a transfer of a redox couple from water (w) to a nonaqueous solvent (s) (70)

$$\Delta(\Delta G_{rc}^{\circ})_{Born}^{s-W} = \frac{e^{2}N}{2}(\frac{1}{\varepsilon_{w}} - \frac{1}{\varepsilon_{s}})(\frac{z^{2}}{r_{ox}} - \frac{z^{2}}{r_{red}})$$
 (17)

where e is the electronic charge, N is Avogadro's Number, $\epsilon_{\rm w}$ and $\epsilon_{\rm s}$ are the (static) dielectric constants in water and the nonaqueous solvent, $Z_{\rm ox}$ and $Z_{\rm red}$ are the charges on the oxidized and reduced species, and $r_{\rm ox}$ and $r_{\rm red}$ are the corresponding radii.

The Born equation for estimation of reaction entropies of a given redox couple in any solvent is given by (70)

$$(\Delta S_{rc}^{\circ})_{Born} = -\frac{e^{2}N}{2\varepsilon T} (\frac{d \ln \varepsilon}{d \ln T}) (\frac{z_{ox}^{2}}{r_{ox}} - \frac{z_{red}^{2}}{r_{red}})$$
 (18)

where T is the absolute temperature, and the other terms have already been defined above.

It is well known that the Born model yields estimates of solvation free energies and entropies for simple monoatomic ions that are often in substantial disagreement with experiment, undoubtedly due in large part to the extensive short-range solvent order induced by such uncoordinated ions (70). This model might be expected to be more

applicable to the estimation of $\Delta(\Delta G_{\mathbf{rc}}^{\circ})^{\mathbf{S-W}}$ for the present work since we are dealing with complex ions with fixed coordination spheres which might act to prevent the approach of solvent molecules to the metal center.

B. SOLVENT DEPENDENCE OF REDOX ELECTRODE KINETICS

1. <u>Evaluation of Activation Free Energies and Other Electrode</u> Kinetic Parameters

In order to evaluate the electrochemical kinetic data in different solvents, it is first necessary to consider the conventional formulations that attempt to describe the factors determining electrochemical reactivity. One such model which is especially applicable to outer-sphere pathways is the "reactive-collision" model (71-73). For electrochemical reactions this model can be expressed as

$$k_{ob} = \kappa Z \exp(-\Delta G^{\neq}/RT)$$
 (19)

 k_{Ob} is the observed electrochemical rate constant (cm sec⁻¹), κ is a transmission (electron tunneling) coefficient, k_{C} is the electrochemical collision frequency and k_{C} is the free energy of activation. The free energy of activation k_{C} can be expressed as the sum of contributions arising from the individual events in the activation

process (73)

$$\Delta G^{\neq} = W_{p} + (\Delta G^{\neq})_{is} + (\Delta G^{\neq})_{os}$$
 (19a)

In this equation W_p is the work (free energy) required to bring the reactant from the bulk solution to the reaction plane at the electrode (i.e., to form the so-called precursor state). $(\Delta G^{\neq})_{is}$ is the "inner-shell" reorganization energy which is the energy required to stretch or compress the metal-ligand bond distances and to change the ligand conformation. $(\Delta G^{\neq})_{os}$ is the "outer-shell" term, the energy required to rearrange and reorient solvent molecules surrounding the reactant. The inner-shell and outer-shell reorganizations must take place prior to electron transfer in order to attain the activated complex and facilitate the electron transfer process.

The ΔG^{\neq} in Equation (19a) can be rewritten as

$$\Delta G^{\neq} = W_{p} + \Delta G_{corr}^{\neq}$$
 (20)

where $\Delta G_{\text{corr}}^{\neq}$ is the work (double-layer) corrected free energy of activation (<u>i.e.</u>, the overall reorganization free energy). Using $\Delta G_{\text{corr}}^{\neq}$, Equation (19) can be expressed as

$$k_{corr} = \kappa Z \exp(-\Delta G_{corr}^{\neq}/RT)$$
 (21)

where $k_{\mbox{corr}}$ is the double-layer corrected rate constant in a given solvent.

The corresponding relationship to Equation (5) for electrochemical kinetics can be derived by noting that the $\Delta G_{\text{corr}}^{\neq}[=G_{\text{corr}}^{\neq}-G_{\text{I}}^{\circ}]$ can be separated into a potential-dependent ("electrical") part $(G_{\text{corr}}^{\neq}-G_{\text{I}}^{\circ})_{\text{e}}$ and a potential-independent ("chemical") part $(G_{\text{corr}}^{\neq}-G_{\text{I}}^{\circ})_{\text{c}}$ (46,47). The former component is related to the potential-dependent part of $(G_{\text{II}}^{\circ}-G_{\text{I}}^{\circ})$, $F\phi_{\text{m}}$ (Equations (2) and (3)) by (46,47,74)

$$(G_{corr}^{\neq} - G_{I}^{\circ})_{e} = \alpha_{corr} F \phi_{m}$$
 (22)

Since in Equation (21) Z should be dependent only on the effective reactant mass (10a), it should be approximately solvent independent. If κ is also solvent independent, the ratio of the double-layer corrected rate constant for a given reaction in water to that in another solvent at a fixed value of ϕ_m , $(k_w/k_s)_{corr}^{\phi_m}$, will be related to the corresponding free energies of activation $(\Delta G_{corr}^{\neq})_{s}^{\phi_m}$ and $(\Delta G_{corr}^{\neq})_{s}^{\phi_m}$ by

RT
$$\ln(k_w/k_s)_{corr}^{\phi_m} = (\Delta G_{corr}^{\neq})_s^{\phi_m} - (\Delta G_{corr}^{\neq})_w^{\phi_m}$$
 (23)

In view of Equation (22), Equation (23) can be written as

RT
$$\ln(k_w/k_s)_{corr}^{\phi_m} = (G_{corr}^{\neq} - G_{I}^{\circ})_{c}^{s} - (G_{corr}^{\neq} - G_{I}^{\circ})_{c}^{w} =$$

$$= \Delta(G_{corr}^{\neq} - G_{ox}^{\circ})_{c}^{s-w} = \Delta(\Delta G_{corr}^{\neq})_{c}^{s-w} \qquad (24)$$

where $\Delta(\Delta G_{\text{corr}}^{\neq})_{\text{c}}^{\text{S-W}}$ is the change in the chemical part of the activation free energy for a given reaction resulting from substituting a given nonaqueous solvent for water.

In order to obtain values of k_{corr} in each solvent from the observed rate constants k_{app} , the following relation can be used (e.g., Reference 75)

$$\ln k_{corr}^{E} = \ln k_{app}^{E} + f(Z_{r} - \alpha_{corr})\phi_{d}$$
 (25)

where k_{corr}^{E} is the double-layer corrected rate constant corresponding to the measured value of k_{app}^{E} at a given electrode potential E, Z_{r} is the charge on the reactant, $f = \frac{F}{RT}$ and α_{corr} is the transfer coefficient after correction for double-layer effects and is given by (9)

$$\alpha_{corr} = \frac{\alpha_{app} - Z_r (\partial \phi_d / \partial_E)_{\mu}}{1 - (\partial \phi_d / \partial_E)_{\mu}}$$
 (26)

In this equation $(\partial \phi_d/\partial_E)_{\mu}$ denotes the dependence of the average diffuse layer potential ϕ_d upon the electrode potential E at a constant electrolyte composition μ , α_{app} is the apparent transfer coefficient. Values of

 $\alpha_{\rm app}$ can be obtained from the experimental Tafel plots using $\alpha_{\rm app} = -f^{-1}(\partial \ln k_{\rm app}/\partial_E)_{\rm u}$ (9).

The evaluation of the quantities $\Delta(\Delta G_{\text{rc}}^{\circ})^{\text{S-W}}$ [Equation (5)] and $\Delta(\Delta G_{\text{corr}}^{\neq})_{\text{c}}^{\text{S-W}}$ [Equation (24)] for a given electrode reaction is of fundamental interest since they provide a monitor of the purely chemical influences brought about by solvent substitution upon the thermodynamics and kinetics of electron transfer. Since neither absolute nor even relative values of ϕ_{m} in different solvents are strictly speaking thermodynamically accessible quantities, the evaluation of $\Delta(\Delta G_{\text{corr}}^{\neq})_{\text{c}}^{\text{S-W}}$ inevitably requires some sort of an extrathermodynamic procedure. As was discussed before, the TATB assumption seems to be a more reliable method than the other procedures. Therefore, the values of k_{corr} evaluated at a fixed electrode potential (versus the TATB scale) can be inserted into Equation (24) to yield estimates of $\Delta(\Delta G_{\text{corr}}^{\neq})_{\text{c}}^{\text{S-W}}$ (see Chapter VI).

2. <u>Solvent Dependence of Intrinsic Barriers</u>

Further insight into the underlying factors which are responsible for the solvent effects on the electrode kinetics can be obtained by separating $\Delta(\Delta G_{\text{corr}}^{\neq})^{\text{S-W}}$ into intrinsic and thermodynamic contributions (10b,74,76,77). The double-layer corrected formal rate constant k_{corr}^{f} (rate constant measured at the formal potential E_{f} and

corrected for double-layer effects or "standard rate constant") can be related directly to the so-called intrinsic free energy of activation ΔG_{1}^{\neq} by (cf. Equation (10) of Reference (10a)).

$$k_{corr}^{f} = \kappa Z \exp(-\Delta G_{1}^{\neq}/RT)$$
 (27)

This intrinsic barrier ΔG_{1}^{\neq} is of particular interest since it represents the value of $\Delta G_{\text{corr}}^{\neq}$ when $G_{1}^{\circ} = G_{11}^{\circ}$, i.e., when the electrical and chemical parts of the overall free energy of reaction just cancel. The significance of the intrinsic barrier in the present context can be seen as follows.

In view of Equation (22), $\Delta G_{\hat{\mathbf{1}}}^{\neq}$ and $\Delta G_{\hat{\mathbf{corr}}}^{\neq}$ are related by

$$\Delta G_{\text{corr}}^{\neq} = \Delta G_{1}^{\neq} + \alpha_{\text{corr}} F(\phi_{\text{m}} - \phi_{\text{m}}^{\circ})$$
 (28)

Therefore from Equations (5) and (28) the alteration in ΔG_1^{\neq} , $\Delta (\Delta G_1^{\neq})^{S-W}$, resulting from changing from water to another solvent is related to $\Delta (\Delta G_{\text{corr}}^{\neq})_{\text{c}}^{S-W}$ and $\Delta (\Delta G_{\text{rc}}^{\circ})^{S-W}$ by

$$\Delta(\Delta G_1^{\neq})^{s-w} = RT \ln(k_w^f/k_s^f)_{corr}.$$
 (29a)

$$= \Delta \left(\Delta G_{corr}^{\neq}\right)_{c}^{s-w} - \alpha_{corr}^{\Delta} \left(\Delta G_{rc}^{\circ}\right)^{s-w}$$
 (29b)

The solvent dependence of the free energy barrier $\Delta(\Delta G_{\text{corr}}^{\neq})_{c}^{S-W}$ is therefore equal to the sum of the "intrinsic" part $\Delta(\Delta G_{1}^{\neq})^{S-W}$, and a "thermodynamic" part α_{corr} (ΔG_{rc}°) $^{S-W}$. The latter is equal to the change in $\Delta G_{\text{corr}}^{\neq}$ expected for a hypothetical transition state having the properties of a stable species with a structure and charge appropriately intermediate between ox and red. Therefore nonzero values of $\Delta(\Delta G_{1}^{\neq})^{S-W}$ signify that there are changes in G_{corr}^{\neq} resulting from solvent substitution that are not reflected in corresponding changes in G_{ox}° and G_{red}° , $G_{\text{i.e.}}^{\circ}$, are unique ("intrinsic") to the transition state (10b,74,76,77).

The intrinsic free energy of activation ΔG_{1}^{\neq} can also be expressed as the sum of the intrinsic outer-shell $(\Delta G_{1}^{\neq})_{\text{os}}$ and intrinsic inner-shell $(\Delta G_{1}^{\neq})_{\text{is}}$ terms, i.e., $\Delta G_{1}^{\neq} = (\Delta G_{1}^{\neq})_{\text{is}} + (\Delta G_{1}^{\neq})_{\text{os}}$. Theoretical models are available for calculation of the latter components. For outer-sphere reactions, the inner-shell term can be obtained by combining vibrational spectroscopic and bond length information assuming the metal-ligand bonds are behaving harmonically (10a,73,78). Estimates of the outer-shell contribution are obtained by treating the solvent as a dielectric continuum (10a,73,78) (see Chapter VI).

CHAPTER IV

SOLVENT PROPERTIES

A. CLASSIFICATION

Although a single classification scheme useful to all areas of nonaqueous solvent study has not yet been devised, a simple classification of solvents into protic and aprotic have proved to be useful (79). Protic solvents such as water, methanol and formamide are strong hydrogen-bond donors and can donate protons. On the other hand, aprotic solvents generally have hydrogens bound only to carbon, have very little affinity for protons, and are incapable of dissociating to form protons. Common aprotic solvents include aliphatic and aromatic hydrocarbons, ether, nitromethane, acetonitrile, propylene carbonate, dimethylsulfoxide, and dimethylformamide.

B. THE DIPOLE MOMENTS AND DIELECTRIC CONSTANTS

The degree of polarity of a bond or a molecule is measured by its dipole moment μ . The net dipole moment of a molecule is given by the vector sum of the bond moments and is a function of the charge separation and geometry of the molecule. Due to the geometry factor and the possibility of partial or complete cancellation of the bond moments, the dipole

moment is probably a less useful measure of the ability of a solvent to promote dissociation of an ionic solute than is the dielectric constant, ϵ (79).

The ratio of the force in vacuum to the force in the medium is a characteristic of the medium and is known as its dielectric constant ε (80). The dielectric constant is one of the important properties of a solvent. There are several factors which contribute to the variation of solvent dielectric constant. Some of these factors are: permanent dipoles, number of dipoles, polarizability of medium, and the extent of association of dipoles arising from shortrange interactions (80). An increase in any of these factors will increase the value of ϵ . The association of dipoles (solvent molecule) can bring the dielectric constant into the range of 20-70 compared with values of 5 to 10 for nonassociated molecules. Indeed, hydrogen-bonded liquids (such as water, formamide and N-methylformamide) have high dielectric constants compared with those of nonassociated liquids (such as ether, benzene and sulfur dioxide).

Therefore, solvents with large dielectric constants promote the dissociation of ionic solutes, which in turn can lower the solution resistance. This process is very important in order to minimize ohmic drops in electrochemical work.

C. THE DONOR- AND ACCEPTOR-NUMBERS

Although different single-parameter approaches have been suggested for characterization of the solvating (ionizing) abilities of solvents, none of them have been successful to represent effectively the donor (nucleophilic) and acceptor (electrophilic) properties of solvents (81).

On the other hand the two-parameter approach, namely donicity or "donor number" and "acceptor number" proposed by Gutmann and coworkers (81) has proved extremely useful in the interpretation and prediction of a vast amount of coordinating interactions in solution.

The so-called "donor number", DN, is defined as the negative molar enthalpy value (in K cal/mol) for the reaction between solvent molecules as the donor and antimony pentachloride as a reference acceptor in 10^{-3} M solution of 1.2-dichloroethane as an inert solvent (81).

DN
$$\equiv -\Delta H_{S \cdot SbCl_5}$$

The donor number of a solvent has been interpreted as a measure of its electron donating ability or basicity (Lewis base), and can be a useful guide in assessing the ionizing power of a solvent. It also reflects the extent of covalent interactions between donor and acceptor.

The second of the two important solvent parameters characterizes the electron acceptor or electrophilic properties of a solvent. An empirical parameter termed the "acceptor number" which is a dimensionless number has been deduced from ³¹P NMR studies on triethylphosphine oxide in different solvents (81).

The values of chemical shifts have been extrapolated to infinite dilution, referred to hexane as reference solvent. In order to emphasize the relationship between acceptor properties and their conjugate donor properties, $SbCl_5$ has been used as a standard for both parameters. The corrected chemical shifts have been related directly to that for the $Et_3PO + SbCl_5$ adduct dissolved in 1,2-dichloroethane by arbitrarily assigning this the value of 100 (81).

Acceptor Number = Corrected Chemical Shift x 100
Corrected Chemical Shift of Et₃PO·SbCl₅

D. SOLVENT "INTERNAL ORDER", "a" PARAMETER

Criss and Salomon (17,20) have pointed out that the structural characteristics of the solvents resulting from hydrogen bonding or strong dipole-dipole interactions play the predominant role in determining ionic entropies, and the solvent basicities play a minor role. They have analyzed the available data for the ionic entropies \overline{S}° of simple univalent ions in various solvents in terms of the structural properties of the solvent. It was noted that \overline{S}° for a given ion in various solvents generally becomes increasingly negative as the degree of "internal order" of the solvent (the degree of association between solvent molecules) decreases, suggesting that a major factor contributing to So is the extent to which the ion can induce additional solvent order within its vicinity (17). The decreases in \overline{S}° generally found for the transfer of a given ion from water to other solvents have been found to be given by a characteristic "a" parameter for each solvent, where the value of "a" decreases as the internal order of the solvent decreases (17,20). Values of "a" (in cal. deg. -1 mole) for different solvents were obtained (see Equation (3) of Chapter I) from the intercepts of linear plots of ionic entropies in a given solvent versus corresponding ionic entropies in water (18). These values are listed in Table 2.

E. POTENTIAL RANGE IN NONAQUEOUS SOLVENTS

One of the most important reasons that nonaqueous solvents are attractive for electrochemical studies is the large potential range that is available at a number of electrodes. A number of aprotic solvents allow a much wider variety of electrode processes to be examined than in water. The practical working (voltage) limits in any solvent depend not only on the solvent intrinsic parameters (its oxidation-reduction properties), but also on the nature of the working electrode material, and the composition of the supporting electrolyte. Table 1 summarizes the practical voltage range (±0.2 V) for some of the aprotic solvents used in this work. These values are for vigorously purified solvents and are reported versus the aqueous saturated calomel reference electrode.

F. CHOICE OF SOLVENT

Although there are a large number of nonaqueous solvent systems that could be studied, it was necessary to use more strongly ionizing solvents for which some double-layer data on mercury electrodes were available (double-layer data are required for electrode kinetics). Dipolar solvents with substantial dielectric constants (ε > 35), which are capable of dissolving multicharged cations and anions were

Voltage Range on Mercury and Platinum in Selected Solvents and Supporting Electrolytes.b Table 1.a

Supporting Electrolyte	Working Electrode	Acetonitrile	Propylene Carbonate	Dimethyl- formamide	Dimethyl- sulfoxide
TEAP ^C	Hg	0.6 to -2.8	0.5 to -2.5	0.5 to -3.0	0.25 to -2.8
	Pt		1.7 to -1.9	1.6 to -2.1	0.7 to -1.85
TBAI ^d	НВ	-0.6 to -2.8		-0.4 to -3.0	-0.4 to -2.85
$NaClO_{m{\mu}}$	НВ			0.5 to -2.0	0.25 to -1.90
	Pt	1.8 to -1.5		1.6 to -1.6	0.7 to -1.85

^aData taken from Table 4-1 of Reference 79.

^bMeasured potentials are in volts, <u>vs</u>. aqueous SCE.

^cTEAP = tetraethylammonium perchlorate.

dTBAI = tetra-n-butylammonium iodide.

used. Employment of these solvents not only minimizes the solution resistance (ohmic drop), but also prevents the extent of ion association in the bulk solution. Table 2 summarizes solvents used in this work along with some of their physical and chemical properties. It is seen that the values of dielectric constant, donor number, acceptor number and solvent internal order "a" parameter vary over a wide range, which should allow the effects of such factors on both the electrode kinetics and thermodynamics to be explored systematically.

Table 2. Some Properties of Various Solvents.

		Dipole ^a	Dielectric	Donor	Acceptor	[] []
Solvent	Structure	Moment	Constant	Number	Number	a
Nitromethane (NM)	CH ₃ NO ₂	3.57	36	2.7	20.9	
Acetonitrile (AN)	CH3CN	3.44	36.0	14.1	18.9	-18.3
Propylene Carbonate (PC)	CH2CHCH3	4.98	64.9	15.1	18.3	- 9.3
Methanol (MeOH)	сн ³ он	1.7	32.6	19	41.3	-10.8
Formamide (F)	HCONH2	3.73	108.7	v24	39.8	- 1.5
N-Methylformamide (NMF)	нсоинсн3	3.83	182		32.1	- 4.8
$N_{\bullet}N-Dimethylformamide (DMF) HCON(CH_3)_2$	$HCON(CH_3)_2$	3.86	36.7	56.6	16.0	-15.9
Dimethylsulfoxide (DMSO)	$(cH_3)_2$ so	3.90	46.7	29.8	19.3	6.6 -
<pre>Hexamethylphosphoramide (HMPA)</pre>	$((cH_3)_2N)_3PO$	84.4	29.6	38.8	10.6	
Water	н ₂ 0	1.85	78.5	1 8	54.8	0.0

DGutmann Donor Number in Kcal.mol-1 from $^{\mbox{a}}\mbox{Dipole}$ moment in Debye from Reference (82). Reference (81).

Table 2. Continued.

^cGutmann Acceptor Number from Reference (81).

dEmpirical "a" parameter in cal.deg⁻¹ mol⁻¹ describing solvent "Internal Order" from Reference (20).

CHAPTER V.

SOLVENT EFFECTS UPON THE THERMODYNAMICS OF M(III)/(II) TRANSITION-METAL REDOX COUPLES

A. INTRODUCTION

Variations in the solvent medium are expected to have large influences upon the thermodynamics of electron transfer reactions. Part of these effects can arise from changes in the composition of coordination shell of the reacting species as well as from reactant-solvent interactions ("inner shell" and "outer shell" effects, respectively). In order to distinguish between these two contributions, we have chosen to do a systematic study of solvent effects upon the thermodynamics of redox couples involving substitutionally inert transition-metal ions. These redox couples in which the oxidized and reduced species are both stable in the solution phase have a general form of $\mathbf{M}^{\mathbf{III}}\mathbf{L}_{\mathbf{n}}/\mathbf{M}^{\mathbf{II}}\mathbf{L}_{\mathbf{n}}$ (where M = Ru, Co, Cr, Fe; L = amines, polypyridines, etc., and n = number of ligands) and involve in a single electron transfer reactions.

The general approach is to determine the formal potential E_f of each redox couple in a range of solvents having suitably different chemical and physical properties. In addition, the temperature dependence of E_f is monitored in each solvent using a nonisothermal cell arrangement, giving values of reaction entropies ΔS_{rc}^{o} for each redox couple. These measurements coupled with extrathermodynamic

methods such as the "ferrocene", and "tetraphenylarsonium-tetraphenylborate" assumptions yield estimates of the free energy and enthalpy of transferring the redox couple from water to other solvents.

B. RESULTS

Four groups of M(III)/(II) transition-metal redox couples were studied; the ferricinium/ferrocene redox couple, cationic redox couples containing polypyridine ligands, cationic redox couples containing ammine and ethylenediamine ligands, and anionic redox couples containing ethylenediaminetetraacetato ligands. Comparison between and within these groups will allow one to determine the effects of central metal ion, ligand, and charge upon the redox thermodynamic parameters as the solvent is varied.

1. Ferricinium-Ferrocene Redox Couple

The ferricinium/ferrocene (Fe(C₅H₅)⁺/Fe(C₅H₅), redox couple was selected in order (i) to be used as an internal reference electrode for estimation of $\Delta \phi_{l,j}^{S-W}$ and hence transfer free energies of other redox couples, and (ii) to find out the possible reasons for the suspected breakdown of the "ferrocene assumption" (see Chapter III). As was discussed in the previous Chapter, the evaluation of ΔS_{rc}° ($=\overline{S}_{red}^{\circ}$ - $\overline{S}_{ox}^{\circ}$) in a given solvent involves a much milder

extrathermodynamic assumption than for the corresponding free energy differences ($\overline{G}_{red}^{\circ}$ - $\overline{G}_{OX}^{\circ}$); the latter requires an absolute Galvani potential difference to be estimated, which is fraught with difficulties. Therefore values of ΔS_{rc}° for ferricinium/ferrocene (Fc⁺/Fc) in different solvent should provide valuable information regarding the extent of solvent interactions with this redox couple.

Formal potentials E_f of the Fc⁺/Fc couple were obtained by cyclic voltammetry using platinum and/or vitreous carbon indicator electrodes. Reversible or quasi-reversible behavior was typically obtained in all solvents studied here in that the separation between the anodic and cathodic voltammetric peaks was 60-80 mV with essentially equal peak currents. In most solvents, identical formal potentials were obtained for either anodic-cathodic voltammograms using dissolved ferrocene, or cathodic-anodic voltammograms using ferricinium picrate as the solute. Indeed, it was found that ferricinium is stable even in solvents of high basicity such as dimethylsulfoxide and dimethylformamide at temperatures up to 50°C for at least six hours, provided that the solutions were deaerated with nitrogen or argon and contained only weakly complexing anions such as perchlorate. These results are in contrast to earlier reports that ferricinium is rapidly decomposed in dimethylsulfoxide and dimethylformamide (83). ever, it was observed that ferricinium decomposes in

hexamethylphosphoramide even on the cyclic voltammetric time scale, as evidenced by reverse (cathodic-going) voltammetric peaks that were markedly smaller than the forward anodic peaks in this solvent using ferrocene as the solute. (Also, cyclic voltammetry of dissolved ferricintum in hexamethylphosphoramide yielded a wave only at a potential characteristic of the $\mathrm{Fe}^{3^+/2^+}$ couple in this solvent.) In water, ferricinium picrate was used as the solute on account of the limited solubility of ferrocene. No precipitation of electrogenerated ferrocene in the vicinity of the electrode appeared to occur during the period of the voltammetric scan in that cyclic voltammograms of reversible shape with equal anodic and cathodic peak currents were consistently obtained using ferricinium picrate concentrations in the range 2 x 10^{-4} to 10^{-3} $\underline{\mathrm{M}}$.

Table 3 summarizes values of ΔS_{rc}° for the Fc⁺/Fc couple, determined in different supporting electrolytes in nine solvents, along with the corresponding formal potentials measured at 25°C. In Table 4, values of ΔS_{rc}° for the Fc⁺/Fc couple measured in 0.1 M TEAP in various solvents are compared with the corresponding estimates of ΔS_{rc}° , $(\Delta S_{rc}^{\circ})_{Born}$, resulting from the dielectric-continuum Born model. The Born estimates of ΔS_{rc}° are given by (70)

$$(\Delta S_{rc}^{\circ})_{Born} = -\frac{e^{2}N}{2\epsilon T} (\frac{d \ln \epsilon}{d \ln T}) (\frac{Z_{ox}^{2}}{r_{ox}} - \frac{Z_{red}^{2}}{r_{red}})$$
 (1)

Reaction Entropies for Ferricinium-Ferrocene Couple in Various Solvents. Table 3.

			ASo b		
Solvent	Electrolyte	E _f a mV	Cal deg ⁻¹ mol ⁻ 1	Temp. Range °C	Working ^c Electrode
Water	$0.1 \overline{ ext{M}} ext{ L1C1O}_{ ext{d}}$	127	-5	3-40	
	0.1 <u>M</u> TEAP 0.1 <u>M</u> KPF ₆	125 ^d 133	-5	3-50	Pt
Formamide	0.1M Liclo,	281	0	4-56	
		245 ^d 269	0	91-11	O
N-Methylformamide	$0.1M \text{ L1ClO}_{4}$	397	ħ	94-5	
	$0.1M$ TEAP $0.5M$ Liclo _{μ}	334 ^d 374	7	5-50	O
Propylene Carbonate	$0.05M \text{ Liclo}_{\text{h}}$	345	. 10	4-56	
	0.1M Liclou	328	11	10-60	
	O.1M TEAP	363	11	5-55	Pt
	0.1M TEAP	270 ^a	11	4-50	
	$0.2M \text{ Liclo}_{\text{l}}$	308	10.5	5-55	

Table 3. Continued.

			Q %SV		
Solvent	Electrolyte	$\mathrm{E}_{\mathbf{f}}^{\mathbf{a}}$ mV	cal deg ⁻¹ . mol ⁻¹	Temp. Range °C	Working ^c Electrode
Acetonitrile	0.1M Liclo _{ll}	342	11	5-45	
		372	11.5	3-45	Pt
	O.1M TEAP	309 ^d	11.5	3-45	
Dimethylsulfoxide	0.025M Liclo ₄	456	13	20-45	
	$0.1M \text{ L1C1O}_{\text{ll}}$	439	12.5	19-55	
	O.1M TEAP	317 ^d	12.5	20-60	Pt
	$0.2 \overline{M} \text{ Liclo}_{f q}$	429	13	20-60	
	$0.5 \overline{ ext{M}}$ Liclo $_{ ext{h}}$	412			
Dimethylformamide	$0.025 \overline{\mathrm{M}}$ Liclo ₄	506	14	4-55	
	$0.05M \text{ Liclo}_{4}$	501	13.5	4-55	
	$0.1M \text{ Liclo}_{4}$	493	14	4-55	Pt
	0.1M TEAP	450	14	4-50	
	0.1M TEAP	363 <mark>q</mark>	13.5	2-50	
	$0.2M \text{ Liclo}_{4}$	473	13.5	4-55	
	$0.5M \text{ Liclo}_{4}$	425	•		

Table 3. Continued.

Solvent	Electrolyte	E _f a mV	ΔS_{rc}^{o} b cal deg ⁻¹ mol ⁻¹	Temp. Range	Working ^c Electrode
Nitromethane	$0.1 \overline{ ext{M}}$ Liclo $_{f \mu}$ 0.1 $\overline{ ext{M}}$ TEAP	147 ^d 270 ^d	14	4-4 <i>6</i> 50-50	Pt
Methanol	0.1M L1ClO ₄ 0.1M TEAP	356 346 ^d	m m	3-43 23-50	O

 $^{
m a}$ Reversible formal potential in mV vs. aqueous KSCE; determined at 25°C by cyclic voltammetry using nonisothermal cell arrangement "a" (see text) unless otherwise noted.

^bReaction of entropy of Fc⁺/Fc in listed solvents at 25°C; determined by using Equation (15) of Chapter III. Experimental precision estimated to be ±0.5-1 e.u., accuracy within 1-2 e.u. (see text).

 $^{\text{c}}$ Working (indicator) electrode; Pt = Platinum "flag" and C = glassy carbon.

dPotentials quoted versus aqueous s.c.e. (filled with saturated NaCl) using cell:

NaSCE(aq)|0.1M TEAP(aq)||0.1M TEAP(solvent)|Pt or C.

Table 4. $\Delta S_{rc}^{\circ} (= \overline{S}_{Fc}^{\circ} - \overline{S}_{Fc}^{\circ} +)$ for the Ferricinium-Ferrocene Redox Couple in Various Solvents. Comparison with Predictions from Born Model.

Solvent	ΔS° a rc Cal deg ^{-l} mol ^{-l}	(AS°c)Born Cal deg-1 mol-1
Water	- 5	2.5
Formamide	0	1.3
Methanol	3	6.4
N-Methylformamide	4	2.0
Propylene Carbonate	11	2.6
Acetonitrile	11.5	4.9
Dimethylsulfoxide	12.5	3.3
Dimethylformamide	14	5.7
Nitromethane	14	5.0

^aReaction entropy of Fc⁺/Fc in listed solvent at 25°C; obtained from temperature dependence of E_f using nonisothermal cell arrangement "b" (see text). Experimental precision ca. ± 0.5 -1 e.u.

bValue of ΔS_{rc}° at 25°C predicted from the Born model; calculated from Equation (2) using dielectric constant data listed in Table 5.

(For definition of the terms used in Equation (1), see Equation (18) of Chapter III). According to the Born model, the reaction entropy for the Fc⁺/Fc couple is $\Delta S_{rc}^{o} = -\overline{S}_{Fc}^{o}+$; therefore the simpler form of Equation (1) can be employed

$$(\Delta S_{rc}^{\circ})_{Born} = -\frac{1}{r} \frac{e^{2}N}{2\epsilon T} (\frac{d \ln \epsilon}{d \ln T})$$
 (2)

in which r is the radius of the ferricinium cation, taken as 3.8 Å (84).. Values of $dln_{\epsilon}/dlnT$ and literature sources for them are given in Table 5.

2. Couples Containing Polypyridine Ligands

Formal potentials and reaction entropies for Fe(bpy) $_3^{3+/2+}$, $Cr(bpy)_3^{3+/2+}$, $Co(bpy)_3^{3+/2+}$, and $Co(phen)_3^{3+/2+}$ (where bpy = 2,2'-bipyridine, and phen = 1,10-phenanthroline) were determined in various solvents. In addition, estimates of free energies of transfer $\Delta(\Delta G_{rc}^{\circ})^{s-w}$, enthalpies of transfer $\Delta(\Delta H_{rc}^{\circ})^{s-w}$, and entropies of transfer $\Delta(\Delta S_{rc}^{\circ})^{s-w}$ for the above redox couples when transferred from water to seven nonaqueous solvents were determined. These redox couples were selected for several reasons. The polypyridine ligands should provide an "insulating shield" around the central metal cation, and are not expected to interact strongly with the solvent so that the dielectric continuum treatments may provide a reasonable description of the

Table 5. Temperature Derivatives of Dielectric Constants for Various Solvents.

Solvent	a e	- dlne dlnT	$-\frac{e^2N}{2\epsilon T}\left(\frac{dln\epsilon}{dlnT}\right)^b$
Water	78.5	1.36 ^c	9.65
Formamide	108.7	0.98 ^d	5.02
N-Methylformamide	182	2.5 ^d	7.65
Propylene Carbonate	64.9	1.14 ^g	9.80
Acetonitrile	36.0	1.2 ^f	18.56
Dimethylsulfoxide	46.7	1.04 ^f	12.43
Dimethylformamide	36.7	1.43 ^d	21.70
Methanol	32.6	1.43 ^e	24.38
Nitromethane	36	1.23 ^h	19.01

^aDielectric constant at 25°C.

^bConstant term in Equations (1) and (2) for a given solvent calculated for $T = 25^{\circ}C$.

^cReference 70.

dS. J. Bass, W. I. Nathan, R. M. Meighan, R. H. Cole, J. Phys. Chem. 68, 509 (1964).

ep. G. Sears, R. R. Holmes, L. R. Dawson, J. Electrochem. Soc. 102, 145 (1955).

fG. J. Janz, R. P. T. Tomkins, "Nonaqueous Electrolyte Handbook", Vol. I., Academic Press, N. Y., 1972.

gR. Payne, I. E. Theodorou, J. Phys. Chem. 76, 2892 (1972).

hc. P. Smyth, W. S. Walls, J. Chem. Phys. 3, 557 (1935).

solute-solvent interactions. Indeed, these couples have been widely employed as inert outer-sphere reagents for homogeneous redox kinetics in aqueous media, and are anticipated to provide valuable model systems for investigating outer-shell solvent effects upon electrochemical as well as homogeneous electron transfer rates. Some measurements of the solvent dependence of E_f for $Fe(phen)_3^{3+/2+}$ and related couples (82) suggested that $\Delta(\Delta G_{rc}^{\circ})^{s_1-s_2}$ may be quite small for such systems. It is therefore of interest to ascertain if such behavior, if confirmed for the other couples, is found for the structurally more sensitive entropic component $\Delta(\Delta S_{rc}^{\circ})^{s_{1}-s_{2}}$, and also to test the ability of the conventional dielectric continuum treatments to predict the magnitudes of these thermodynamic quantities. The comparison between $Fe(bpy)_3^{3+/2+}$, $Cr(bpy)_3^{3+/2+}$, and $Co(bpy)_3^{3+/2+}$ is of particular interest for exploring the influence of the electronic structure of the metal center upon the redox thermodynamics. Thus the iron and chromium couples involve electron transfer into a t_{2g} orbital (28), so that the charge should be extensively delocalized around the bipyridine rings via back bonding with the empty π -orbitals on the ligand (85). The cobalt couple involves the transition $t_{2g}^6 \rightarrow t_{2g}^5 e_g^2$ (28) so that the added electron will be localized at the metal center and the cobaltnitrogen bond distances will be substantially increased in the lower oxidation state (85). Markedly larger values

of ΔS_{rc}° have been seen in aqueous media for $Co(bpy)_3^{3+/2+}$ and $Co(phen)_3^{3+/2+}$ (both 22 e.u. for ionic strength μ = 0.05 M) (21) compared with those for the low spin couples $Fe(bpy)_3^{3+/2+}$, $Fe(phen)_3^{3+/2+}$, and $Ru(bpy)_3^{3+/2+}$ (2, 3, and 1 e.u., respectively, for μ = 0.05 - 0.1 M (21,24)); these effects have been attributed to differences in the extent of orientation of water molecules in the vicinity of the polypyridine rings (21,24). It is therefore of interest to find out if such electronic structural effects upon ΔS_{rc}° are obtained in other solvents.

Table 6 summarizes the formal potentials $\mathbf{E}_{\mathbf{f}}$ obtained for the polypyridine redox couples in each solvent at 25°C quoted relative to the corresponding values of $\mathbf{E}_{\mathbf{f}}$ for ferricinium/ferrocene (Fc⁺/Fc), [i.e., $E_f^{Fc} = E_f$ (redox couple) $\underline{\text{vs.}}$ s.c.e. - $E_f(Fc^+/Fc)$ $\underline{\text{vs.}}$ s.c.e.], along with corresponding reaction entropies $\Delta S_{\mathbf{rc}}^{\circ}$. The formal potentials for each redox couple were obtained using either the oxidized or the reduced form of the reactant in the bulk solution as convenient, usually at a concentration of 1 mM. Reversible or quasi-reversible behavior was normally obtained in that the cathodic-anodic peak separations were typically 60-80 mV. About 25 mM of bipyridine or phenanthroline was added (as appropriate) in order to inhibit dissociation of the reduced complexes in solution. The absence of significant dissociation was confirmed from the equality of the anodic and cathodic peak currents and the lack of a

Formal Potentials and Reaction Entropies for M(III)/(II) Polypyridine Redox Couples in Various Solvents. Table 6.

		Co(pher	Co(phen) ^{3+/2+}	Co(bpy) ₃	3+/2+	Fe(bpy	Fe(bpy) ₂ $\frac{3+/2+}{2}$	$(cr(bpy)_{2}^{3+/2+}$	3+/2+	+ 54	
Solvent	Electrolyte	Frca f	ΔSO b	a or I		E P P P P P P P P P P P P P P P P P P P	ASO b	a or I	ASO b	E C	(AS ^o) d re Born
Water	0.1M Liclo	18	22	-57	22	718	2	-607	4	127	7.1
Formamide	0.1M Liclo	-35	28	-86	28	₽Đ	fJ	-627	14	281	3.7
N-Methyl- formamide	0.1M Liclo	-72	34	-127	37.5	po	ę,	-675	19	397	5.6
Propylene Carbonate	$0.1\overline{M}$ Liclo	-22	43	-92	97	657	25	-648	27	328	7.2
	0.2M Liclo			-90	45	859	56			308	
Aceto- nitrile	0.1M Liclo	-15	75	-72	43	670	23	-650	29	342	13.7
Dimethyl- sulfoxide	0.1M Lic10,	-105	47.5	ų	ч	po	f.	069-	4 1	439	9.1
	$0.2\overline{M}$ Liclo	-104	46.5	ਖ	h	₽Ū	f			429	
Dimethyl-	O.05M Liclo	-81	67	ਖ	ч	620	75			501	15.9
formamide	0.1M Liclo	-85	48.5	ч	ų	624	41.5	<i>-</i> 697	34	493	
	0.2M L1C10	-82	47	ч	h					473	
Nitrc- methane	0.1M Liclo	43	57.5	-22	96	727	75	009-	32	147 ^e	14.0

Table 6. Continued.

 $^{
m a}$ Formal potential for redox couple in solvent given in far left column, quoted in mV vs. $^{
m E}_{
m f}$ for ferricinium/ferrocene couple in same electrolyte ($E_{\rm f}^{\rm Fc}$ = $E_{\rm f}$ (redox couple) - $E_{\rm f}({\rm Fc}^{\dagger}/{\rm Fc})$). Obtained using cyclic voltammetry (see text).

 $^{\mathrm{b}}_{\mathrm{Reaction}}$ entropy of redox couple in listed solvent obtained from temperature dependence of $\mathrm{E_{f}}$ using nonisothermal cell arrangement a (see text for details). Units are cal. deg⁻¹ mol⁻¹.

^CFormal potential for ferricinium-ferrocene couple in each electrolyte, mV vs. KSCE immersed in same electrolyte unless otherwise noted. desction entropy for $M(bpy)_3^{3+/2+}$ couples (cal. deg⁻¹ mol⁻¹) calculated from the Born model for each solvent (Equation (1)) using the radius r = 6.8 A and constant values for each solvent listed in Table 5.

eusing cell arrangement s.c.e. $|0.1\underline{M}$ LiCl $0_4(aq)||0.1\underline{M}$ LiCl $0_4(solvent)|$ Pt, C, or Hg.

ferratic voltammetric behavior precluded measurement of $\Delta S^{O}_{r_G}$.

<code>gelectrooxidation</code> of background precluded determination of $\mathbf{E}_{oldsymbol{ extsf{f}}}.$

 $^{
m h}$ Highly irreversible behavior (cathodic-anodic peak separation $_{
m >}$ (120 mV) precluded determination of $^{
m E}_{
m f}$ and

dependence of E_f upon the added ligand concentration. The derived values of E_f were usually reproducible to within 1-2 mV. [As mentioned before (Equation (14) of Chapter III) the actual values of E_f will generally differ slightly from the experimental estimates due to the inequality of the diffusion coefficients for the oxidized and reduced species. However, this difference is generally small (2-3 mV) and, most importantly, is similar for all the systems studied here so that it generally cancels when differences in E_f are considered, as in the present work.] For some systems, particularly with $Co(bpy)_3^{3+/2+}$, larger peak separations (90-100 mV) were obtained, presumably resulting from slow electrode kinetics so that the derived values of E_f were known only approximately (±5-10 mV) under these circumstances.

Listed in Table 7 are estimates of the change in $(\overline{G}_{red}^o - \overline{G}_{OX}^o)$ for the polypyridine redox couples resulting from substituting the various nonaqueous solvents for water, $\Delta(\Delta G_{rc}^o)^{s-w}$, obtained from the corresponding values of $(\Delta E_f^{Fc})^{s-w}$ using Equation (3).

$$\Delta(\Delta G_{rc}^{\circ})^{s-w} = -F_{\Delta}(E_{f}^{Fc})^{s-w} + \Delta(\Delta G_{rc}^{\circ})_{Fc}^{s-w}$$
(3)

(See Equation (8) of Chapter III for details.)

The appropriate values of $\Delta(E_{\mathbf{f}}^{\mathrm{Fc}})^{\mathbf{s-w}}$ were obtained from the

Free Energies, Enthalpies, and Entropies of Transfer of M(III)/(II) Poly pyridine Redox Couples from Water to Various Solvents, Calculated from Data in Table 6. (Free Energies and Enthalpies in Kcal.mol-1; Entropies in cal.deg-1 mol-1.) Table 7.

	Cr (1	Cr (bpy)3+/2+	2+	Fe (Fe(bpy)3+/2+	+7	q) 00	Co(bpy)3+/2+	+
Solvent	А	В	C	А	В	ນ	А	В	C
Formam1de	(0.5)	2.0	10				(0.6)	2.7	9
N-Methylformamide	(1.6) -0.4	4.1	15				(1.6)	4.3	15.5
Propylene Carbonate	(1.0)	5.9	23	(1.4) -0.6	6.3	23	(0.8)	0.9	24
Acetonitrile	(0.6)	9.4	25	(1.1) -2.4	3.9	21	(0.3)	3.1	21
Dimethylsulfoxide	(1.9)								
Dimethylformamide	(2.0)	8.0	30	(2.4)	11.2	39.5			
Nitromethane	(-0.2) -1.7	6.7	28	(-0.2) -1.7	10.3	40	(0.8)	7.9	34

Table 7. Continued.

		Co(phen)3+/2+		Fc ⁺ /Fc*
Solvent	А	В	೮	$-\Delta(\Delta G_{\Gamma C}^{o})_{FC}^{S-W}$
Formamide	(1.2)	2.0	9	1.5
N-Methylformamide	(2.1)	3.7	12	2.0
Propylene Carbonate	(0.9)	5.2	21	2.0
Acetonitrile	(0.8)	3.3	20	3.5
Dimethylsulfoxide	(2.8) 0.3	7.9	25.5	2.5
Dimethylformamide	(2.4)	7.0	26.5	3.0
Nitromethane	(-0.6)	8.5	35.5	1.5

Table 7. Continued.

aqueous solvent listed. Obtained from formal potentials $\mathrm{E}_{m{ au}}^{\mathrm{HC}}$ for each redox couple versus ing that $\Delta(\Delta G_{rc}^{o})_{Fc}^{S-W}=0$ (i.e., using ferrocene assumption); lower values obtained using estimates of $\Delta(\Delta G_{rc}^{o})_{Fc}^{S-W}$ given in far right-hand column (i.e., using TATB assump-A = Free energy of transfer of redox couple $\Delta(\Delta G_{p,c}^o)^{S-W}$ (kcal.mol⁻¹) from water to non- $^+$ /Fc given in Table 6 using Equation (3). Values in parentheses obtained by assumtion - see text).

aqueous solvent listed. Obtained from corresponding free energies (TATB scale) and entropies of transfer using $\Delta(\Delta H_{rc}^o)^{S-W} = \Delta(\Delta G_{rc}^o)^{S-W} + T\Delta(\Delta S_{rc}^o)^{S-W}$. B = Enthalpy of transfer of redox couple $\Delta(\Delta H_{rc}^{o})^{S-W}$ (Kcal.mol⁻¹) from water to nonC = Entropy of Transfer of redox couple $\Delta(\Delta S_{rc}^{o})^{S-W}$ (cal.deg⁻¹ mol⁻¹) from water to nonaqueous solvent listed. Obtained from differences between appropriate values of ΔS_{rc}° listed for each solvent (in 0.1 M LiClO $_{\mu}$) in Table 6.

and TATB assumptions. ΔG_{t}^2 data for most solvents taken from compilation in Table 12.VI of Reference 48; for nitromethane taken from Reference (83); value given for N-methylfrom water to nonaqueous solvent listed. Obtained from difference in apparent values of transfer free energy ΔG_{t}^{o} of ΔG_{t}^{o} o * Estimates of free energy of transfer for ferricinium-ferrocene couple (Kcal.mol $^{-1}$) formamide is estimated. Most values of $\Lambda(\Lambda G_{
m rc}^{
m o})_{
m Fc}^{
m S-W}$ quoted are probably accurate to within ca. ±1 Kcal.mol⁻¹ formal potential listed in Table 6, and inserted into Equation (3) along with the corresponding estimates of $\Delta(\Delta G_{rc}^{\circ})_{Fc}^{s-w}$. (The estimates of $\Delta(\Delta G_{rc}^{\circ})_{Fc}^{s-w}$ are also listed in Table 7.) Values of $\Delta(\Delta G_{rc}^{\circ})_{Fc}^{s-w}$ obtained by assuming that $\Delta(\Delta G_{rc}^{\circ})_{Fc}^{s-w} = 0$, i.e., by using the ferrocene rather than the TATB assumption, are listed in parentheses in Table 7.

The corresponding variations in ΔS_{rc}^{o} when changing from water to other solvents, $\Delta (\Delta S_{rc}^{o})^{s-w}$, were obtained directly from the values of ΔS_{rc}^{o} given in Table 6 and are also listed in Table 7. The corresponding enthalpies of transfer $\Delta (\Delta H_{rc}^{o})^{s-w}$ that are also given in Table 7 were obtained from the relation

$$\Delta(\Delta H_{rc}^{\circ})^{s-w} = \Delta(\Delta G_{rc}^{\circ})^{s-w} + T_{\Delta}(\Delta S_{rc}^{\circ})^{s-w}$$
(4)

As shown in Table 6, the values of ΔS_{rc}° were found to be essentially independent of ionic strength (1 e.u.). Also, the variations in E_f with ionic strength for the M(III)/(II) polypyridine couples were found to be approximately the same. (within 2-3 mV) as those for the Fc⁺/Fc couple; consequently the derived values of $\Delta (\Delta G_{rc}^{\circ})^{S-W}$ listed in Table 7 are essentially independent of the electrolyte concentration, at least on the ferrocene scale.

3. Couples Containing Ammine and Ethylenediamine Ligands

Formal potentials and reaction entropies for couples containing ammine and ethylenediamine ligands were eval-These systems were selected in order to explore the possibility that specific ligand-solvent interactions . could play an important role in determining the redox thermodynamics. These redox couples are substitutionally inert and can be prepared as anhydrous crystalline solids that are stable and structurally well defined. Couples containing these ligands are considerably smaller and more polar than the polypyridines, containing relatively acidic amine hydrogens which might be expected to interact specifically with surrounding solvent molecules, especially those having strong electron donating capability. Previous study of solvent effects on the formal potential for the $Co(en)_3^{3+/2+}$ couple (en = ethylenediamine) has shown that $\mathbf{E}_{\mathbf{f}}$ becomes markedly more negative with increasing basicity of the solvent as measured by the socalled "Donor Number" (81).

As for the M(III)/(II) polypyridine couples, it is also of interest to compare the behavior of amine and ethylenediamine redox couples having the same charge type and ligand composition, but differing in the electronic state of the central metal cation. The comparison between the behavior of $\text{Co(en)}_3^{3+/2+}$, $\text{Ru(en)}_3^{3+/2+}$, and $\text{Ru(NH}_3)_6^{3+/2+}$ is of particular interest since as mentioned before the reduction

of Co(III) involves the electronic conversion $t_{2g}^6 + t_{2g}^5 e_g^2$, whereas the reduction of Ru(III) involves the transformation $t_{2g}^5 + t_{2g}^6$; these differences are reflected in a markedly greater expansion of the cobalt center upon reduction (86). Also comparison of the capped trisethylenediamine ("sepulchrate") couple $Co(sep)^{3+/2+}$ (70,105) with the trisethylenediamine and hexammine couples should be interesting since the former is structurally rigid (45,87) and contains only one hydrogen coordinated to each amine nitrogen, compared to two and three hydrogens, respectively, for the latter two couples.

Table 8 summarizes the formal potentials, E_f obtained for $Ru(NH_3)_6^{3+/2+}$, $Ru(en)_3^{3+/2+}$, $Co(en)_3^{3+/2+}$, $Co(sep)_3^{3+/2+}$, and $Ru(NH_3)_5NCS_6^{2+/+}$ in 0.1~M LiClO $_4$ in each solvent at 25°C quoted relative to E_f for the ferricinium/ferrocene (Fc $^+$ /Fc) couple in the same solution [i.e., E_f^{Fc}] = E_f (redox couple) vs. s.c.e. - E_f (Fc $^+$ /Fc) vs. s.c.e.], along with the corresponding reaction entropies ΔS_{rc}° . $Ru(NH_3)_6^{3+/2+}$, $Ru(en)_3^{3+/2+}$, $Ru(NH_3)_5NCS_6^{2+/+}$, and $Co(sep)_3^{3+/2+}$ all gave essentially reversible behavior (peak separations 60-70 mV) as expected from the substitution inertness of both oxidation states and the rapidity of their electron exchange. Since $Co(en)_3^{2+}$ is substitutionally labile, this species can dissociate in the absence of added ligand (especially in aqueous solution). However, it was found that only small concentrations of ethylenediamine (2-10 mM)

Formal Potentials and Reaction Entropies for M(III)/(II) Amine and Ethylenediamine Redox Couples in Various Solvents. Table 8.

		Ru(NH ₃) ^{3+/2+}		Ru(en	Ru(en)3+/2+	Co(en)3+/2+	3+/2+
Solvent	(ASrc)Born	E.F.ca	ے م	$_{ m f}^{ m Fc}$ a	ΔS° b	${ m E}_{ m f}^{ m Fc}$	ΔS_{rc}^{o} b
Water	14.0	-305	19	-187	13	-587	37
Formamide	7.2	-553	29	₽0	മ	-813	42
N-methylformamide	13.4	-707	33	£C	ಬ	-945	917
Propylene Carbonate	14.0	-373 ^h	$_{41}^{ m h}$	೯೮	മ	-633 ¹	501
Acetonitrile	26.5	4 -1	J	ᠳ	ÇĮ	-589 ¹	471
Dimethylsulfoxide	17.8	-781 ^h	4 ⁰ ħ	-594	33	-1039	52
Dimethylformamide	31.0	-739 ^h	49ħ	-596	36	-970 ¹	511
Nitromethane	27.1	f	Ĵ	¢٦	J	-4881	451

Table 8. Continued.

	Go(sen) 3+/2+	2+	B11 (NH) NGG 2+/+	NGG2+/+	+
Solvent	F. B. B. B. F. S. F. F. S. F. F. S. F. S. F. S. F. S. F. S. F. F. F. S. F. F. F. S. F.	ASo b	Fr a Ef	AS° b	Fc /Fc E _f c
Water	-667	19	-265	15	127
Formamide	-897	34	-491	19	281
N-Methylformamide	966-	0 17	-670	25	397
Propylene Carbonate	-888	48	-441	34	328
Acetonitrile	6 -1	4	ಟ	₽0	342
Dimethylsulfoxide -	-1112	7 17	-719	56	439
Dimethylformamide	ಶು	5 0	-750	33	493
Nitromethane	£	f	f	f	147 ^e

Table 8. Continued.

LiClO4 as supporting electrolyte unless otherwise noted; quoted in mV. versus ferricin- $^{
m a}$ Formal potential for redox couple in solvent given in far left column, using 0.1 M Obtained using cyclic voltammetry (see jum/ferrocene couple in same electrolyte.

^bReaction entropy of redox couple in listed solvent obtained from temperature dependence a and b; units are cal. deg-1 mol-1 of $\mathbf{E}_{\mathbf{f}}$ using nonisothermal cell arrangement

^cFormal potential for ferricinium-ferrocene couple in 0.1 \underline{M} LiClO $_{f q}$, mV. versus s.c.e. immersed in same electrolyte unless otherwise noted. dReaction entropy calculated from the Born model for each solvent (Equation (1)) using radius r=3.5 Å (appropriate for the small amine couples (73)) and the appropriate dielectric constant data (11sted in Table 5); units are cal. deg⁻¹ mol⁻¹.

eusing cell arrangement s.c.e. $|0.1\underline{\mathrm{M}}|$ LiClO $_{\mathrm{H}}(\mathrm{aq})||0.1\underline{\mathrm{M}}|$ LiClO $_{\mathrm{H}}(\mathrm{solvent})|$ Pt, C, Hg.

 $^{
m f}$ Insolubility precluded measurement of ${
m E}_{
m f}$.

 $^{
m g}{
m Erratic}$ voltammetric behavior precluded measurement of ${
m E_{
m f}}.$

hobtained in 25 mM Liclo $_{\mu}$.

 $^1\mathrm{Obtained}$ in 0.1 $\underline{\mathtt{M}}$ tetraethylammonium perchlorate.

were required in order to prevent the dissociation of $\operatorname{Co(en)}_3^{2+}$ produced in the cathodic segment of the cyclic voltammogram, since equal cathodic and anodic peak currents were then obtained together with peak potential separations that were typically in the range ca. 60-90 mV. Measurements of E_f values for $\operatorname{Ru}(\operatorname{NH}_3)_6^{3+/2+}$, $\operatorname{Ru}(\operatorname{en})_3^{3+/2+}$, $\operatorname{Ru}(\operatorname{NH}_3)_5^{5}\operatorname{NCS}^{2+/+}$, and $\operatorname{Co(sep)}^{3+/2+}$ in acetonitrile and nitromethane were precluded by solubility restrictions; in addition, $\operatorname{Ru}(\operatorname{en})_3^{3+/2+}$ yielded irreproducible and illdefined cyclic voltammograms in several solvents which restricted further the useful data that could be obtained for this couple.

Estimates of the change in $(\overline{G}_{red}^{\circ} - \overline{G}_{ox}^{\circ})$ for amine redox couples resulting from substituting the various nonaqueous solvents for water, $\Delta(\Delta G_{rc}^{\circ})^{S-W}$, were obtained from Equation (3) and are listed in Table 9. (These estimates are obtained using similar treatments employed for polypyridne M(III)/(II) couples.)

The corresponding variations in ΔS_{rc}° for a given amine redox couple, $\Delta(\Delta S_{rc}^{\circ})^{S-W}$, were obtained directly from the differences between the appropriate values of ΔS_{rc}° given in Table 8, and are also listed in Table 9 along with the corresponding enthalpies of transfer $\Delta(\Delta H_{rc}^{\circ})^{S-W}$ that were obtained from Equation (4).

The values of the formal potentials E_f relative to Fc^+/Fc for all five amine couples were typically found to be

Free Energies (A), Enthalpies (B), and Entropies (C), of Transfer of M(III)/(II) Amine and Ethylenediamine Redox Couples from Water to Various Solvents, Calculated from Data in Table 8 (Free Energies and Enthalpies in Kcal.mol-1; Entropies in cal.deg-1 mol-1). 6 Table

	Ru (N	Ru(NH ₃) ^{3+/2+}	+	Ru (e	Ru(en)3+/2+	+) o)	Co(en)3+/2+	
Solvent	A	В	၁	А	В	ນ	А	В	O
Formam1de	(5.7) 4.2	7.2	10				(5.2)	5.5	5
N-Methylformamide	(9.3)	11.5	14				(8.3)	0.6	6
Propylene Carbonate	(1.6) -0.4	6.2	22				(1.1) -0.9	3.0	13
Acetonitrile							(0.0)	-0.5	10
Dimethylsulfoxide	(11.0) 8.5	14.8	21	(6.4)	12.9	20	(10.4) 7.9	12.4	15
Dimethylformamide	(10.0) 7.0	15.1	27	(6.4)	13.3	23	(8.8)	10.0	14
Nitromethane							(-2.3) -3.8	-1.4	ω

Table 9. Continued.

	000	Co(sep)3+/2+	+	Ru (NH	Ru(NH ₂) ₅ NCS ^{2+/+}	+	
Solvent	A .	В	ວ	A	В	ರ	A(AG°)S-W
Formamide	(5.3)	8.3	15	(5.4) 3.9	5.1	ħ	0.85
N-Methylformamide	(7.6) 5.6	11.9	21	(9.5)	10.5	10	1.7
Propylene Carbonate	(5.1)	11.8	59	(4.2) 2.2	7.9	19	9.0-
Acetonitrile							-3.2
Dimethylsulfoxide	(10.3)	15.3	25	(10.6)	11.4	11	-2.0
Dimethylformamide				(11.4) 8.4	13.8	18	-3.4
Nitromethane							-3.4

Table 9. Continued.

assuming that $\Delta(\Delta G_{rc}^o)_{Fc}^{s-w}=0$ (1.e., using ferrocene assumption); lower values obtained using estimates of $\Delta(\Delta G_{rc}^o)_{Fc}^{s-w}$ given in Table 7 (1.e., using TATB assumption - see text). A = Free energy of transfer of redox couple $\Delta(\Delta G_{rc}^o)^{S-W}$ (Kcal.mol⁻¹) from water to nonversus Fc $^+/$ Fc given in Table 8 using Equation (3). Values in parentheses obtained by aqueous solvent listed. Obtained from formal potentials $\mathbf{E}_{\mathbf{f}}^{\mathbf{FC}}$ for each redox couple

aqueous solvent listed. Obtained from corresponding free energies (TATB scale) and B = Enthalpy of transfer of redox couple $\Delta(\Delta H_{rc}^o)^{S-W}$ (Kcal.mol⁻¹) from water to nonentropies of transfer using $\Delta(\Delta H_{rc}^{o})^{S-W} = \Delta(\Delta G_{rc}^{o})^{S-W} + T\Delta(\Delta S_{rc}^{o})^{S-W}$.

C = Entropy of transfer of redox couple $\Delta(\Delta S_{rc}^{o})^{S-W}$ (cal. $\deg^{-1} \mod^{-1}$) from water to nonaqueous solvent listed. Obtained from differences between appropriate values of ΔS_{rc}° listed for each solvent in Table 8. *Free energy of transfer of redox couple (Kcal.mol $^{-1}$) calculated from the Born model for each solvent (Equation (6)) using radius r = 3.5 Å (appropriate for the small amine couples) and the appropriate dielectric constant data listed in Table 2. approximately independent (within 5 mV or so) of the ionic strength μ in the range μ = 0.025 - 0.2 \underline{M} (Table 10). The values of $\Delta S_{\mathbf{rc}}^{\mathbf{o}}$ were also found to be essentially independent (±1 e.u.) of ionic strength within this range (Table 10).

4. Anionic Redox Couples

Formal potentials and reaction entropies for two anionic redox couples, $Co(EDTA)^{-/2-}$ and $Fe(EDTA)^{-/2-}$ (where EDTA = ethylenediaminetetraacetato) were evaluated. These complex anions were selected in order to investigate the solvent-dependent behavior of redox couples containing net negative charges and to compare them with cationic redox couples. These redox couples are substitutionally inert; also the EDTA ligand in $Co(EDTA)^{-/2-}$ has been shown to be hexadentate in both oxidation states (88). Some measurements of the solvent dependence of E_f for anionic redox couples such as $Fe(CN)_6^{3-/4-}$ and $Mn(CN)_6^{3-/4-}$ suggested that E_f becomes more positive with increasing electron accepting properties of the solvent (89-92), as measured by the so-called "Acceptor Number" (81).

In Table 11 are summarized the formal potentials obtained for $\text{Co}(\text{EDTA})^{-/2-}$ and $\text{Fe}(\text{EDTA})^{-/2-}$ in 0.1 M LiClO $_4$ in each solvent at 25°C quoted vs both KSCE, E_f , and Fc^+/Fc redox couple, E_f^{Fc} , along with the corresponding values of $\Delta \text{S}_{\text{rc}}^{\circ}$. Both anionic redox couples gave essentially reversible

Formal Potentials and Reaction Entropies for M(III)/(II) Amine and Ethylenediamine Redox Couples in Different Ionic Strength. Table 10.

		Ru(NH ₃)	Ru(NH ₃) ₅ NCS ^{2+/+}	Ru(en	$Ru(en)^{3+/2+}_{3}$	Ru(NH,	3)3+/2+	$\cos(\text{en})^{3+/2+}$		Co(sep) ³⁺ /2+
Solvent	Electrolyte	E ^{FC} B	$\Delta S_{\mathbf{rc}}^{\mathbf{o}}$	ь Г.	F ^{rca} Asob	F. Ca	$\mathbf{F_f^{Fc^a}}$ $\Delta \mathbf{S_{rc}^{O}}$	Erca ASob		$\mathbf{F_f^{Fc}}^{\mathbf{a}}$ $\Delta_{\mathbf{S^o}}^{\mathbf{b}}$
DMF	0.025M LiClO ₄ -745	-745	33			-739 . 46	. 46		₽Đ	ы
	0.05M Liclo,	-747	35	-600 34	34	-743	45		₽Đ	ත
	O.1M Liclo,	-750	33	-596 36	36				മ	മ
	$0.2M \text{ Liclo}_{2}^{\prime}$	-751	34						рŋ	рυ
DWSO	0.025M Liclo	-723	25			-781	39			
	0.05M Liclo ₂	-721				-778	70			
	O.1M Liclo,	-719	56	-594 33	33			-1039 52	-1112	77
	$0.2M \text{ Liclo}_{2}^{1}$							-1036 51		
PC	$0.1M \text{ LiClO}_4$	-441	34	p 0	93	t	J		-888 48	48
	0.2M Liclo			рņ	рŋ	çı	4 1		-885 48	48

See notes for Table 8 for explanation of a, b, f and g.

Formal Potentials and Reaction Entropies for Fe(EDTA) $^{-/2}$ and Co(EDTA) $^{-/2}$ -Redox Couples in Various Solvents. Table 11

	Fe	Fe(EDTA)-/2-			Co(EDTA)-/2-	
Solvent	Ef	E ^{Fc} a	ΔS° c	Е ^р	EFca f	ΔS° C
н ₂ о	-132 ^g	-250	-3.5	119	- 12	- 7.5
Methanol	-191	-547	7.5	95	-300	15
Formam1de	-235	-516	ı	f.	6 -4	£
N-Methylformamide	-261	-658	2	÷,	G 1	J.
Propylene Carbonate	р	ರ	þ	Φ	Φ	Φ
Acetonitrile	р	ಥ	р	-350	-695	41
Dimethylsulfoxide	-527	996-	6	Ą	4	f)
Dimethylformamide	-483	916-	7	£,	Çų	Ţ

^aFormal potential for redox couple in given solvent, using $0.1 \frac{M}{M}$ LiClO $_{\psi}$ as supporting electrolyte; quoted in mV vs Fc⁺/Fc couple in same electrolyte. Obtained with HMDE using cyclic voltammetry.

^bFormal potential, quoted in mV <u>vs</u> saturated calomel reference electrode (KSCE), using cell arrangement "a" (see text).

Table 11. Continued.

^cReaction entropy of redox couple in listed solvent obtained from temperature dependence of $\rm E_f$ using nonisothermal cell a, units are cal. $\rm deg^{-1}\ mol^{-1}$.

 $^d\mathrm{Insolubility}$ precluded measurements of E_f and $^{\Delta\mathrm{S}^o}_{rc}$.

 $^{
m e}$ Erratic voltammetric behavior precluded measurements of $^{
m E}_{
m f}$ and $^{
m AS^o}$.

 $^f\text{Totally}$ irreversible behavior precluded determination of E_f and $\Delta \text{S}^{\text{o}}_{\text{rc}}$.

 $g_{\rm pH}$ of the solution = 2.7.

 h pH of the solution = 4.3.

behavior with peak separations of 60 - 70 mV. Measurements of $E_{\rm f}$ for Fe(EDTA)^{-/2-} in acetonitrile and propylene carbonate were precluded by solubility restrictions; in adtition, ${\rm Co(EDTA)}^{-/2-}$ gave ill-defined and totally irreversible cyclic voltammograms in several solvents.

Estimates of $\Delta(\Delta G_{rc}^{\circ})^{s-w}$ for $Co(EDTA)^{-/2-}$ and $Fe(EDTA)^{-/2-}$ were obtained from Equation (3) and are listed in Table 12. The corresponding variations in ΔS_{rc}° , $\Delta(\Delta S_{rc}^{\circ})^{s-w}$, along with the enthalpies of transfer $\Delta(\Delta H_{rc}^{\circ})^{s-w}$ for the two anionic redox couples are also listed in Table 12.

C. DISCUSSION

1. Ferricinium-Ferrocene Couple

The results presented in Table 4 for Fc^+/Fc redox couple indicate that in contrast to the Born estimates $(\Delta S_{rc}^{\circ})_{Born}$, which are uniformly small and positive (1-6 e.u.), the experimental reaction entropies increase markedly from a small negative value in water (-5 e.u.) to substantial positive values (11-14 e.u.) in several dipolar aprotic solvents. These results clearly indicate that there are significant differences in the nature and extent of solvent polarization between ferricinium and ferrocene that are sensitive to the microscopic solvent structure.

It was noted in Chapter IV, that the decreases in $\overline{S_+^\circ}$ found for the transfer of a given cation from water to other solvents have been found by Criss and Salomon

Data in Table 11 (Free Energies and Enthalpies in Kcal.mol⁻¹; Entropies in Free Energies, Enthalpies, and Entropies of Transfer of Fc(EDTA) $^{-/2}$ and Co(EDTA) $^{-/2}$ Redox Couples from Water to Various Solvents Calculated from cal. $deg^{-1} mol^{-1}$). Table 12.

		Fe(EDTA)-/2-			Co(EDTA)-/2-	
Solvent	Δ(ΔG°)S-wa	$\Delta(\Delta H_{\Gamma C}^{o})^{S-W}^{b}$	Δ(ΔS°) ^{S-w°}	Δ(ΔG°)S-wa	Δ(ΔH°)S-wb	Δ(ΔS°)S-w ^C
Methanol	(6.8) 1.8	5	11	(6.7) 1.7	8.4	22.5
Formamide	(6.1) 4.6	5.9	4.5			
N-methyl- formamide	(9.4) 7.4	6.6	8.5			
Acetonitrile]e			(15.7) 12	26.4	48.5
Dimethyl- sulfoxide	(16.5)	17.7	12.5			
Dimethyl- formamide	(16.7) 13.7	16.8	10.5			

^aFree energy of transfer of redox couple $\Delta(\Delta G_{rc}^o)^{s-w}$ (Kcal.mol⁻¹) from water to non-aqueous solvent, obtained from formal potentials E_f^{Fc} for each redox couple given in

Table 12. Continued.

 $\Delta(\Delta G_{rc}^{\circ})_{Fc}^{S-W}=0$ (i.e., using ferrocene assumption); lower values obtained using estimates of $\Delta(\Delta G_{rc}^{\circ})_{Fc}^{S-W}$ given in Table 7, for methanol $\Delta(\Delta G_{rc}^{\circ})_{Fc}^{S-W}=-5$ (i.e., using TATB assumption) Table 11 using Equation (3). Values in parentheses obtained by assuming that

 $^{\rm b}$ Enthalpy of transfer of redox couple $\Delta(\Delta H^o_{rc})^{\rm S-W}$ (Kcal.mol⁻¹) from water to nonaqueous solvent listed, obtained from corresponding $\Delta(\Delta G^o_{rc})^{\rm S-W}$ (TATB scale) and $\Delta(\Delta S^o_{rc})^{\rm S-W}$ using Equation (4).

^cEntropy of transfer of redox couple $\Delta(\Delta S_n^o)^{s-w}$ (cal. deg⁻¹ mol⁻¹) from water to nonaqueous solvent listed, obtained from differences between appropriate values of $\Delta S_{\Gamma C}^{o}$ given for each solvent in Table 11.

(17, 20) to be given by a characteristic "a" parameter for each solvent, where the value of "a" decreases as the internal order of the solvent decreases. As shown in Figure 2 (open symbols) it is seen that the experimental increases in $(\overline{S}^{\circ}_{Fc}$ - $\overline{S}^{\circ}_{Fc}$ +) in going from water to the other solvents do roughly parallel the corresponding "a" values in most solvents, as would be expected if $\cdot \overline{\mathbb{S}}_{Fc}^o+$ varies with the solvent in a similar manner to $\overline{\mathbb{S}}^{\circ}_+$ for simple univalent cations, and if \overline{S}^{o}_{Fc} is not strongly dependent on the solvent. (Significant variations in $\overline{S}^{\circ}_{Fc}$ may occur, but will be of no consequence to the validity of the ferrocene assumption as long as they are accompanied by comparable variations in \overline{S}_{Fc}^{o} .) It is interesting to note that the variations of $(\overline{S}_{Fc}^{o} - \overline{S}_{Fc}^{o})$ for the most part do not correlate with the expected basicity of the solvent, as measured for example by "Donor Number" D.N. (81) (Figure 3 (open symbols)). A similar finding has been noted previously for monoatomic cations (20).

The small negative value of $(\overline{S}_{Fc}^{\circ} - \overline{S}_{Fc}^{\circ})$ in water has been noted previously (24). This unexpected result has been ascribed to the delocalization of the reducing electron around the cyclopentadienyl rings leading to a net increased polarization of adjacent water molecules in the lower oxidation state (24). The enhancement of the water structure from the hydrophobic nature of the ferrocene molecule ("solvation of the second kind") (53,54) may also be a factor along with the involvement of quadrupole-dipole

interactions (54). Such solvent polarization around the neutral ferrocene molecule may also occur in the other solvents, but is presumably outweighed by the greater tendency of the ferricinium cation to induce solvent ordering via ion-dipole interactions. In any case, the ferrocene assumption is clearly unsuited for estimating entropies of single ion transfer between different solvents, especially involving water or other hydrogen-bonded solvents.

In view of the substantially larger observed variations in ΔS_{rc}^{o} in changing from water to other solvents, $\Delta (\Delta S_{rc}^{o})^{S-W}$, for the Fc +/Fc couple (Table 4), compared with the corresponding dielectric-continuum predictions $\Delta(\Delta^{So}_{rc})^{S-W}_{Born}$, it is of interest to compare these experimental results with the disparities noted previously between the values of transfer free energies for single ions ΔG_{\pm}° obtained using the ferrocene and alternative extrathermodynamic assumptions (48). As was mentioned in Chapter III, aside from the ferrocene procedure the most widely accepted approaches (1) the "tetraphenylarsonium-tetraphenylborate" (TATB") procedure; and (2) the "zero liquid junction potential" procedure (48). Methods (1) and (2) have been shown to yield consistently similar values of ΔG_{t}^{o} (usually within ca. 1 Kcal mole⁻¹) between a wide range of solvents (48,55). However, the values of $\Delta G_{\rm t}^{\rm o}$ for ion transfer from water to other solvents, $(\Delta G_t^o)_{Fc}^{s-w}$, obtained using the

ferrocene procedure have been found to be consistently less positive than the corresponding values, $(\Delta G_{t}^{\circ})_{1}^{s-w}$ and $(\Delta G_{t}^{\circ})_{2}^{s-w}$, obtained using methods (1) and (2), respectively. Assuming for the moment that methods (1) and (2) yield the "true" transfer free energy $(\Delta G_{t}^{\circ})_{true}^{s-w}$, the alteration in the free energy difference $(\overline{G}_{Fc}^{\circ} - \overline{G}_{Fc}^{\circ} +)$ between ferrocene and ferricinium upon transfer from water to another solvent, $\Delta(\overline{G}_{Fc}^{\circ} - \overline{G}_{Fc}^{\circ} +)^{s-w}$, can be obtained from

$$\Delta(\overline{G}_{Fc}^{\circ} - \overline{G}_{Fc+}^{\circ})^{S-W} = (\Delta G_{t}^{\circ})_{Fc}^{S-W} - (\Delta G_{t}^{\circ})_{true}^{S-W}$$
 (5)

Table 13 consists of estimates of $\Delta(\overline{G}_{FC}^{\circ} - \overline{G}_{FC}^{\circ})^{S-W}$ obtained using Equation (5) from values of ΔG_{C}° for Ag and Cu tabulated in References 48 and 50, along with the corresponding values of $T\Delta(\overline{S}_{FC}^{\circ} - \overline{S}_{FC}^{\circ})^{S-W}$ extracted from the data given in Table 4. It is seen that the increasing values of $-\Delta(\overline{G}_{FC}^{\circ} - \overline{G}_{FC}^{\circ})^{S-W}$ obtained for solvents of decreasing structure and ionizing ability are typically paralleled by comparable or larger values of $T\Delta(\overline{S}_{FC}^{\circ} - \overline{S}_{FC}^{\circ})^{S-W}$, although inevitably there are some disparities in the estimates of $\Delta(\overline{G}_{FC}^{\circ} - \overline{G}_{FC}^{\circ})^{S-W}$ obtained using methods (1) and (2). Since the values of $T\Delta(\overline{S}_{FC}^{\circ} - \overline{S}_{FC}^{\circ})^{S-W}$ do not rely critically on any particular extrathermodynamic assumption, this finding can be taken as additional evidence that methods (1) and (2) are indeed more trustworthy than the ferrocene assumption. If the estimates of $\Delta(\overline{G}_{FC}^{\circ} - \overline{G}_{FC}^{\circ})^{S-W}$

(5), Compared with Corresponding Transfer Entropies T($\overline{\rm S}_{\rm Fc}$ - $\overline{\rm S}_{\rm Fc+}$)^{8-W} for T=25°C. from Water to Various Other Solvents $\Delta(\vec{G_{P_C}}-\vec{G_{P_C}}+)^{S-W}$ Obtained using Equation Estimates of Transfer Free Energies for Ferricinium-ferrocene Redox Couple Table 13.

	$-\Delta(\overline{G}_{P_G}^{\bullet})$	$-\Delta(\overline{G}_{F_C}^o - \overline{G}_{F_C}^o +)^{s-w^a}$ Kcal mol ⁻¹	nol ⁻ l	$T_{\Delta}(\overline{S}_{P_{G}}^{o} - \overline{S}_{P_{G}}^{o})^{f}$
Solvent	Method (1) ^{b,d}	Method (2) ^{b,e}	Method (2) ^{C,e}	Kcal mol ⁻¹
Formamide	1.1	2.0	1	1.5
Propylene Carbonate	1.8	3.3	3.4	4.7
Dimethylsulfoxide	2.6	3.0	2.8	5.0
Dimethylformamide	2.7	3.7	4.1	5.8
Acetonitrile	3.1	4.2	5.6	4.9
Methanol	4.6	5.0	7.5	2.4

^aVariation in $(G_{F_C}^o - G_{F_C}^o +)^{s-w}$ in changing from water to solvent listed; estimated from Equation (5) using the method indicated.

^bFrom Equation (5), using ion transfer energies for Ag⁺ calculated from data in Table 12VI of Reference 48.

dvalues of $(\Delta G_{t}^{o})_{true}^{s-w}$ assumed to equal those given by "Ph $_{\mu}$ AsPh $_{\mu}$ B Assumption" [Method (1); ^cFrom Equation (5), using ion transfer energies for Cu²⁺ from Table VI of Reference 50.

Table 13. Continued.

^eValues of $(\Delta G_t^{0})_{true}^{S-W}$ assumed to equal those given by "zero liquid junction potential assumption" [Method (2); see text].

fvariation in ($\overline{S_F^o}$ - $\overline{S_F^o}$ +) in changing from water to solvent listed; obtained from values given in Table 4 for jonic strength μ = 0.1 \underline{M} . by either method (1) and (2) are approximately correct, then from the data in Table 13 it follows that typically $-\Delta(\overline{G}_{Fc}^{\circ}+-\overline{G}_{Fc}^{\circ}+) \sim T\Delta(\overline{S}_{Fc}^{\circ}-\overline{S}_{Fc}^{\circ}+); \ \underline{i.e.}, \ \text{that} \ \Delta(\overline{H}_{Fc}^{\circ}-\overline{H}_{Fc}^{\circ}+) \sim 0.$ This suggests that a primary reason for the probable break-down of the ferrocene assumption is simply the greater tendency of solvent dipoles to be polarized by the ferricinium cation compared with the ferrocene molecule, to an extent which is greater than predicted from the Born model and sensitive to the microscopic structure of the solvent.

2. Polypyridine Redox Couples

The data presented in Tables 6 and 7 for polypyridine couples exhibit three interesting features. First, the values of ΔS_{rc}° are markedly larger in nonaqueous solvents compared to water, especially in aprotic media where $\Delta(\Delta S_{rc}^{\circ})^{s-w} \sim 20-40$ e.u.. Second, there is consistently an approximate compensation between $\Delta(\Delta S_{rc}^{\circ})^{s-w}$ and $\Delta(\Delta H_{rc}^{\circ})^{s-w}$ so that the values of $\Delta(\Delta G_{rc}^{\circ})^{s-w}$ are uniformly small and negative in the range 0 to -3 Kcal mol⁻¹ for all four polypyridine couples on the basis of the TATB assumption employed here. Third, although the absolute values of ΔS_{rc}° for the Co(III)/(II) couples are 15-20 e.u. larger than for Cr(bpy) $\frac{3}{3}^{+/2+}$ and Fe(bpy) $\frac{3}{3}^{+/2+}$ (Table 6), the values of $\Delta(\Delta S_{rc}^{\circ})^{s-w}$ in a given solvent are approximately the same for all four polypyridine couples (Table 7):

The simplest theoretical treatment of such outer-shell

solvent effects is to utilize the Born dielectric continuum theory. This model might be expected to be more applicable to the estimation of $\Delta(\Delta G_{rc}^o)^{s-w}$ for the present systems since the polypyridine ligands should act to shield somewhat the solvent from the metal cation, and several complicating factors may cancel out in the measured difference of transfer free energies between the oxidized and reduced forms. The Born estimates of $\Delta(\Delta G_{rc}^o)^{s-w}$ can be obtained from Equation (6)

$$\Delta(\Delta G_{rc}^{\circ})_{Born}^{s-w} = \frac{e^{2}N}{2} \left(\frac{1}{\varepsilon_{w}} - \frac{1}{\varepsilon_{s}}\right) \left(\frac{z_{ox}^{2}}{r_{ox}} - \frac{z_{red}^{2}}{r_{red}}\right)$$
 (6)

Calculations using $Z_{\rm ox}=3$, $Z_{\rm red}=2$, and radii appropriate for the M(III)/(II) polypyridines ($r_{\rm ox}=r_{\rm red}\approx6.8$ Å (73)) yielded values of $\Delta(\Delta G_{\rm rc}^{\rm o})_{\rm Born}^{\rm S-W}$ for the various solvents here that lie in the range -1.5 to 1 Kcal mol⁻¹. Bearing in mind that the experimental values of $\Delta(\Delta G_{\rm rc}^{\rm o})^{\rm S-W}$ are probably trustworthy only to within ca 1 Kcal mol⁻¹ due to the likely uncertainties in the TATB assumption (48), the agreement can be considered to be reasonable.

The comparison between the experimental and Born estimates of the reaction entropies is of greater interest since it enables the applicability of the Born model to be tested in a single solvent. Values of $(\Delta S_{rc}^{\circ})_{Born}^{s-w}$ calculated from Equation (1) for $r_{ox} = r_{red} = 6.8$ Å are given for each solvent in Table 6. The experimental values of ΔS_{rc}° are seen to be typically in marked disagreement with corresponding

Born predictions $(\Delta S_{rc}^{\circ})_{Born}$. A milder test of the Born model is to compare the observed solvent dependence of ΔS_{rc}° , $\Delta (\Delta S_{rc}^{\circ})^{s-w}$, with the corresponding differences in $(\Delta S_{rc}^{\circ})_{Born}$, $\Delta (\Delta S_{rc}^{\circ})_{Born}^{s-w}$.

Figure 1 contains plots of $\Delta(\Delta S_{rc}^{\circ})^{s-w}$ against $\Delta(\Delta S_{rc}^{\circ})_{Born}^{s-w}$. It is seen that a rough correlation between these quantities is obtained, although there is considerable scatter and the average slope is somewhat larger than the predicted value of unity.

These comparisons suggest that a substantial part of the observed values of $\Delta S_{\mathbf{rc}}^{\mathbf{o}}$ in the various solvents arise from extensive short-range polarization in the higher oxidation state which is partly dissipated upon reduction, this factor being superimposed upon the milder long-range cationsolvent interactions which are more likely to be described successfully by the Born dielectric continuum model. typically $\Delta S_{rc}^{o} > (\Delta S_{rc}^{o})_{Born}$ (Table 6), indicating that the enhancement of solvent polarization ("ordering") in the tripositive versus the dispositive oxidation states is in most cases greater than predicted from macroscopic dielectric considerations, probably as a result of dielectric saturation in the vicinity of the solute. The Born model also fails to account for the markedly larger values of ΔS_{no}^{o} seen for $Co(bpy)_3^{3+/2+}$ and $Co(phen)_3^{3+/2+}$ compared with $Cr(bpy)_3^{3+/2+}$ and $Fe(bpy)_3^{3+/2+}$ in each solvent.

In recent years there have been a number of attempts

Figure 1. Plots of Δ(ΔS°_{rc})^{S-W} for each polypyridine redox couple against the corresponding Born estimates $\Delta(\Delta S^{\circ}_{rc})^{S-W}_{Born}$ obtained from the values of $(\Delta S^{\circ}_{rc})_{Born}$ calculated for water and the appropriate nonaqueous solvent using Equation (1) (see text).

Key to this and Figures 2 and 3. Redox couples:

Cr(bpy)^{3+/2+}, Fe(bpy)^{3+/2+}, Co(bpy)^{3+/2+},

Co(phen)^{3+/2+}, Fe(bpy)^{3+/2+}, Co(bpy)^{3+/2+},

Co(phen)^{3+/2+}, O Ferricinium/ferrocene.

Solvents: 1, formamide; 2, N-methylformamide;
3, propylene carbonate; 4, dimethylsulfoxide;
5, dimethylformamide; 6, acetonitrile; 7, nitro-

methane.

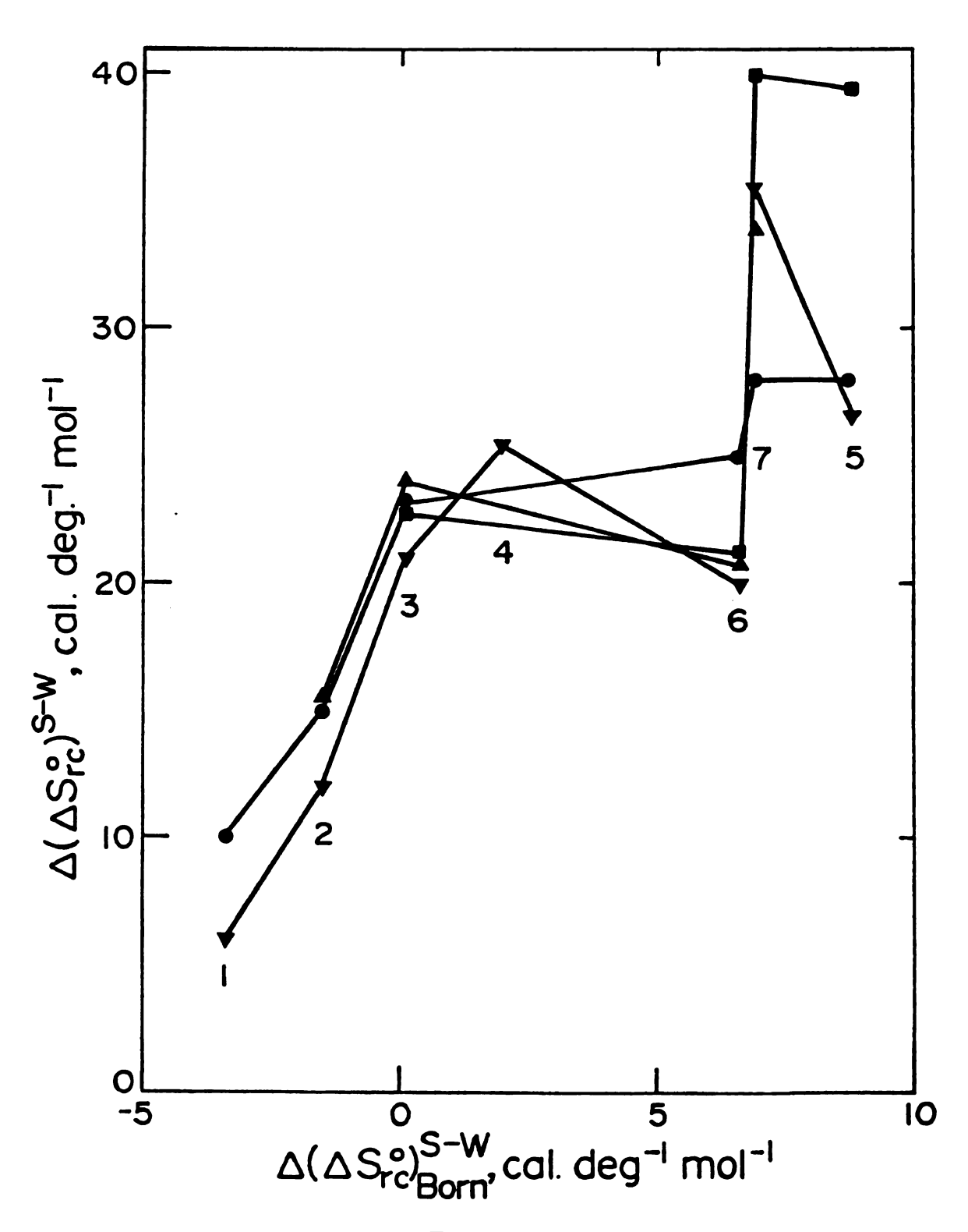


Figure 1

to provide more successful treatments of ion solvation, either by modifications to the Born model (93) or by the development of fundamentally new approaches (94a). However, most effort has been devoted to the utilization of these treatments for the estimation of solvation free energies in aqueous solution, and little attention has been paid to the estimation of solvation entropies, particularly in nonaqueous media (94b). It has been found that reasonable agreement with experimental solvation entropies for monatomic cations in various aprotic solvents can be obtained using a modified Born model where the first solvation layer was assumed to be dielectrically saturated (94b). Direct application of this approach to the present systems does indeed yield estimates of $\Delta S_{\mbox{\scriptsize rc}}^{\mbox{\scriptsize o}}$ that are larger than $(\Delta S_{rc}^{o})_{Rorm}$ and in some cases closer to the experimental values. However, it is uncertain that the model is entirely appropriate to the present systems where the first solvation sphere is occupied by the coordinated ligands, and in any case it is unable to account for the observed variations of $\Delta S_{\mbox{\scriptsize rc}}^{\mbox{\scriptsize o}}$ with the metal spin state or the small values of ΔS_{rc}^{o} seen in hydrogen-bonded solvents. More sophisticated solvation treatments which take into account the molecular structure of the polar solvent (94a) should ultimately yield accurate descriptions of the experimental results. However, these models in their present form are not entirely applicable to the present systems since neither chemical interactions between the complexes and their immediate environment nor dielectric saturation effects are fully taken into account (94a). Such effects should provide an important influence upon the redox thermodynamic parameters considered here since these quantities reflect the change in solvent polarization resulting from decreasing the solute charge from +3 to +2. The remaining discussion will therefore be concerned with the utilization of more "intuitive chemical" approaches for rationalizing the experimental behavior.

The uniformly positive values of $\Delta(\Delta S_{rc}^{\circ})^{s-W}$ indicate that the increase of the metal oxidation state from +2 to +3 yields a relatively greater enhancement in the extent of solvent polarization ("ordering") in the vicinity of the complex for nonaqueous solvents compared with the same process in water. Such differences can be simply explained by the unusually high degree of internal order exhibited by liquid water. Thus the additional cationic charge carried by the oxidized compared to the reduced form of the redox couple will generate a greater degree of solvent polarization in the vicinity of the solute in solvents having a smaller degree of internal order due to the relative ease by which solvent molecules can be disturbed from their bulk orientation in response to the electric field. If the same factors that determine the ionic entropies of univalent ions $\overline{\mathbb{S}}^{\circ}$ also influence the values of \overline{S}^{o}_{OX} relative to \overline{S}^{o}_{red} for the

M(III)/(II) polypyridine couples, it would be expected that $\Delta(\Delta S_{rc}^{\circ})^{S-W}$ would be linearly related to -a. Such a plot is given in Figure 2. It is seen that there is indeed an approximate correlation between the values of $\Delta(\Delta S_{rc}^{\circ})^{S-W}$ for all four polypyridine couples (closed symbols) and -a. Thus relatively small values of $\Delta(\Delta S_{rc}^{\circ})^{S-W}$ (§15 e.u.) are observed in formamide and NMF that are expected to be polymerized to some extent via hydrogen bonding (17). Larger values of $\Delta(\Delta S_{rc}^{\circ})^{S-W}$ (20-40 e.u.) are seen for the aprotic solvents PC, DMSO, DMF, and acetonitrile which are expected to have relatively small degrees of internal order. These solvents have sizable dipole moments which should encourage additional solvent ordering around M(III) compared to the corresponding M(II) polypyridine complexes via ion-dipole interactions.

There is also the possibility that the observed solvent dependence of ΔS_{rc}^{o} may arise from variations in the ability of the solvents to engage in donor-acceptor interactions with the M(III) state to a greater extent than with M(II). If this factor does indeed provide a major contribution to ΔS_{rc}^{o} , then a correlation between $\Delta (\Delta S_{rc}^{o})^{S-W}$ and the donicity of the solvents would be expected. Although it is difficult to formulate quantitative scales which reflect the electron donating abilities (or basicity) of solvents, one such measure which has proved useful is the so-called Donor Number (D.N.) (81). Figure 3 contains plots of

Figure 2. Plots of the variation in the reaction entropy $\Delta(\Delta S_{rc}^{\circ})^{s-w}$ for a given polypyridine redox couple when changing from water to various nonaqueous solvents against -a, where "a" is a parameter related to the degree of "internal order" of each solvent (17,20). Values of $\Delta(\Delta S_{rc}^{\circ})^{s-w}$ taken from Table 7. The straight lines are drawn between adjacent points for a given redox couple in the various solvents. Key to redox couples and solvents as in notes to Figure 1.

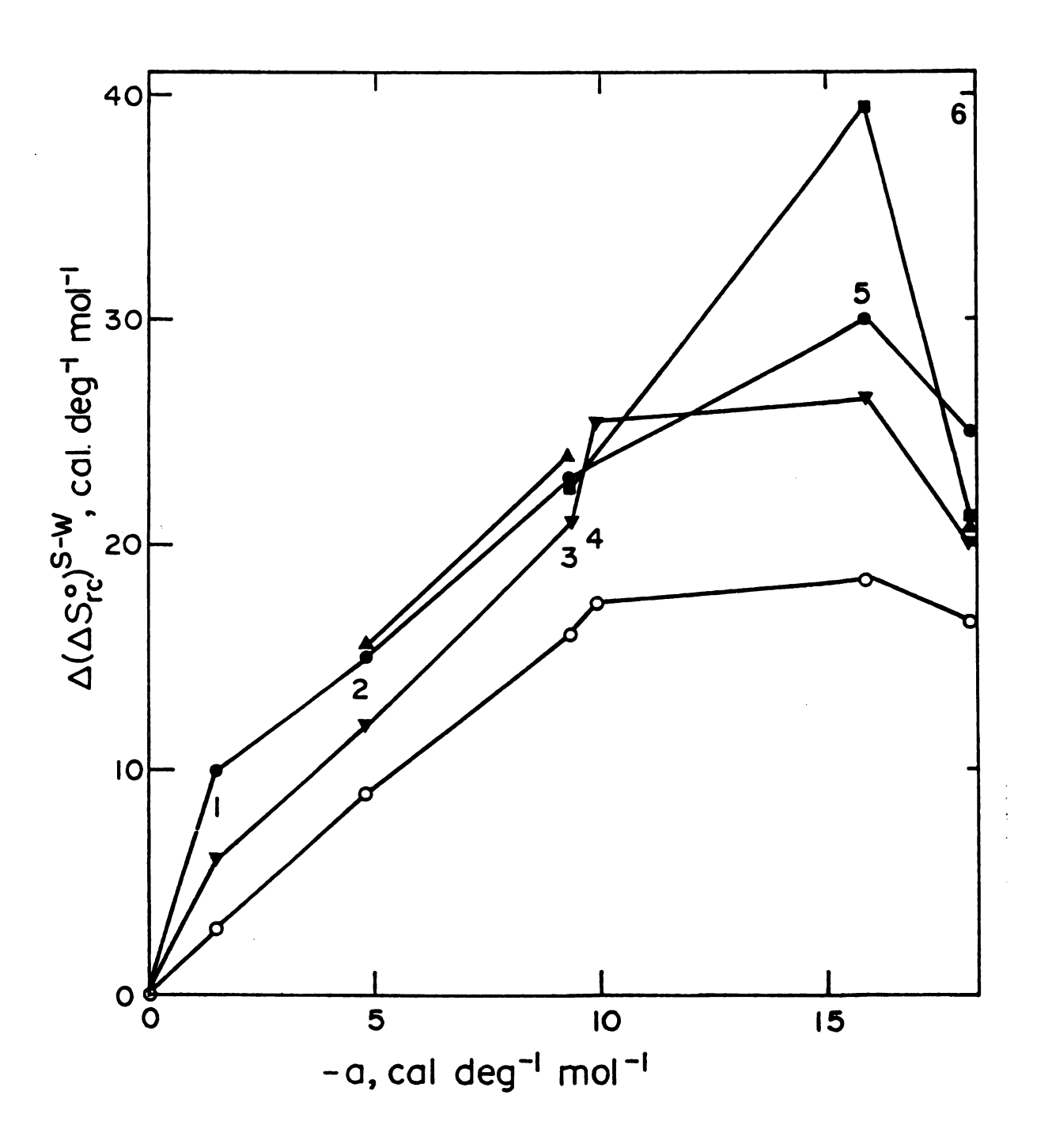


Figure 2

Figure 3. Plots of $\Delta(\Delta S_{rc}^{\circ})^{s-w}$ for each polypyridine redox couple against the "Donor Number" for the various nonaqueous solvents (81). Key to redox couples and solvents as in notes to Figure 1.

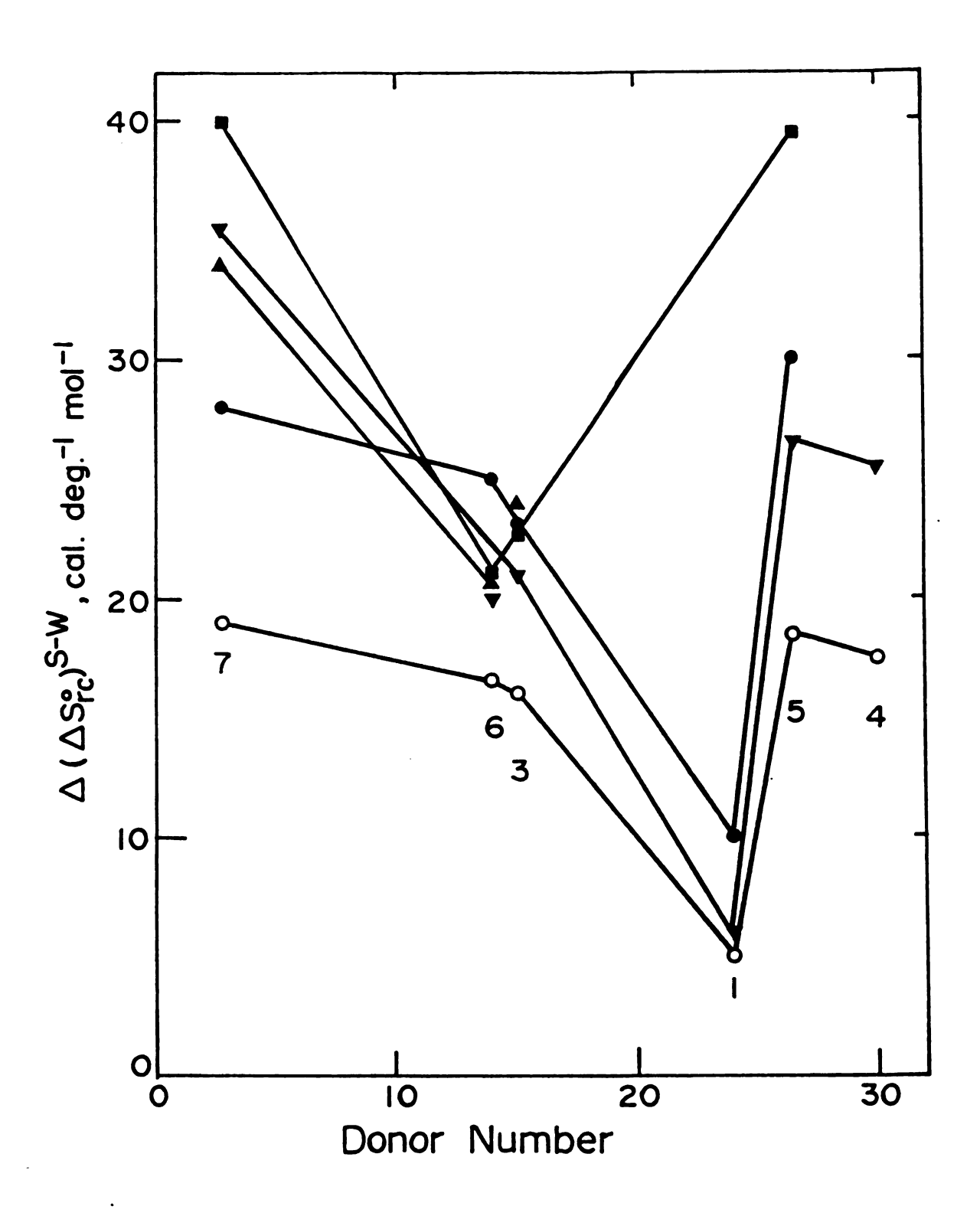


Figure 3

 $\Delta(\Delta S_{rc}^{\circ})^{s-w}$ against the values of D.N. quoted in Reference 81. In contrast to Figures 1 and 2, it is seen that there is no correlation between the values of D.N. for the various solvents and $\Delta(\Delta S_{rc}^{\circ})^{s-w}$.

On the basis of Figures 1-3, it therefore appears that the large changes in $\Delta S_{\mbox{\scriptsize rc}}^{\mbox{\scriptsize o}}$ observed when the solvent is varied are primarily determined by the relative ability of the tripositive M(III) polypyridine complex compared to the corresponding M(II) species to disturb the bulk solvent structure and reorient solvent molecules within its vicinity. The use of the macroscopic dielectric constant in the Born model presumes that such solvent polarization is minor. Nevertheless, it is interesting to note that at least qualitatively similar variations in ΔS_{ro}^{o} with the nature of the solvent are predicted by the "a" parameter, and the simple Born treatment, inasmuch as the corresponding plots in Figures 2 and 1 have similar shapes. This similarity reflects the interrelationship between the internal order of solvents and their macroscopic dielectric properties, and suggests that both these factors play a major role in determining the alterations in the degree of solvent ordering induced by M(III) vs. M(II) polypyridines as the solvent is varied. In contrast, the almost complete lack of correlation between $\Delta(\Delta S_{rc}^{o})^{S-W}$ and the solvent Donor Number suggests that the changes in relative solvent polarization on the nature of solvent only depend to a minor extent, if

at all, on the ability of the solvent to coordinate to the cationic solute. Although there may well be substantial variations in solvent polarization in the vicinity of the M(III) polypyridine complexes as the solvent is altered arising from variations in the solvent coordinative abilities, if present they appear to be largely compensated by similar changes for the corresponding M(II) complexes.

Nevertheless, the apparent sensitivity of $\Delta S_{\mathbf{rc}}^{\circ}$ to the symmetry of the orbital occupied by the reducing electron suggests that the extent of solvent polarization in the oxidized state relative to the corresponding reduced form in a given solvent is indeed sensitive to local, and presumably short-range, solvation factors. The strikingly smaller values of $\Delta S_{\mathbf{rc}}^{\circ}$ (1-4 e.u.) seen in aqueous solution for $Cr(bpy)_3^{3+/2+}$, $Fe(bpy)_3^{3+/2+}$ (Table 6), $Fe(phen)_3^{3+/2+}$, and $Ru(bpy)_3^{3+/2+}$ (21,24) compared with the values for Co- $(bpy)_3^{3+/2+}$ and $Co(phen)_3^{3+/2+}$ (22 e.u.) probably arise from the delocalization of the reducing t_{2g} electron around the aromatic rings for the Fe(III)/(II), Ru(III)/(II), and Cr(III)/(II) couples; this delocalization will be largely absent for the Co(III)/(II) couples which involve the electronic transition $t_{2g}^6 \rightarrow t_{2g}^5 e_g^2$. As noted previously (21,24), this electron delocalization may influence ΔS_{rc}^{o} by inducing an increase in solvent polarization in the vicinity of the aromatic rings in the reduced state compared with the oxidized form which will counteract the

normal entropy increase resulting from the decrease in solvent polarization close to the metal redox center. Evidence supporting this contention includes the negative value of ΔS_{rc}° (-5 e.u.) found for Fc⁺/Fc in aqueous solution (2⁴). The structure of Fc⁺/Fc differs from the polypyridine couples in that the compact "sandwich" structure of the former couple should prevent the close approach of solvent molecules to the metal redox center that can occur along the channels formed by the more open polypyridine rings. Therefore the only major factor contributing to ΔS_{rc}° for the Fc⁺/Fc couple is presumed to be the additional solvent polarization in the reduced state arising from the delocalization of the added ligand around the cyclopentadienyl rings, yielding a negative value of ΔS_{rc}° (2⁴).

As noted above, the values of ΔS_{rc}^{o} for $Co(bpy)_{3}^{3+/2+}$ and $Co(phen)_{3}^{3+/2+}$ compared with those for $Cr(bpy)_{3}^{3+/2+}$ and $Fe(bpy)_{3}^{3+/2+}$ are also consistently 15-20 e.u. larger, not only in water, but also in all seven nonaqueous solvents (Table 6). This simple result is surprising; the tendency of the various solvents to be oriented by the delocalized electron might be expected to be dependent to some extent upon solvent properties such as the extent of internal order or the ability to act as an electron acceptor. However, the behavioral simplicity may be misleading in that it could arise from a fortuitous cancellation between several effects. Thus the degree of internal order of several of

the solvents used here vary roughly with their expected tendency to act as electron acceptors as measured by the so-called "acceptor number" (81). The extent of solvent orientation induced near the aromatic ligands could remain similar when changing, for example, from water to DMF since to the degree of internal order and electron accepting a bility of the solvent are thereby diminished.

The approximate compensation between corresponding values of $T\Delta(\Delta S_{rc}^{\circ})^{S-W}$ and $\Delta(\Delta H_{rc}^{\circ})^{S-W}$ for polypyridine couples yielding markedly smaller values of $\Delta(\Delta G_{rc}^{\circ})^{S-W}$ (Table 7) has often been observed for entropic and enthalpic quantities in electrolyte solutions (95). Such a compensation is expected since the (entropically unfavorable) orientation of solvent molecules as a result of ion-dipole interactions, for example, would necessarily yield favorable enthalpic changes. Although $\Delta(\Delta G_{rc}^{\circ})^{S-W}$ is frequently close to zero, the values are typically negative (at least on the TATB scale) so that the entropic factors appear to provide the Predominant influence upon the free energies of transfer.

Measurements of reaction entropies for the Fe(phen) $_3^{3+/2+}$ and related redox couples having methyl groups substituted around the phenanthroline ring have been previously compared in acetonitrile and water (26). The value of ΔS_{rc}^{o} given for Fe(phen) $_3^{3+/2+}$ in acetonitrile (25 e.u., μ = 0.1 (26)) is close to our value for Fe(bpy) $_3^{3+/2+}$ in this solvent (23 e.u., Table 6). However, the value of ΔS_{rc}^{o} reported in

Reference (26) for Fe(phen) $_3^{3+/2+}$ in water (-20.5 e.u.) is markedly different than the previous determinations for Fe(phen) $\frac{3}{3}^{+/2+}$ and Fe(bpy) $\frac{3}{3}^{+/2+}$ (3 and 2 e.u., respectively, μ = 0.05 (21)). Since values of ΔS_{rc}^{o} close to zero have also been given earlier for these and other low-spin M(III)/-(II) polypyridine couples in aqueous solution (96), the disparate value for Fe(phen) $\frac{3+}{3}$ quoted in Reference 26 is presumably in error. One possible source of this discrepancy is the confusion that can be caused by the indiscriminate use of alternative entropy scales without clearly identifying which scales are being employed. As **pointed** out in Reference (21), the values of ΔS_{rc}^{o} obtained from a nonisothermal cell arrangement as employed here differ markedly from the frequently quoted "reaction en- $\texttt{tropies"}\ \Delta S_{H}^{\textbf{o}}$ that actually refer to the overall entropy change for an electrochemical cell containing a hydrogen reference electrode; it can be shown that (24) ΔS_{rc}^{o} = ΔS_{H}^{o} + 20.5 e.u. Some, but not all, of the "reaction entropies" quoted in Reference 26 are actually values of ΔS_{H}° rather than ΔS_{rc}° .

In the next section values of ΔS_{rc}^{o} and $\Delta (\Delta G_{rc}^{o})^{s-w}$ obtained for ammine and ethylenediamine redox couples will be discussed and compared with those for polypyridine couples.

3. Ammine and Ethylenediamine Couples

Inspection of the data presented in Tables 8 and 9 reveals that substantial changes in the redox thermodyramics of ammine and ethylenediamine redox couples occur when the solvent is varied. Two main features are apparent. Firstly, the values of $\Delta(\Delta G_{rc}^{o})^{s-w}$ vary over a wide \rightarrow ange, from ca. -4 Kcal mol⁻¹ in nitromethane to around 8 ightharpoonup cal mol⁻¹ in DMSO, the values being usually within ca. ○.5 - 1 Kcal mol⁻¹ for all four amine couples in a given \Longrightarrow olvent. Even larger variations in $\Delta(\Delta H_{rc}^{o})^{S-W}$ are seen (ca. -1.5 to 15 Kcal mol⁻¹). The solvent sensitivity of \triangle (\triangle G $^{\circ}_{rc}$) $^{s-w}$ contrasts with the behavior of the M(III)/- \langle II) polypyridine couples, where the values of $\Delta(\Delta G_{rc}^{o})^{S-W}$ were typically small and negative (Table 7). Secondly, the values of ΔS_{rc}^{o} are uniformly and markedly larger in nonaqueous media compared with water, especially in aprotic solvents where $\Delta(\Delta S_{rc}^{o})^{s-w}$ approaches 30 e.u. Broadly similar values of $\Delta(\Delta S_{rc}^{o})^{s-w}$ have also been observed for the Polypyridine couples, so that the differences in $\Delta(\Delta G_{rc}^{o})^{s-w}$ between the saturated amine and polypyridine couples are Chiefly due to the enthalpic component $\Delta(\Delta H_{rc}^{o})^{s-w}$. However, the values of ΔS_{rc}^{o} in a given solvent are, as before, sensitive to the nature of both the metal and the co-Ordinated ligands.

As for polypyridine couples, it is instructive to compare the experimental values of $\Delta(\Delta G_{rc}^o)^{s-w}$, ΔS_{rc}^o , and

 $\Delta(\Delta S_{rc}^{\circ})^{S-W}$ for amine and ethylenediamine couples with the corresponding predicted values from the Born model $\Delta(\Delta G_{rc}^{\circ})_{Born}^{S-W}$, $(\Delta S_{rc}^{\circ})_{Born}^{S-W}$, and $\Delta(\Delta S_{rc}^{\circ})_{Born}^{S-W}$. These latter quantities were obtained from Equations (1) and (6).

Values of $(\Delta S_{rc}^{\circ})_{Born}$ and $\Delta(\Delta G_{rc}^{\circ})_{Born}^{S-W}$ calculated from Equations (1) and (6) for $Z_{ox} = 3$, $Z_{red} = 2$, and $r_{ox} = r_{red} = 3.5$ Å (appropriate for the small amine couples (73)) are given in Tables 8 and 9, respectively.

Comparison of $\Delta(\Delta G_{rc}^{\circ})_{Born}^{s-w}$ with the corresponding exightharpoonup erimental values $\Delta(\Delta G_{
m rc}^{\circ})^{
m S-W}$ (Table 9) reveals, not unexpectedly, that the Born predictions are frequently in 1 arge and even qualitative disagreement with experiment. In particular, large positive values of $\Delta(\Delta G_{rc}^{\circ})^{s-w}$ (ca. 5-8.5 Kcal mol⁻¹) are observed for all five amine couples in the strongly basic solvents DMSO and DMF (D.N. = 29.8 and 26.6, respectively (81)) in contrast to the negative \mathbf{v} alues of $\Delta(\Delta G_{rc}^{o})_{Born}^{s-w}$ predicted for these solvents (Table 9). Nevertheless for the other five, less basic, non- \mathbf{a} queous solvents the values of $\Delta(\Delta G_{rc}^{\circ})^{s-w}$ and $\Delta(\Delta G_{rc}^{\circ})_{Born}^{s-w}$ agree at least qualitatively and are indeed in close agreement for the weakly basic solvents propylene carbonate, acetonitrile, and nitromethane (D.N. = 15.1, 14.1 and 2.7, respectively (81)) for which negative values of $\Delta(\Delta G_{rc}^{o})^{S-W}$ are observed (Table 9). [Although these transfer free energies naturally rely upon the choice of water as the reference solvent, water also appears to be a relatively

weak electron donor (D.N. ≈ 18 (81)).] These considerations therefore suggest that long-range solvation influences may provide an important part of the additional solvation energy for the oxidized versus the reduced forms of these redox couples, at least in solvents of low basicity where short range solvent-solute interactions of the donor-acceptor type should be relatively weak.

However, if donor-acceptor interactions are instead providing the predominant contribution to the solventdependent redox thermodynamics of $Co(en)_3^{3+/2+}$, as suggested by Mayer et al. (97), as well as for the other amine couples considered here, a linear correlation between the experi**m**ental values of $\Delta(\Delta G_{rc}^{o})^{s-w}$ or $\Delta(\Delta H_{rc}^{o})^{s-w}$ and the solvent Donor Number (or a related measure of the solvent basicity) would be expected. Figure 4 consists of such plots for $Co(en)_3^{3+/2+}$ and $Ru(NH_3)_6^{3+/2+}$. [Similar plots were obtained for Ru(en) $_3^{3+/2+}$, Ru(NH₃)₅NCS^{2+/+}, and Co(sep) $_3^{3+/2+}$ but are omitted for clarity.] It is seen that there is indeed a reasonably linear correlation for both $\Delta(\Delta G_{rc}^{o})^{S-W}$ and $\boldsymbol{\triangle} \; (\Delta H_{\boldsymbol{\mathcal{T}}\boldsymbol{\mathcal{C}}}^{o})^{S-W}$ with the solvent D.N. for both couples in the Six nonaqueous solvents for which Donor Numbers are available, although the values of $\Delta(\Delta G_{rc}^{o})^{S-W}$ and $\Delta(\Delta H_{rc}^{o})^{S-W}$ in nitromethane are decidedly less negative than expected. A related plot of E_f for $Co(en)_3^{3+/2+}$ [measured versus the "reference solute" couple bisbiphenylchromium (I/O)] against D.N. for a number of nonaqueous solvents has previously

Figure 4. Plots of the variation in the free energy of reaction, $\Delta(\Delta G_{rc}^{\circ})^{S-W}$, and the enthalpy of reaction, $\Delta(\Delta H_{rc}^{\circ})^{S-W}$, for $Co(en)_3^{3+/2+}$ and $Ru(NH_3)_6^{3+/2+}$ when changing from water to various nonaqueous solvents against the "Donor Number" for each solvent (81): Closed symbols: $\Delta(\Delta G_{rc}^{\circ})^{S-W}$. Open symbols: $\Delta(\Delta H_{rc}^{\circ})^{S-W}$. Redox couples:

•, 0, $Co(en)_3^{3+/2+}$;•, □, $Ru(NH_3)_6^{3+/2+}$. Solvents in this and Figures 5, 6 and 7: 1, formamide; 2, N-methylformamide; 3, propylene carbonate; 4, dimethylsulfoxide; 5, dimethylformamide; 6, acetonitrile; 7, nitromethane. The straight lines are drawn between adjacent points for a given redox couple in the various solvents.

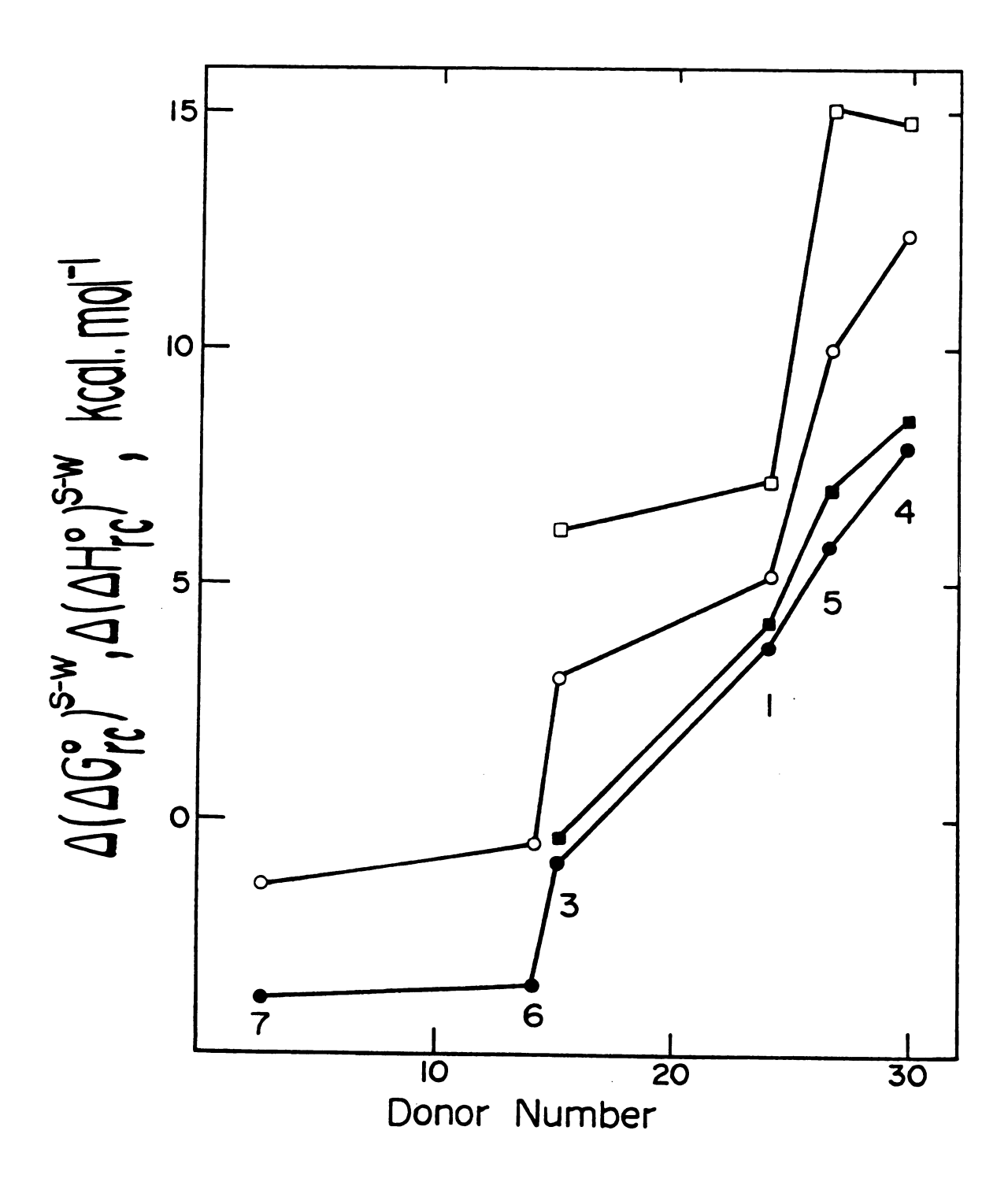


Figure 4

been shown by Mayer et al. to be approximately linear (97). This result provided the chief basis for their assertion that donor-acceptor interactions between the solvent and the acidic amine hydrogens on Co(en)3+ provided the prevailing contribution to the solvent influence upon the $rac{1}{2}$ edox thermodynamics of Co(en) $\frac{3+}{2}$. Although the present ata do not entirely contradict this conclusion, they sugest instead that such short-range interactions may be of predominant importance only with the more highly basic solvents. Nevertheless, the uniformly large positive values $oldsymbol{\circ}$ $\Delta (\Delta G_{rc}^{\circ})^{s-w}$ obtained in DMSO and DMF for the five amine couples in comparison with the small and negative corresponding values for the polypyridine couples that have ro electron acceptor sites provides strong evidence for the importance of donor-acceptor interactions to the redox thermodynamics for the former systems.

However, the comparable values of $\Delta(\Delta G_{rc}^{\circ})^{S-W}$ obtained for $Ru(NH_3)_6^{3+/2+}$, $Ru(en)_3^{3+/2+}$ and $Co(en)_3^{3+/2+}$, and $Co(sep)_3^{3+/2+}$ couples that contain eighteen, twelve, and Six amine hydrogens, respectively, is somewhat surprising on this basis. One plausible explanation is that there is only one solvent molecule strongly coordinated to each amine center anyway as a consequence of electrostatic and steric limitations. Another surprising result is the apparent insensitivity of $\Delta(\Delta G_{rc}^{\circ})^{S-W}$ to the electronic structure of the metal center in the reduced state. For

example, Ru(en) $_3^{3+/2+}$ and Co(en) $_3^{3+/2+}$ yield comparable values of $\Delta(\Delta G_{rc}^o)^{s-w}$ in both DMSO and DMF (Table 9). This behavioral simplicity may well have some utility in that values of ΔE_f^{Fc} could presumably be predicted with some confidence for redox couples for which measurements of E_f are impractical $[\underline{e.g.}, Co(NH_3)_6^{3+/2+}]$.

One inevitable difficulty in interpreting such experimental estimates of $\Delta(\Delta G_{rc}^{\circ})^{S-W}$ lies in the uncertainties inherent in the extrathermodynamic assumption required for their evaluation. Thus the values of $\Delta(\Delta G_{rc}^{\circ})^{S-W}$ based on the ferrocene scale (given in parentheses in Table 9) are up to 3.5 Kcal mol⁻¹ larger than those based on the TATB scale; the former values are uniformly positive except in nitromethane (Table 9) so that it would be concluded that the Born model is noticeably less successful for predicting $\Delta(\Delta G_{rc}^{\circ})^{S-W}$ if the ferrocene rather than the TATB scale had been employed. However, the available evidence suggests that the TATB scale provides estimates of single-in transfer energies [and hence values of $\Delta(\Delta G_{rc}^{\circ})^{S-W}$] that are trustworthy at least to within 1-2 Kcal mol⁻¹ (48).

Turning now to the entropy data, as might be anticipated the values of $(\Delta S_{rc}^{\circ})_{Born}$ are generally in poor agreement with the experimental quantities (Table 8). Also, plots of $\Delta(\Delta S_{rc}^{\circ})^{S-W}$ versus $\Delta(\Delta S_{rc}^{\circ})_{Born}^{S-W}$ for the three small amine couples exhibit considerable scatter (Figure 5). In view

Figure 5. Plots of the variation in the reaction entropy $\Delta(\Delta S_{rc}^{\circ})^{S-W} \text{ for a given amine redox couple when changing from water to various nonaqueous solvents against the corresponding Born estimates <math display="block">\Delta(\Delta S_{rc}^{\circ})^{S-W}_{Born} \text{ obtained from the values of } (\Delta S_{rc}^{\circ})_{Born} \text{ calculated for water and the appropriate nonaqueous solvent using Equation (1) (see text). Redox couples: <math>\bullet$, $\operatorname{Co(en)}_3^{3+/2+}$; \bullet , $\operatorname{Ru(NH}_3)_6^{3+/2+}$; \bullet , $\operatorname{Ru(en)}_3^{3+/2+}$. Key to solvents as in notes to Figure 4.

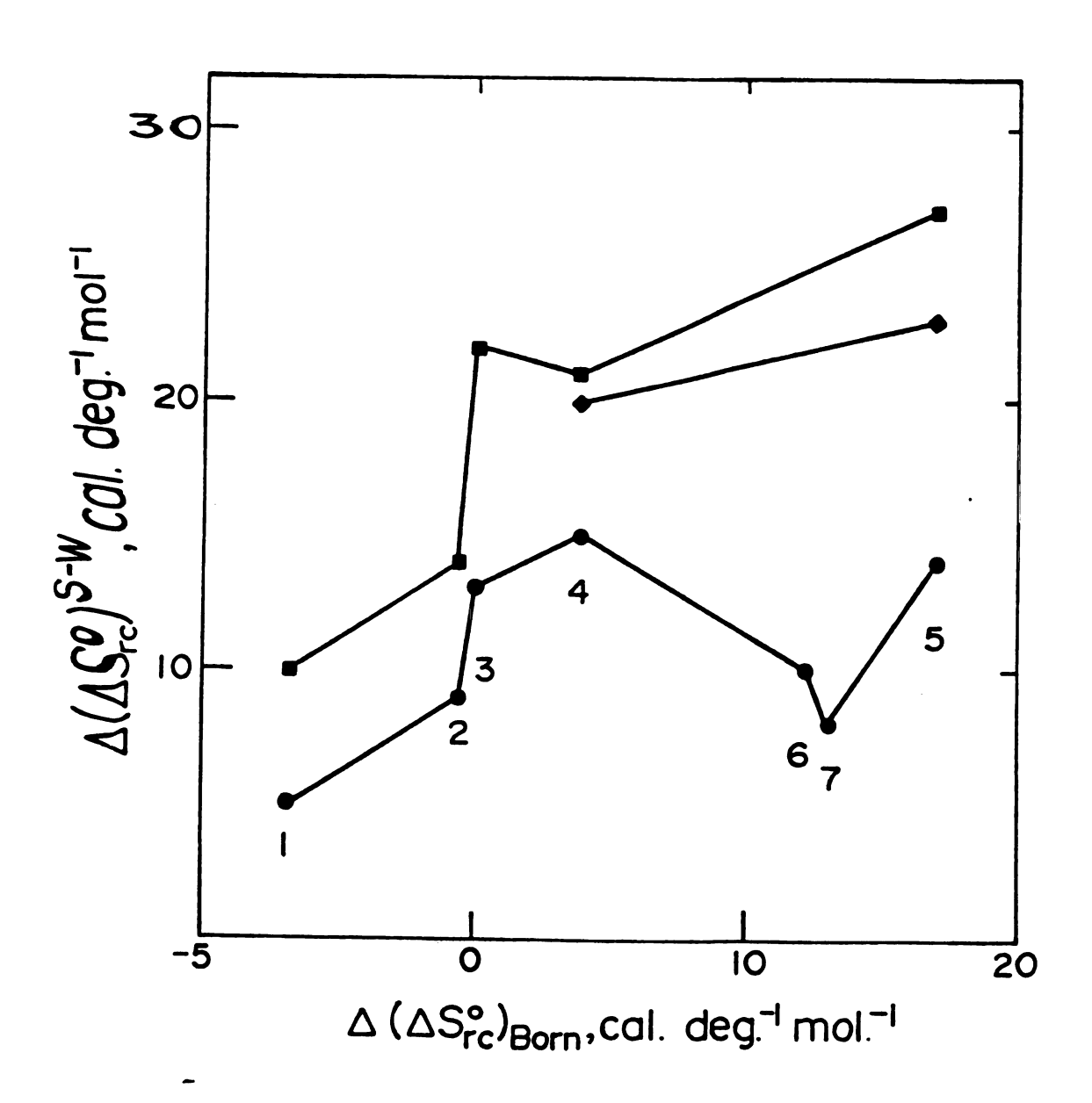


Figure 5

of the reasonable correlations obtained between $\Delta(\Delta G_{rc}^{o})^{s-w}$ and $\Delta(\Delta H_{rc}^{o})^{S-W}$ with the solvent Donor Number (Figure 4) it is of interest to ascertain if a similar relationship exists between $\Delta(\Delta S_{rc}^{o})^{S-W}$ for each redox couple and D.N. Such plots are given for the four amine couples in Figure It is seen that in contrast to Figure 4, there is little any correlation between $\Delta(\Delta S_{rc}^{\circ})^{s-w}$ and D.N. Thus, so 1 vents of relatively low basicity such as propylene carbonate and nitromethane give rise to values of $\Delta(\Delta S_{rc}^{o})^{s-w}$ that are comparable to, or even larger than, those obtained in the strongly donating solvents DMSO and DMF. Also, if such donor-acceptor interactions were important It would be expected that the values of $\Delta(\Delta S_{rc}^{o})^{s-w}$ in a given solvent would be greater for couples containing likely electron acceptor sites compared to couples of similar size and charge type not containing such ligand sites. fact the opposite appears to be the case. For example, the values of $\Delta(\Delta S_{rc}^{o})^{s-w}$ in each nonaqueous solvent listed in Tables 7 and 9 increase in the sequence $Co(en)_3^{3+/2+}$ < $Co(sep)^{3+/2+} < Co(bpy)_3^{3+/2+} \approx Co(phen)_3^{3+/2+}$ even though $Co(en)_3^{3+/2+}$ and $Co(sep)_3^{3+/2+}$ contain a total of twelve and six amine hydrogens, respectively, and the last two couples contain no amine hydrogens or other clearly identifiable acceptor sites.

A more successful correlation than Figure 6 is obtained by plotting the experimental values of $\Delta(\Delta S_{rc}^{o})^{s-w}$

Figure 6. Plots of $\Delta(\Delta S_{rc}^{\circ})^{s-w}$ for each amine redox couple against the "Donor Number" for the various non-aqueous solvents. Redox couples: \bullet , Co(en) $_3^{3+/2+}$; \bullet , Ru(NH $_3$) $_6^{3+/2+}$; \bullet , Ru(en) $_3^{3+/2+}$; \bullet , Co(sep) $_3^{3+/2+}$.

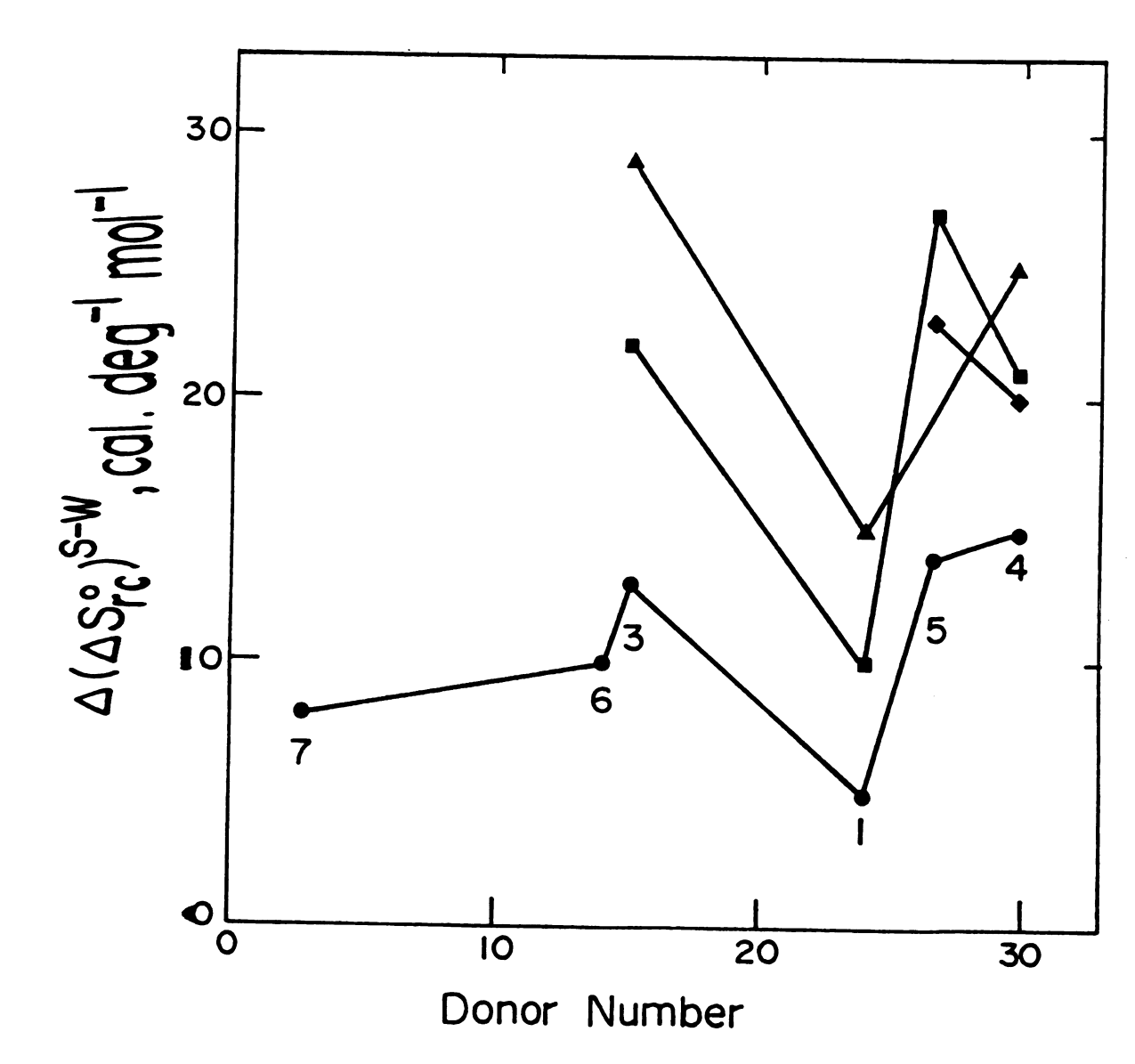


Figure 6

for each couple against -a for each nonaqueous solvent (Figure 7), where "a" is an empirical parameter (17,20) that provides a measure of the degree of "internal order" (the extent of association between solvent molecules in the bulk liquid (17)). It is seen that Δ(ΔS_{rc})^{S-W} increases almost uniformly with decreasing solvent internal order. These plots have similar shapes to those for the polypyridine redox couples (Figure 2), although the present plots are significantly less linear and have smaller slopes. The success of this correlation suggests that the values of ΔS_{rc} are at least partly determined by the ease by which surrounding solvent molecules are able to reorientate away from their bulk structure in response to the enhanced electric field around the oxidized versus the reduced forms of the redox couple.

These results therefore argue against the predominant importance of solvent-solute donor-acceptor interactions in termining the degree of this additional solvent polarization. Although at first sight surprising, this conclusion is quite compatible with the apparent sensitivity of the ee energy term $\Delta(\Delta G_{rc}^{\circ})^{S-W}$ to solvent basicity since the tropic terms ΔS_{rc}° and hence $\Delta(\Delta S_{rc}^{\circ})^{S-W}$ should respond to the extent of solvent ordering induced, rather than the tength of the donor-acceptor interactions themselves.

Figure 7. Plots of $\Delta(\Delta S_{rc}^{\circ})^{s-w}$ for each amine redox couple against -a, where "a" is a parameter related to the degree of "internal order" of each solvent. Redox couples: \bullet , $Co(en)_3^{3+/2+}$; \bullet , $Ru(NH_3)_6^{3+/2+}$; \bullet , $Ru(en)_3^{3+/2+}$; \bullet , $Co(sep)_3^{3+/2+}$. Key to solvents as in notes to Figure 4.

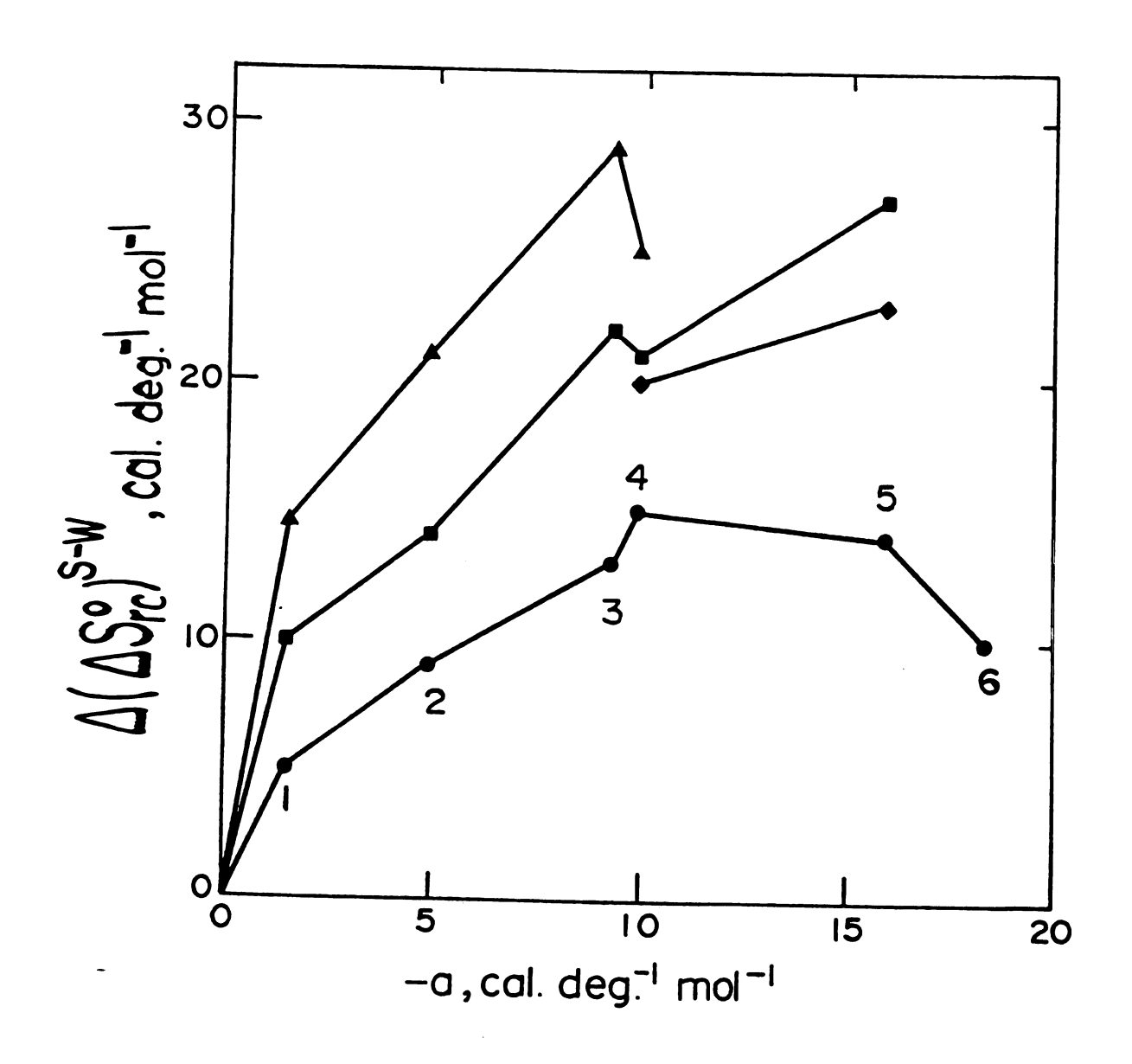


Figure 7

contact with the amine ligands are strongly oriented, variations in the strength of the donor-acceptor interactions may have only a relatively minor influence upon the extent of this orientation. Indeed, the markedly larger experimental values of ΔS_{rc}^{o} in a given solvent compared to the Born predictions (Table 8) suggest that there commonly is extensive additional short-range solvent polarization induced by the oxidized form of the redox couple, most likely involving oriented solvent molecules in the first solvation sphere.

Nevertheless, some influence of solvent donicity upon $\Delta S_{\mathbf{rc}}^{\mathbf{o}}$ for couples containing electron acceptor sites might be expected. Indeed, a comparison of the plots of $\Delta (\Delta S_{rc}^{\circ})^{s-w}$ versus D.N. for the saturated amine couples (Figure 6) with the corresponding plots for the polypyridine couples (Figure 3) reveals that the values of $\triangle (\Delta S_{rc}^{\circ})^{s-w}$ for the former systems tend to increase more C → r decrease less) with increasing D.N. in comparison with those for the latter systems. Further, a number of aquo r = dox couples of the form $M(OH_2)_6^{3+/2+}$ exhibit values of $\Delta \lesssim_{rc}^{\circ}$ that are markedly (20-30 e.u.) larger than for structrally similar amine redox couples $M(NH_3)_6^{3+/2+}$ in aqueous S Olution (21). These differences are most likely due, at \perp east in part (23), to the greater extent of hydrogen bonding between the more acidic hydrogens on the aquo I i gands with surrounding oriented water molecules (21).

In view of the foregoing discussion it is interesting to examine the effects of donor-acceptor interactions between anionic redox couples and solvent molecules upon the redox thermodynamics. These effects are now discussed in the following section.

4. Anionic Couples

Inspection of the data presented in Tables 11 and 12 indicates that the redox thermodynamics of Fe(EDTA)^-/2- and $\text{Co}(\text{EDTA})^{-/2-}$ vary considerably with the nature of the solvent. Similar to the cationic redox couples, the values of ΔS_{rc}° are larger in nonaqueous media than in water, which results in uniformly positive values of $\Delta (\Delta S_{rc}^{\circ})^{\text{S-W}}$. The formal potentials for the two anionic redox couples (quoted versus Fc⁺/Fc) become more negative (<u>i.e.</u>, the values of $\Delta (\Delta G_{rc}^{\circ})^{\text{S-W}}$ become more positive) when water is replaced by other protic and subsequently aprotic solvents. These data indicate that the predominant contribution to $\Delta (\Delta G_{rc}^{\circ})^{\text{S-W}}$ arises from the enthalpic component $\Delta (\Delta H_{rc}^{\circ})^{\text{S-W}}$.

As expected the simple dielectric continuum Born model is unable to predict the observed variations in $\Delta(\Delta G_{rc}^{\circ})^{S-W}$ for the anionic redox couples. Similar to the cationic redox couples the interactions of Fe(EDTA)^{-/2-} and Co-(EDTA)^{-/2-} with the solvent molecules can be discussed in terms of donor-acceptor interactions. It has been sugset sted by Gutmann and coworkers (89-91) that the solvent

generally can be regarded as an electron acceptor when interacting with anions. Figure 8 consists of plots of values of $\Delta(\Delta G_{rc}^o)^{s-w}$ and $\Delta(\Delta H_{rc}^o)^{s-w}$ against the solvent acceptor number (73) for $Fe(EDTA)^{-/2}$ couple. It is seen that there is a reasonably good correlation between $\Delta(\Delta G_{rc}^{o})^{S-W}$ or $\Delta(\Delta H_{rc}^{o})^{S-W}$ and the acceptor number. In order to explain these observations, one should consider the interaction of solvent molecules with both the oxidized and the reduced forms of the redox couple. In the two anionic complexes considered here a charge decrease in the central metal ion upon reduction will lead to a more net negative charge on the reduced species which in turn enhances its donor property and stabilization compared to the oxidized form. Such a difference in stabilization of the reduced and oxidized forms of the redox couple shifts the formal potential to a positive direction (i.e., $\Delta(\Delta G_{na}^{o})^{S-W}$ shifts toward smaller value) as the acceptor number of the solvent increases.

Similar to the cationic complexes containing polypyridine and amine ligands, it is interesting to note that the values of $\Delta(\Delta G_{rc}^{\circ})^{s-w}$ for $Co(EDTA)^{-/2-}$ and $Fe(EDTA)^{-/2-}$ are also insensitive to the electronic structure of the metal center. Table 12 reveals that there is an excellent agreement between values of $\Delta(\Delta G_{rc}^{\circ})^{s-w}$ for the two (EDTA) complexes when water is replaced by methanol. These results along with those obtained for cationic complexes (Tables 7

Figure 8. Plots of the variation in the free energy of reaction, $\Delta(\Delta G_{rc}^{\circ})^{S-W}$, and the enthalpy of reaction, $\Delta(\Delta H_{rc}^{\circ})^{S-W}$ for Fe(EDTA)^{-/2-} when changing from water to various nonaqueous solvents against the "Acceptor Number" for each solvent (81): closed symbols: $\Delta(\Delta G_{rc}^{\circ})^{S-W}$. Open symbols: $\Delta(\Delta H_{rc}^{\circ})^{S-W}$.

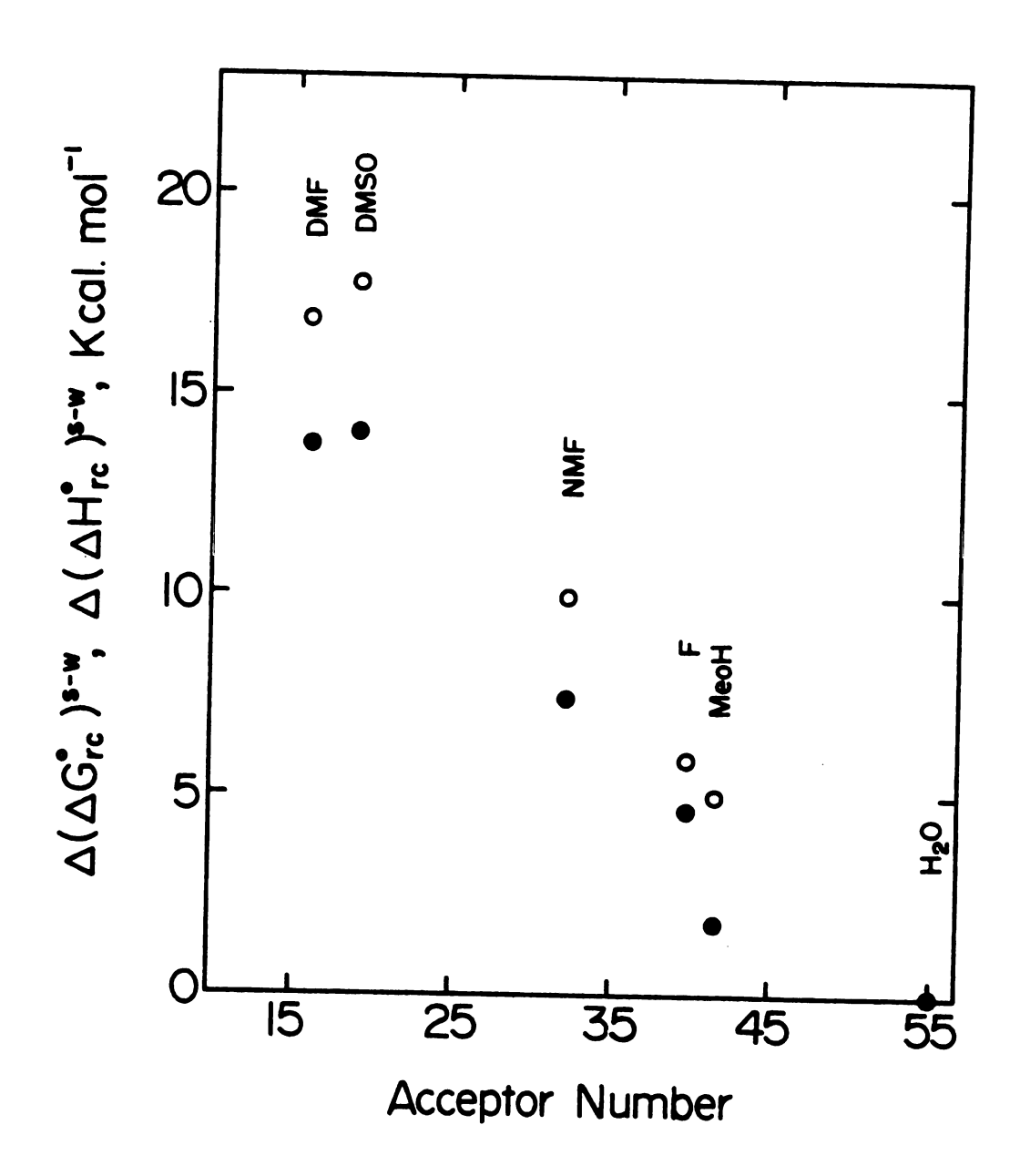


Figure 8

and 9) indicate that values of $\Delta(\Delta G_{rc}^{\circ})^{s-w}$ for couples containing different central metal ions are mainly determined by their charge, the nature of the coordinated ligands and the surrounding solvent molecules.

Turning now to the entropy data, Equation (1) predicts that the values of $(\Delta S_{rc}^{\circ})_{Born}$ for anionic couples $Fe(EDTA)^{-/2-}$ and $Co(EDTA)^{-/2-}$ in all solvents studied here (except water) are in qualitative disagreement with the experimental quantities. In view of the more negative charge residing on the reduced form of the redox couple compared to the oxidized form, one would expect negative experimental values of ΔS_{rc}^{o} in all solvents. In fact, the positive values of ΔS_{rc}^{o} obtained in all nonaqueous solvents (Table 11), suggest that the interaction of solvent molecules (as electron acceptor) with the negative ion (as electron donor) is not the only factor that can contribute toward the thermodynamics and particularly the entropies of anionic redox couples. These positive values of $\Delta S_{\mbox{\scriptsize rc}}^{\mbox{\scriptsize o}}$ for the Fe(EDTA) $^{-/2}$ and the Co(EDTA) $^{-/2}$ couples obtained in nonaqueous solvents indicate that the enhancement of solvent ordering in the vicinity of the oxidized form is greater than that of the reduced form. Although these two anionic redox couples have a net negative charge, this charge is not distributed spherically on each molecule. As a result part of the molecule (containing nitrogen atoms) is less negative compared to the other part (containing

acetate groups). Therefore solvent molecules in this case can also be regarded as electron donors and they can interact with the positive center of the redox couple. Indeed this is confirmed by the approximate linear correlation observed for the plot of $\Delta(\Delta G_{rc}^{\circ})^{S-W}$ versus solvent donor number for $Fe(EDTA)^{-/2-}$ redox couple (although this plot is less linear and has a smaller slope than the corresponding plot of $\Delta(\Delta G_{rc}^{\circ})^{S-W}$ versus acceptor number). Therefore the extent of solvent polarization (ordering) in the vicinity of the oxidized form (where the central metal ion has an oxidation state of +3) is greater than the reduced form (where the central metal ion has an oxidation state of +2). This explains the positive values of ΔS_{rc}° obtained for $Fe(EDTA)^{-/2-}$ and $Co(EDTA)^{-/2-}$ in all non-aqueous solvents studied here (Table 11).

Based on the foregoing discussion, the negative experimental values of $\Delta S_{\text{rc}}^{\circ}$ obtained in water for Fe(EDTA)^{-/2-} and Co(EDTA)^{-/2-} are somewhat surprising. One possible explanation is that the two anionic redox couples gain some water molecules upon reduction. This is probably due to greater extent of hydrogen bonding between oxygen atoms of the acetate groups (in the EDTA molecule) and the surrounding oriented water molecules in the reduced compared to the oxidized forms. Indeed the values of $\Delta S_{\text{rc}}^{\circ}$ shift toward positive as the extent of solvent hydrogen bonding decreases in the sequence water > formamide > N-methylformamide

(Table 11).

Plots of ΔS_{rc}° versus donor number or acceptor number for the two (EDTA)-complexes exhibit little correlation. On the other hand, similar to the cationic redox couples containing polypyridine and amine ligands a more successful correlation is obtained by plotting the experimental values of ΔS_{rc}° versus "a" (Figure 9). Figure 9 shows that ΔS_{rc}° increases almost uniformly as the extent of association between solvent molecules decreases. These results further indicate that the values of ΔS_{rc}° when the solvent is varied are mainly determined by the ease by which surrounding solvent can be disturbed from their bulk structure in response to the electric field.

It is apparent from the above considerations that a number of molecular factors can contribute towards the thermodynamics of outer-shell solvation even for the archetypically simple one-electron redox couples considered here. Nevertheless, an encouraging overall feature of these results is that the dependence of the redox thermodynamic parameters upon the nature of the central metal, the coordinated ligands, and the surrounding solvents fall into clear patterns which should allow predictions of the solvent-dependent behavior of structurally related redox couples to be made with some confidence.

Figure 9. Plots of ΔS_{rc}^{o} for Fe(EDTA)^{-/2-} against -a for the various solvents.

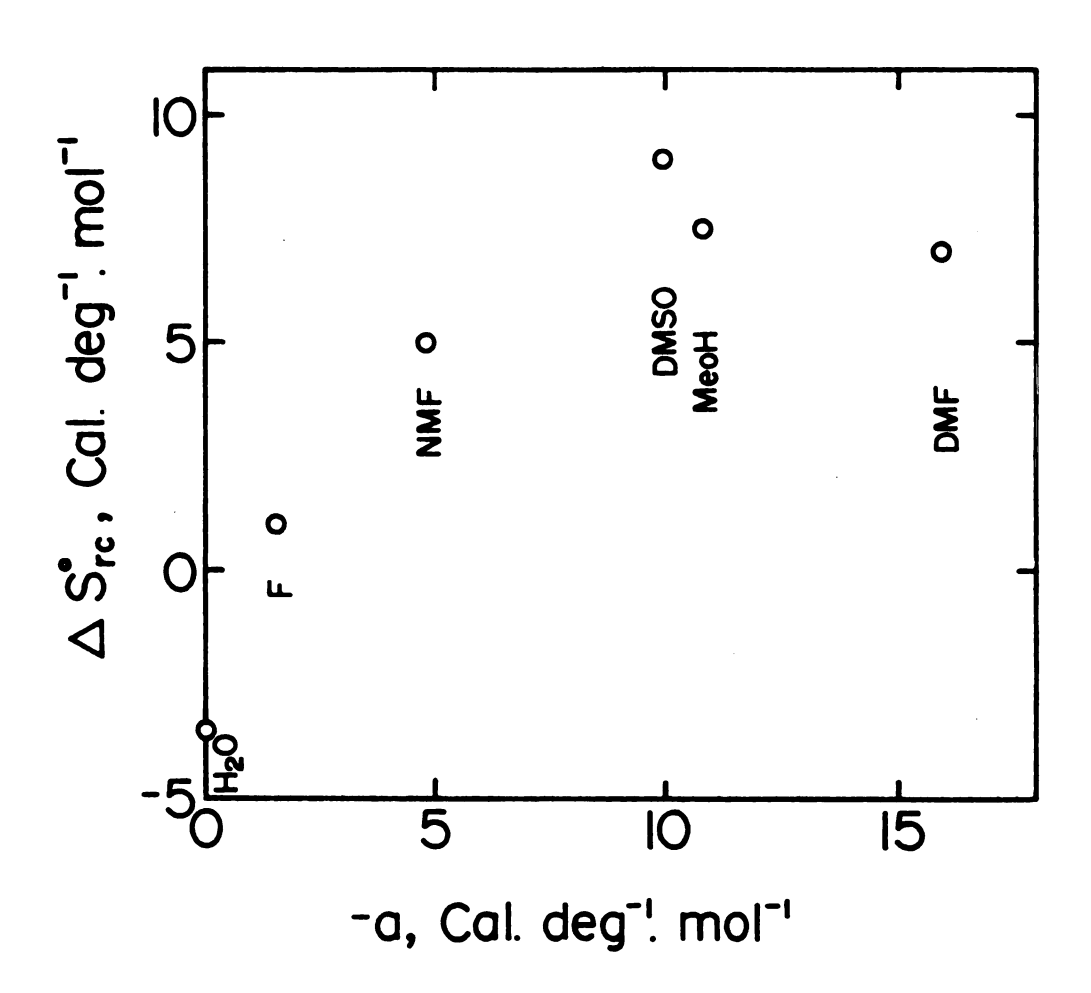


Figure 9

CHAPTER VI

SOLVENT EFFECTS ON THE KINETICS OF SIMPLE ELECTROCHEMICAL REACTIONS:

COMPARISON OF THE BEHAVIOR OF Co(III)/(II)TRISETHYLENEDIAMINE AND AMINE COUPLES WITH
THE PREDICTIONS OF DIELECTRIC CONTINUUM THEORY

A. INTRODUCTION

As noted in Chapter I, the majority of studies of solvent substitution on the kinetics of electrode reactions have employed substitutionally labile cations where the observed effects can arise from changes in the composition of the coordination shell (inner-shell effect), as well as variations in the energy required to reorganize solvent molecules beyond the primary coordination shell (outer-shell contribution).

In this chapter electrode kinetics of substitutionally inert reactants are presented. Electrode kinetic parameters for $Co(en)_3^{3+/2+}$ couple evaluated at mercury electrodes in water and six nonaqueous solvents are discussed. In addition, the solvent dependencies of the rate parameters are compared with the predictions of the dielectric continuum model formulated by Marcus (10a). Rate-potential data are also given for the reduction of the structurally similar complexes $Co(NH_3)_6^{3+}$ and $Co(NH_3)_5^{F^{2+}}$ in these solvents.

Ach of the three reactants studied here are expected to chavior at the mercury-aqueous (13,75) and mercury-non-queous interfaces (see Chapter VII).

B. EXPERIMENTAL

Heterogeneous rate constants k_{app} as a function of electrode potential (13) were obtained for the reduction of $Co(en)_3^{3+}$, $Co(NH_3)_6^{3+}$, and $Co(NH_3)_5F^{2+}$ at a dropping mercury electrode (d.m.e.) by means of d.c. and normal pulse polarography. The d.m.e. had a mechanically controlled drop time of 2 sec. Reactant concentrations between 0.5 and 1 mM were usually employed. The analyses of polarographic waves utilized the methods due to Koutecky (98), and Oldham and Parry (99). These methods are very suitable for irreversible polarograms, and allow rate constants in the range of 10^{-4} to 4 x 10^{-2} cm/sec to be evaluated reliably. The reductions of $Co(NH_3)_6^{3+}$ and $Co(NH_3)_5^{2+}$ are totally irreversible (i.e., no significant back reaction) since the products rapidly yield solvated Co(II) which cannot be reoxidized to Co(III) except at markedly more positive potentials (13). The greater stability of $Co(en)_3^{2+}$ can result In significant anodic back reaction contributions to the \triangleright olarographic reduction of Co(en) $_3^{3+}$ in several solvents as cidenced by the presence of significant anodic current on he return scan of cathodic-anodic cyclic voltammograms. Wever, this unwanted complication was eliminated where Cessary by adding a small (≤5 mM) concentration of Ni²⁺ \sim z_n^{2+} . These cations preferentially complex the ethyleneamine released upon formation of Co(II) which acts to en- \sim urage dissociation of the remaining $Co(en)_3^{2+}$ and therefore eliminate the anodic back reaction. Values of k_{app} for Co(en)_3^{3+} could therefore be determined at significant cathodic under-potentials as well as over-potentials which assisted the evaluation of rate parameters in media where the measured formal (i.e., "standard") rate constants k_{app}^f were fairly large (>10⁻² cm/sec). The measured rate constants were generally reproducible to within ca. 10-20%. Formal potentials for the $\text{Co(en)}_3^{3+/2+}$ couple were obtained in the same electrolytes using cathodic-anodic cyclic voltammetry as was described in Chapter V.

An aqueous saturated calomel electrode (s.c.e.) was used as the reference electrode, although for convenience electrode potentials were quoted here versus the formal potential for the ferricinium/ferrocene redox couple (Fc⁺/Fc) determined in the same solvent and supporting electrolyte.

Further experimental details are given in Chapter II.

C. RESULTS

Table 14 summarizes rate-potential data for the oneextraction of $Co(en)_3^{3+}$ in each solvent expressed
an apparent (experimental) cathodic rate constant k_{app}^{-800} assured at -800 mV versus the ferricinium-ferrocene (Fc⁺/Fc)
cuple in the same electrolyte. Also listed are the apparent
thodic transfer coefficients α_{app} obtained from the
experimental Tafel plots using $\alpha_{app} = -f^{-1}(\partial \ln k_{app}/\partial E)_{\mu}$ ere f = F/RT, and μ denotes a given electrolyte composition
end of the extent

Malle 14, Solvent Dependence of Electrochemical Kinetic Parameters for the Co(en)3+/2+ Couple at Mercury Electrodes at 25°C.

		kapp	a _{app}	kcorr	-Ed	k e kapp	k ^f f
Solvent	Electrolyte	cm.s-1		cm.s-1	mV vs Fc+/Fc	cm.s-1	cm.s-1
Water	0.1M KPF6 ^g 0.4M KPF6 ^g	~100j ~30 ^j	0.95	~50 ~30	565 580	3x10 ⁻² 5x10 ⁻²	3x10 ⁻² 2.5x10 ⁻²
Formamide	0.1 <u>M</u> Licio ₄ 0.1 <u>M</u> TEAP ^h 0.5 <u>M</u> Licio ₄	3x10 ⁻³ 2x10 ⁻³ 3.5x10 ⁻³	1.0	1x10 ⁻³	813 806 800	4.5x10 ⁻³ 2.5x10 ⁻³ 3.5x10 ⁻³	1.3x10 ⁻³
NMF	$0.1\underline{M}$ L1ClO $_{\mu}$	3.5x10 ⁻⁵ 2.5x10 ⁻⁵	0.95	1.5x10 ⁻⁵	945 943	7×10 ⁻³ 4×10 ⁻³	6.5x10 ⁻⁴
PC	0.1 <u>M</u> L1C1O ₄ 0.1 <u>M</u> TEAP ^h	4x10 ⁻² 2x10 ⁻²	9.0	1.1x10 ⁻³	632 633	4.5x10 ⁻³ 4.5x10 ⁻³	3×10 ⁻⁴
AN	0.1 <u>M</u> L1C1O ₄ 0.1 <u>M</u> TEAP ¹	0.35 0.25j	7.0	4×10 ⁻³	290	1.0×10 ⁻³	1.3×10 ⁻³
DMSO	0.1M L1C104 0.1M TEAP ^h 0.5M L1C10 ₁₁	3x10 ⁻⁶ 2x10 ⁻⁶ 1.0x10 ⁻⁶	0.85	2,5x10 ⁻⁷ 2x10 ⁻⁷ 4x10 ⁻⁷	1040	8.5x10 ⁻³	8x10 ⁻⁶ 2x10 ⁻⁵

Table 14. Continued.

$ \begin{array}{cccccccccccccccccccccccccccccccccccc$								
olvent Electrolyte $_{\rm cim.s}^{-1}$ $_{\rm cim.s}^{\rm mV}$ $_{\rm vs}^{\rm s}$ $_{\rm re.s}^{\rm re}$ $_{\rm Fc}^{\rm t/Fc}$ $_{\rm cm.s}^{\rm -1}$ 0.95 $_{\rm rx10}^{\rm re}$ $_{\rm pro}^{\rm s}$ $_{\rm pro}^{\rm s}$ 0.95 $_{\rm s.5x10}^{\rm ro}$ $_{\rm pro}^{\rm s}$ $_{\rm pro}^{\rm s}$			k_800 ^a	α_{app}	k _{corr}	-Efd	kf e app	k ^f f
0.1M L1ClO _{μ} 5x10 ⁻⁶ 0.95 7x10 ⁻⁷ 968 3x10 ⁻³ 0.1M TEAP ^h 5x10 ⁻⁶ 0.95 8.5x10 ⁻⁷ 970 μ x10 ⁻³	Solvent	Electrolyte	cm.s-1		сш.з-1	mV vs Fc+/Fc	cm.s	cm.s-1
	DMF	0.1М L1С1О ₄ 0.1М ТЕАР ^ћ	5×10 ⁻⁶ 5×10 ⁻⁶	0.95	7×10 ⁻⁷ 8.5×10 ⁻⁷		3×10 ⁻³ 4×10 ⁻³	1x10-5

^aApparent (experimental) rate constant for Co(en) $^{3+}$ reduction in solvent and electrolyte indicated, measured at -800 mV vs. formal potential for ferricinium-ferrocene couple $\Re c^{+}$ / Fc) in same media.

 $^{
m b}$ Apparent cathodic transfer coefficient in solvent and electrolyte indicated, obtained from $\alpha_{app} = -(RT/F)(\partial \ln k_{app}/\partial E)\mu$. ^cDouble-layer corrected rate constant at -800 mV vs Fc⁺/Fc, obtained from corresponding value of k-800 using Equation (1) assuming that $Z_{\rm r}$ = 3 and $\alpha_{\rm I}$ \sim 0.6-0.7 (see text). Sources of electrode capacitance data used to estimate q^m - E curves and hence values of ϕ_d employed in Equation (1): Water, Reference 101; formamide, Reference 106; NMF, Reference 100b; AN, R. Payne, J. Phys. Chem., 71, 1548(1967); PC, DMSO, DMF, R. Payne,

^dFormal potential for Co(en) $_3^{3+}$ couple against Fc⁺/Fc, determined in stated media using cyclic voltammetry (see text).

 $^{\rm e}$ Apparent "formal" rate constant ($\frac{1.e.}{1.e.}$, measured at ${\rm E}_{\rm f}$) in stated media.

f Double-layer corrected formal rate constant, obtained from corresponding value of k_{app}^f using Equation (1) assuming that Z_r = 3 and α_{corr} $^{\circ}$ 0.6-0.7 (see text).

hsolution contained $\sim 5 \text{ mM}$ Ni²⁺. ¹Solution contained ~ 5 JExtrapolated value. golution contained ~2 mM H⁺.

of data extrapolation that was required, and provided a convenient basis for the kinetic analysis described below.) Since the Tafel plots were essentially linear over the ca. 200 mV overpotential range that was typically accessible, a single value of $\boldsymbol{k}_{\text{app}}$ and $\boldsymbol{\alpha}_{\text{app}}$ suffice to describe the rate parameters in a given electrolyte. Values of the apparent formal rate constants k_{ann}^{f} for $Co(en)_3^{3+/2+}$ were determined by interpolation or extrapolation to the appropriate formal potential $\mathbf{E}_{\mathbf{f}}$ in each electrolyte. In most cases the electrolyte composition was chosen to be 0.1 M lithium perchlorate or 0.1 M tetraethylammonium perchlorate (TEAP). These electrolytes probably exhibit negligible specific adsorption at the small to moderate negative electrode charge densities q^{m} where the kinetics were monitored in nonaqueous media (100), and perchlorate anions have only a small tendency to form ion pairs with the cationic reactant. In aqueous media 0.1 M and 0.4 M potassium hexafluorophosphate were sed as supporting electrolytes since the kinetics were easured at small positive values of q^m where perchlorate mecific adsorption is quite noticeable. Hexafluorophos-Plate adsorption is sufficiently weak so that small posi-Two values of the potential across the diffuse layer ϕ_d re obtained under these conditions (75, 101, 102).

The choice of these electrolytes therefore enabled the equired diffuse-layer corrections to the cathodic rate arameters to be made with some confidence using the

relation (e.g., Reference 75)

$$\ln k_{corr}^{E} = \ln k_{app}^{E} + f(Z_{r} - \alpha_{corr})\phi_{d}$$
 (1)

where k_{corr}^E is the "double-layer corrected" rate constant corresponding to the measured value k_{app}^E at a given electrode potential E, Z_r is the charge on the reactant, and α_{corr} is the transfer coefficient after correction for double-layer effects. This last quantity can be obtained from α_{app} using

$$\alpha_{corr} = \frac{\alpha_{app} - Z_r(\partial \phi_d / \partial E)_u}{1 - (\partial \phi_d / \partial E)_u}$$
 (2)

Equations (1) and (2) involve the assumptions that the reaction site lies at the outer Helmholtz plane (o.H.p.) and that discreteness-of-charge effects are negligible (75). However, they have been shown (13,75) to be approximately consistent with experimental kinetic data for (III) amine reductions in a wide range of aqueous supprting electrolytes when ϕ_d is calculated from doublewayer compositional data using the Gouy-Chapman-Stern (GCS) heory (103). The required values of ϕ_d in aqueous media ere obtained from the double-layer data in Reference 101 of References 75 and 102). The values of ϕ_d in

nonaqueous media were determined as follows. Electrode charge-potential $(q^m - E)$ plots were obtained by integrating the appropriate capacitance-potential curves taken from the literature (see footnote (c) to Table 14 for sources) along with the p.z.c. values determined in the present work. These p.z.c. values obtained in 0.1 M perchlorate media are (vs. Fc +/Fc, values vs. s.c.e. given in parentheses): formamide, -729 mV (-448 mV); NMF, -732 mV (-335 mV); PC, -601 mV (-273 mV): AN, -622mV (-250 mV); DMSO, -717 mV (-278 mV); DMF, -691 mV (-198 mV). The values of q^{m} at the required electrode potentials were then read off from these plots and inserted into the GCS expression (103) to find the corresponding values of ϕ_d . Values of α_{corr} were also determined in a similar manner from the corresponding values of α_{app} (Table 14) using Equation (2); they varied typically in the range ca. 0.5 - 0.7. (Although the quantitative validity of these estimates of α_{corr} is questionable, this uncertainty has little influence upon the extent of the double-layer correction since $Z_r >> \alpha_{corr}$.)

The resulting values of $k_{\rm corr}^{-800}$ and $k_{\rm corr}^{\rm f}$ are also listed in Table 14. In a given solvent, it was found that the corresponding values of $k_{\rm corr}$ determined in the various electrolytes, including 0.5 M LiClO₄ as well as 0.1 M LiClO₄ are typically in reasonable agreement (Table 14), which supports the approximate validity of the double-layer corrections.

It is seen that the values of k_{corr}^{f} as well as k_{corr}^{-800} vary markedly with the nature of the solvent, being substantially smaller in nonaqueous media, particularly DMSO and DMF, compared with the corresponding rate constants in water. In view of these marked solvent influences upon the electrode kinetics of $Co(en)_3^{3+/2+}$, it is of interest to ascertain if the structurally simpler $Co(NH_3)_6^{3+/2+}$ couple exhibits similar behavior. The kinetic parameters for $Co(NH_3)_6^{3+}$ reduction are summarized in Table 15, along with those for $Co(NH_3)_5F^{2+}$ reduction. The latter exhibits similar rate parameters to the $Co(NH_3)_6^{3+}$ reduction in aqueous media (13) yet carries a smaller net charge so that the possible influence of varying Z_r upon the solvent effects can be assessed. Inspection of Table 15 reveals that the corresponding values of k_{corr}^{-800} for $Co(NH_3)_6^{3+}$ and $Co(NH_3)_5^{2+}$ reduction in most solvents are within a factor of three or so of each other, whereas those for $Co(en)_3^{3+}$ reduction tend to be between five and tenfold smaller.

D. DISCUSSION

Following the treatment given in Chapter III for evaluation of electrode kinetic parameters in different solvents Equation (3) (Equation (24) of Chapter III) was used to obtain estimates of $\Delta(\Delta G_{\text{corr}}^{\neq})_{\text{c}}^{\text{S-W}}$, the change in the chemical part of the activation free energy for a given reaction when a nonaqueous solvent was substituted for water.

electron Reduction of Co(NH $_3$) $_6^3$ and Co(NH $_3$) $_5$ F 2 + at Mercury Electrodes at Solvent Dependence of Electrochemical Kinetic Parameters for the One-Table 15.

		Co(NH ₃	$co(NH_3)_6^{3+}$ Reduction	tion	Co(NH ₃)	Co(NH ₃) ₅ F ²⁺ Reduction	ıction
		k-800 ^a	dapp	kcorr	kapp	app b	k-800°
Solvent ^d	Electrolyte	cm.s-1		cm.s-1	cm.s-1		cm.s-1
Water	O.1M KPF ₆	72	0.65	n5	κ	0.58	رم.
Formamide	0.1M Liclou	5×10 ⁻³	0.95	1.5x10 ⁻³	3.5×10^{-3}	92.0	$2x10^{-3}$
NMF	$0.1M \text{ Liclo}_{\mu}$	$2x10^{-4}$	06.0	9×10 ⁻⁵	1.2x10 ⁻⁴	99.0	7×10 ⁻⁵
PC	0.1M Liclou	0.3	0.65	8x10 ⁻³	$2x10^{-2}$	99.0	2.5×10^{-3}
DMSO	0.1M Liclou	1.5×10 ⁻⁵	1.0	1.5x10 ⁻⁶	7×10 ⁻⁶	0.65	1.7×10 ⁻⁶
DMF	0.1M L1ClO $_{f \mu}$	1.1×10 ⁻⁴	0.9	1.5x10 ⁻⁵	3.5×10 ⁻⁵	2.0	1.0x10 ⁻⁵

 $^{\rm a}{\rm Apparent}$ (experimental) rate constant in solvent and electrolyte indicated, measured at -800 mV vs. formal potential for ferricinium-ferrocene couple in same media.

^bApparent transfer coefficient in solvent and electrolyte indicated, obtained from $\alpha_{app} = (-RT/F)(3 \ln k_{app}/3E)_{\mu}$.

^cDouble-layer corrected rate constant corresponding to quoted value of $k_{\rm app}^{-800}$; obtained using Equation (1) assuming that $Z_{\rm r}=3$ for Co(NH₃) $_6^3$ and $Z_{\rm r}=2$ for Co(NH₃) $_5^{\rm F}$ reduction, respectively. (For further details, see text and footnote (c) to Table 14.)

dKinetic data were not obtained in acetonitrile due to insufficient reactant solubility in this solvent.

RT ln
$$(k_w/k_s)_{corr}^{\phi_m} = \Delta(\Delta G_{corr}^{\neq})_c^{s-w}$$
 (3)

In this equation $k_{\tilde{W}}$ and $k_{\tilde{S}}$ are the double layer corrected rate constants measured at a constant Galvani potential in water and nonaqueous solvents, respectively.

As mentioned in Chapter III evaluation of $\Delta(\Delta G_{COTT}^{\neq})_{C}^{S-W}$ like $\Delta(\Delta G_{rc}^{o})^{S-W}$ requires an extrathermodynamic assumption. If the ferrocene assumption is correct, then the values of k_{corr} evaluated at a fixed electrode potential (-800 mV) versus Fc +/Fc given in Tables 14 and 15 can be inserted directly into Equation (3) to yield estimates of $\Delta(\Delta G_{COTT}^{\neq})_{c}^{S-W}$. Since, the "tetraphenylarsonium-tetraphenylborate" (TATB) assumption is a more reliable procedure than the ferrocene assumption (see Chapters III and V), it is preferable to apply a correction to the electrode potentials employed in each of the various nonaqueous solvents in order to take into account the likely deficiencies of the Fc +/Fc and convert the free energies to the TATB scale. Therefore the value of k_{corr} in each nonaqueous solvent that was inserted into Equation (3) was obtained at an electrode potential differing from -800 mV vs. Fc⁺/Fc by an amount ΔE found from

$$-F\Delta E = \Delta (\Delta G_{rc}^{o})_{Fc}^{s-w}$$
 (4)

where $\Delta(\Delta G_{rc}^{o})_{Fc}^{s-w}$ is the value of $\Delta(\Delta G_{rc}^{o})^{s-w}$ for the Fc⁺/Fc

couple in a given nonaqueous solvent on the TATB scale. [Literature estimates of $\Delta(\Delta G_{rc}^{\circ})_{Fc}^{s-w}$ are given in Table 7.] The resulting values of $\Delta(\Delta G_{corr}^{\neq})_{c}^{s-w}$ for $Co(en)_{3}^{3+}$ and $Co(NH_{3})_{6}^{3+}$ reduction on the TATB scale are listed in Table 16, along with the corresponding estimates of $\Delta(\Delta G_{rc}^{\circ})_{s-w}^{s-w}$ for the $Co(en)_{3}^{3+/2+}$ couple which are taken from Table 9. (Although there are inevitable uncertainties in the use of such extrathermodynamic procedures, the values of $\Delta(\Delta G_{rc}^{\neq})_{c}^{s-w}$ similar to the values of $\Delta(\Delta G_{rc}^{\circ})_{c}^{s-w}$ are probably accurate to about ± 1 Kcal mol⁻¹.)

It is seen that the values of $\Delta(\Delta G_{rc}^{\neq})_c^{s-w}$ for $\mathrm{Co(en)}_3^{3+}$ reduction are uniformly positive and larger than the corresponding values of $\Delta(\Delta G_{rc}^{\circ})^{s-w}$; i.e., the destabilization of the transition state for $\mathrm{Co(en)}_3^{3+}$ reduction relative to the bulk reactant when substituting nonaqueous for aqueous media is uniformly greater than that for the bulk product. Although values of $\Delta(\Delta G_{rc}^{\circ})^{s-w}$ for $\mathrm{Co(NH}_3)_6^{3+/2+}$ are unobtainable, they are likely to be closely similar to those for $\mathrm{Co(en)}_3^{3+/2+}$ (Chapter V) so a similar result probably also applies to the amine couple.

It was shown in Chapter V that the values of $\Delta(\Delta G_{rc}^{\circ})^{S-W}$ for M(III)/(II) amine and ethylenediamine couples are much larger than the dielectric continuum (Born) predictions; they were interpreted in terms of donor-acceptor interactions between the amine hydrogens and the solvent molecules. Thus $\Delta(\Delta G_{rc}^{\circ})^{S-W}$ has been shown to increase

Table 16. Estimates of the Variations in the Potential-independent Free Energy of Activation $\Delta(\Delta G_{\text{corr}}^{\neq})_{\text{c}}^{\text{S-W}}$ for Co(en)_3^{3+} and $\text{Co(NH}_3)_6^{3+}$ Reduction Resulting From Substituting Various Nonaqueous Solvents for Water.

	Δ(ΔG [≠] _{corr}) ^{s-w} ,	kcal.mol ⁻¹	$\Delta(\Delta G_{rc}^{\circ})^{s-wb}$ Kcal.mol ⁻¹
Solvent	$Co(en)_3^{3+} red^{\underline{n}}$	$Co(NH_3)_6^{3+} red^{\underline{n}}$	Co(en)3+/2+
Formamide	5.5	4.0	3.7
NMF	7.5	5.5	6.3
PC	5.5	3.0	- 0.9
AN	4.0		- 3.5
DMSO	10.0	7.0	7.9
DMF	8.0	6.0	5.8

activation (on TATB scale) resulting from altering solvent from water to solvent indicated. Obtained from rate data in Table 14 using Equation (3); values of k_{corr} evaluated at -800 mV. vs. Fc /Fc in water and at potentials of (-800- Δ E) mV. vs. Fc +/Fc in each nonaqueous solvent, where Δ E is given by Equation (4) (see text). [Resulting values of $\Delta(\Delta G_{corr}^{\neq})_{c}^{s-w}$ are rounded off to nearest 0.5 kcal.

^bChange in free energy of $Co(en)_3^{3+/2+}$ couple (on TATB scale) when solvent altered from water to solvent indicated at ionic strength μ = 0.1. Taken from Table 9.

monotonically with increasing basicity of the solvent, suggesting that there are strong ligand-solvent interactions in the tripositive (oxidized) state which are partly dissipated upon reduction as a consequence of the smaller charge of the product. At first sight, the even larger values of $\Delta(\Delta G_{\text{corr}}^{\neq})_{\text{c}}^{\text{S-W}}$ are surprising on this basis since the transition state is expected to have a solvent structure that is suitably intermediate between those for the reactant and product.

As noted in Chapter III, $\Delta(\Delta G_{\text{corr}}^{\neq})_{\text{c}}^{\text{s-w}}$ can be separated into intrinsic and thermodynamic contributions by

$$\Delta(\Delta G_{i}^{\neq})^{s-w} = \Delta(\Delta G_{corr}^{\neq})_{c}^{s-w} - \alpha_{corr} \Delta(\Delta G_{rc}^{\circ})^{s-w}$$
 (5)

and $\Delta(\Delta G_1^{\neq})^{S-W}$ is given by

$$\Delta(\Delta G_1^{\neq})^{S-W} = RT \ln(k_w^f/k_s^f)_{corr}$$
 (6)

(See Equations (29a) and (29b) of Chapter III for more detailed explanations.)

Table 17 contains values of $\Delta(\Delta G_1^{\neq})^{S-W}$ for the $Co(en)_3^{3+/2+}$ couple obtained using Equation (6) from the standard rate constants listed in Table 14. As expected from Equation (5) given that $\Delta(\Delta G_{corr}^{\neq})_c^{S-W} > \Delta(\Delta G_{rc}^{\circ})_c^{S-W}$ (Table 16) it is seen that the values of $\Delta(\Delta G_1^{\neq})_c^{S-W}$ are uniformly positive; they approach 5 Kcal mol⁻¹ for DMSO

Table 17. Experimental Estimates of the Variations in the Intrinsic Barrier $\Delta(\Delta G_1^{\neq})^{S-W}$ for $Co(en)_3^{3+/2+}$ Resulting from Substituting Various Nonaqueous Solvents for Water. Comparison with Predicted Variations $\Delta(\Delta G_1^{\neq})_{calc}^{S-W}$ from Dielectric Continuum Theory.

	Δ(ΔG [≠] _i) ^{s-w}	Kca	G≠)s-w ^b i)calc 1.mol1
Solvent	Kcal.mol ^{-la}	$R_e = \infty^c$	$R_e = 2(a+L)^d$
Formamide	1.8	-0.9	-0.3
NMF	2.3	-0.8	-0.2
PC	2.7	-0.8	-0.2
AN	1.8	-0.3	0.3
DMSO	4.9	- 1.3	-0.6
DMF	4.7	-1.0	-0.3

^aObtained from values of k_{corr}^{s} listed in Table 14 using Equation (6).

^bDifference between dielectric continuum estimate of the outer-shell intrinsic barrier $(\Delta G_{1}^{\neq})_{OS}$ in given nonaqueous solvent and that for water obtained from Table 18 using Equation (7).

^cSee footnote c of Table 18.

dSee footnote d of Table 18.

and DMF. As noted above, it is likely that the maintenance of a constant ligand composition around the reactant will keep the inner-shell contribution to the reorganization energy, and hence to ΔG_1^{\neq} , approximately constant as the surrounding solvent is varied. It is therefore probable that any variations in ΔG_1^{\neq} resulting from altering the solvent are due to variations in the outer-shell contribution $(\Delta G_1^{\neq})_{OS}$.

As mentioned in Chapter III the usual theoretical model for outer-shell reorganization treats the surrounding solvent as a uniform dielectric continuum, which according to Marcus (10a,78,104) yields the following expression for the intrinsic barrier:

$$(\Delta G_{i}^{\neq})_{os} = \frac{e^{2}}{8} \left(\frac{1}{a} - \frac{1}{R_{e}}\right) \left(\frac{1}{\varepsilon_{op}} - \frac{1}{\varepsilon_{s}}\right) \tag{7}$$

where e is the electronic charge, $\varepsilon_{\rm op}$ and $\varepsilon_{\rm s}$ are the optical and static solvent dielectric constants, a is the radius of the (spherical) reactant, and R_e is twice the distance from the reacting species in the transition state to the electrode surface; <u>i.e.</u>, the distance from the ion to its "image" in the metal. The (1/R_e) term in Equation (7) therefore describes the stabilization of the transition state relative to the reactant ground state afforded by the presence of imaging interactions with the metal

electrode (10a,104). However, it has been pointed out that this term could overestimate the importance of image forces since Equation (7) ignores the screening effect of the surrounding ions (105). It appears to be likely that the reaction sites for Co(III) amine reduction lie outside the primary inner layer of solvent molecules, and close to the outer Helmholtz plane (13) (o.H.p.) where some diffuse-layer screening of the image interactions can be expected. Consequently, values of $(\Delta G_1^{\neq})_{OS}$ were calculated from Equation (7) for the various solvents in two ways (Table 18). Either R_{a} was set equal to infinity (<u>i.e.</u>, imaging was neglected) or taken as 2(a + L), where a is the reactant radius and L is the length of the solvent molecule L, since there is evidence that the thickness of the inner layer in some nonaqueous solvents roughly corresponds to L (106). The value of L was taken as 3 $^{\rm A}$ for water (107), and 6 Å for the nonaqueous solvents (106); a was taken to be 3.5 Å (appropriate for $Co(en)_3^{3+/2+}$ and $Co(NH_3)_6^{3+/2+}$ (73)).

Values of $\Delta(\Delta G_{\mathbf{i}}^{\neq})_{\mathrm{calc}}^{\mathbf{s-w}}$ obtained from the difference between the corresponding calculated values of $(\Delta G_{\mathbf{i}}^{\neq})_{\mathrm{os}}$ in each nonaqueous solvent with that in water given in Table 18 and are also listed in Table 17, both for $R_{\mathbf{e}} = \infty$ and $R_{\mathbf{e}} = 2(\mathbf{a} + \mathbf{L})$. It is seen that in both cases small negative values of $\Delta(\Delta G_{\mathbf{i}}^{\neq})^{\mathbf{s-w}}$ are typically obtained, in contrast to the larger and positive experimental values

Table 18. Calculated Values of the Outer-shell Intrinsic Barrier for $Co(en)_3^{3+/2+}$ from Dielectric Continuum Theory.

Solvent	$\epsilon_{op} = n^{2^a}$	$(\Delta G_{1}^{\neq})_{os}^{b,c}$ $(\Delta G_{1}^{\neq})_{os}^{b,c}$	(ΔG [≠] _i) _{os} Kcal.mol ⁻¹
Water	1.775	6.3	4.7
Formamide	2.090	5.4	4.4
NMF	2.050	5.5	4.5
PC	2.013	5.5	4.5
AN	1.800	6.0	5.0
DMSO	2.178	5.0	. 4.1
DMF	2.036	5.3	4.4

 $^{^{\}rm a}$ Values of $\epsilon_{\rm op}$ for each solvent obtained from refractive indices n listed in "Handbook of Chemistry and Physics", CRC Press, Cleveland, Ohio.

^bEstimate of the outer-shell intrinsic barrier $(\Delta G_{1}^{\neq})_{os}$ calculated from Equation (7), (e²/8 = 40.29), for listed solvents. Values of ε_{s} are listed in Table 2.

^cCalculated from Equation (7) assuming that a = 3.5 Å, and $R_e = \infty$.

^dCalculated from Equation (7) assuming that a = 3.5 Å, $R_e = 2 (a + L)$, where L = 3 Å in water and 6 Å in non-aqueous solvents (see text).

obtained for $\text{Co(en)}_3^{3+/2+}$. (Similar results were also obtained using other plausible values of a and R_{e}). It is therefore concluded that the solvent dielectric continuum model is unable to account for the observed solvent dependence of the electrochemical kinetics of $\text{Co(en)}_3^{3+/2+}$.

Values of $\Delta(\Delta G_1^{\neq})^{S-W}$ cannot be obtained for $\mathrm{Co(NH_3)}_3^{3+/2+}$ since the formal potentials for this couple are unknown. However, the values of $\Delta(\Delta G_{\mathtt{corr}}^{\neq})_c^{S-W}$ for $\mathrm{Co(NH_3)}_3^{3+}$ reduction are only marginally smaller than those for $\mathrm{Co(en)}_3^{3+}$ reduction (Table 16), and consistently larger than the values of $\Delta(\Delta G_{\mathtt{rc}}^{\circ})^{S-W}$ for $\mathrm{Co(en)}_3^{3+/2+}$ and other amine redox couples (including $\mathrm{Ru(NH_3)}_6^{3+/2+}$) (Table 9). Therefore given that $\alpha_{\mathtt{corr}}$ is 0.5-0.7 (13), it follows from Equation (5) that $\mathrm{Co(NH_3)}_6^{3+/2+}$ as well as $\mathrm{Co(en)}_3^{3+/2+}$ would likely yield values of $\Delta(\Delta G_1^{\neq})^{S-W}$ which are in qualitative disagreement with the dielectric continuum predictions.

Two factors appear most likely to be responsible for these apparent discrepancies between theory and experiment. First, it seems feasible that the electron tunneling probability within the transition state (i.e., the transmission coefficient κ in Equations (21) and (27) of Chapter III) could be substantially smaller in some non-aqueous solvents than in water as a result of the probable differences in inner-layer thickness that were noted above.

Such a situation would render Equation (6) invalid and yield values of $\Delta(\Delta G_i^{\neq})^{S-W}$ that are falsely large. If the distance D between the reaction plane and the electrode surface (= 0.5 R_a) is given roughly by D = (a + L), D may well increase from 6.5 $ilde{A}$ in water to around 8-9 $ilde{A}$ in nonaqueous solvents of intermediate molecular weight such as those considered here. Although the question of whether outer-sphere electron transfer is commonly nonadiabatic ($\kappa << 1$) or adiabatic ($\kappa \sim 1$) has been the subject of extensive debate (108), the likely dependencies of K upon the distance between and the nature of the redox centers are largely unsettled. However, recent electron tunneling calculations (109) for $Fe(OH_2)_6^{3+/2+}$ selfexchange in homogeneous solution indicate that κ falls rapidly as the internuclear distance increases above about 6 Å (e.g., $\kappa \sim 10^{-3}$ at 6.9 Å (109)). Comparable results have been obtained with tunneling calculations performed for heterogeneous $Fe(OH_2)_6^{3+/2+}$ exchange (110). If the reactant indeed does not penetrate the inner layer of solvent molecules in the transition state for electron transfer (i.e., outer-sphere electrode reaction pathways are followed (9,111), then the resulting increases in D when substituting nonaqueous solvents for water could be responsible for the smaller values of k_{corr}^f in the former media via smaller values of k rather than larger values of ΔG_{i}^{\neq} (Equation (27) of Chapter III).

Nevertheless, it seems likely that the observed behavior is at least partly due to variations in $(\Delta G_1^{\not f})_{os}$ arising from the more extensive changes in short-range solvent structure that may be necessary in order to surmount the Franck-Condon barrier in nonaqueous media. Although the likely contribution of such short-range reactantsolvent interactions has been widely recognized (71), it is difficult to provide theoretical estimates of their contribution to $(\Delta G_1^{\neq})_{OS}$. However, a valuable experimental monitor of the extent of solvent structural changes accompanying electron transfer can be obtained from measurements of reaction entropy $\Delta S_{\mathbf{rc}}^{\mathbf{o}}$ of individual redox couples (21). As mentioned in Chapter V, experimental values of reaction entropy have been found to be sensitive both to the nature of the coordinated ligands and the surrounding solvent to a much greater extent than predicted by the dielectric continuum (Born) model. This illustrates the importance of short-range ligand-solvent interactions to the changes in solvent polarization ("ordering") brought about by electron-transfer.

It was shown in Chapter V that the values of ΔS_{rc}° for $Co(en)_3^{3+/2+}$ (and also $Ru(NH_3)_6^{3+/2+}$ and $Ru(en)_3^{3+/2+}$) are substantially (up to 30 e.u.) larger in nonaqueous media, particularly DMSO and DMF, compared to the corresponding quantity in water. These variations in ΔS_{rc}° , $\Delta (\Delta S_{rc}^{\circ})^{S-W}$, were found to increase as the extent of

"internal order" (17) of the bulk solvent decreases; <u>i.e.</u>, when going from highly structured solvents, especially water, to polar yet more weakly associated liquids, especially PC, DMF, and DMSO.

Such sensitivities of $\Delta S_{\text{rc}}^{\circ}$ to the solvent medium might be expected to be reflected also in variations in the outer-shell part of the intrinsic barrier (74). Thus the formation of the transition state for $Co(en)_3^{3+}$ reduction in DMSO, for example, is expected to involve a much greater decrease in solvent polarization than the corresponding process in water in view of the large positive value of $\Delta(\Delta S_{rc}^{\circ})^{s-w}$ for DMSO (15 e.u. (Table 9)). This difference will not affect the intrinsic barrier if $\Delta(\Delta G_{corr}^{\neq})^{s-w} = \alpha_{corr} (\Delta G_{rc}^{\circ})^{s-w}$ (Equation (5)); <u>i.e.</u>, when the solvent effect upon the transition-state stability is that expected for a (hypothetical) stable cation with a structure identical to that of the transition state but having the charge $(Z_r - \alpha_{corr})$. However, in actuality the transition state is reached via the reorganization of nuclear coordinates while the reactant charge remains fixed, electron transfer occurring rapidly $(\sim 10^{-16} \text{ sec})$ once the transition state is formed (112). The required solvent reorientation will therefore be unaided by a concomitant variation in the reactant charge so that these solvent structural changes should involve an additional component of the activation energy which will contribute

to the intrinsic barrier. Generally, therefore, the presence of greater differences in the extent of solvent polarization between the oxidized and reduced halves of the redox couple would be expected to yield larger values of $(\Delta G_1^{\neq})_{os}$. However, the likely magnitude of the effect is difficult to assess.

Figure 10 is a plot of $\Delta(\Delta G_1^{\neq})^{s-w}$ for the Co(en) $\frac{3+/2+}{3}$ couple (Table 17) against the corresponding values of $\Delta S_{\mathbf{r}\mathbf{c}}^{\circ}$ in each solvent, taken from Table 8. It is seen that there is a roughly linear correlation between $\Delta(\Delta G_1^{\neq})^{S-W}$ and ΔS_{rc}° , suggesting that there is indeed a contribution to ΔG_{i}^{\neq} arising from specific short-range solvent polarization not considered in the dielectric continuum treatment. Thus ΔG_{1}^{\neq} as well as ΔS_{rc}° increases as the extent of association between bulk solvent molecules decreases, such as the extent of hydrogen bonding in the sequence water, formamide, NMF, and DMF. The progressively greater decreases in the extent of solvent polarization that attend the formation of $Co(en)_3^{2+}$ from $Co(en)_3^{3+}$ in this sequence also appear to require that additional energy be expended to reach the required degree of nonequilibrium solvent polarization in the transition state. A similar correlation between ΔS_{rc}^{o} and ΔG_{i}^{\neq} has been demonstrated for a series of outer-sphere electron transfer processes in homogeneous aqueous media, including reactions where the reorganization of outer-shell solvent provides the

Figure 10. The variation in the intrinsic free energy of activation for $\text{Co(en)}_3^{3+/2+}$ resulting from substituting various nonaqueous solvents for water, $\Delta(\Delta G_1^{\neq})^{\text{S-W}}$, plotted against the corresponding reaction entropies $\Delta S_{\text{rc}}^{\circ}$. Values of $\Delta(\Delta G_1^{\neq})^{\text{S-W}}$ obtained from formal rate constants k_{corr}^{f} given in Table 14 using Equation (6). Values of $\Delta S_{\text{rc}}^{\circ}$ (determined at μ = 0.1) taken from Table 8.

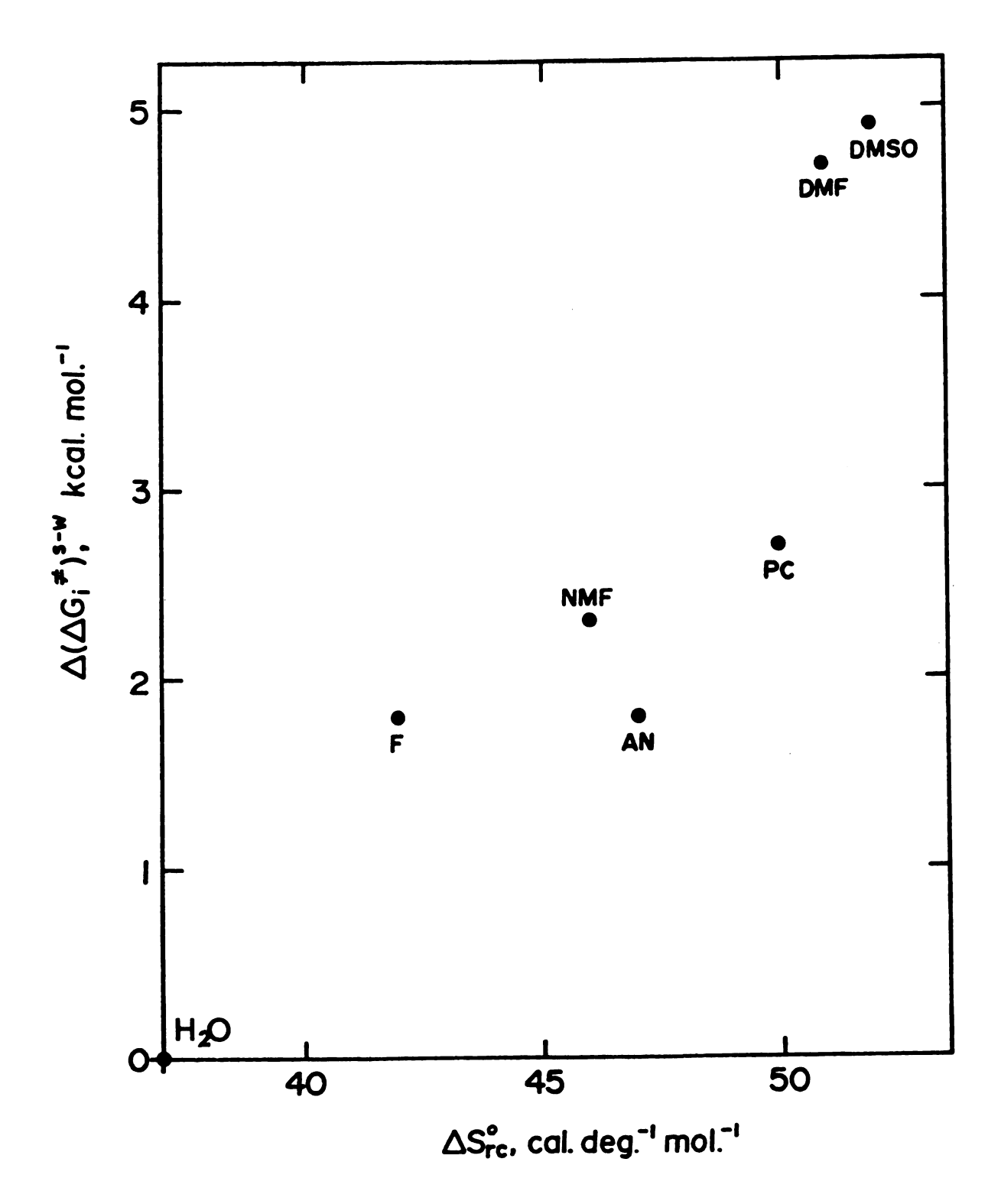


Figure 10

dominant contribution to ΔG_{i}^{\neq} (23).

Other kinetic data for simple outer-sphere redox processes involving substitutionally inert reactants in nonaqueous solvents are sparse, both at electrodes and in homogeneous solution. However, the values of $\mathbf{k}_{_{\mathbf{P}\mathbf{Y}}}$ the rate constant for the homogeneous self-exchange of Fe(phen) $_{3}^{3+/2+}$ and related couples are 1-2 orders of magnitude smaller in acetonitrile than in water (113,114). These reactivity differences are not predicted by the conventional dielectric continuum model of electron transfer. Thus inserting the relevant dielectric constants into the usual expression for the outer-shell barrier to homogeneous self-exchange (115) (assuming that the distance between the reacting centers in the transition state is twice the reactant radius of 6.8 Å (73), yields the prediction that k_{ex} should be very similar in water and acetonitrile (about 20% larger in the latter solvent). Interestingly, this decrease in $k_{\mbox{ex}}$ is again accompanied by a substantial increase in ΔS_{nc}^{o} (Table 6). This behavior indicates that the observed decreases in $k_{\mbox{\scriptsize ex}}$ arise from the greater changes in short-range solvent polarization around the polypyridine complexes that are apparently required in order to induce electron transfer in acetonitrile. The variations of k_{ex} for the ferricinium/ferrocene couple between different nonaqueous solvents have also been reported to differ from the dielectric continuum predictions (116).

It should be noted that the likely limitations of the conventional dielectric continuum model in describing both the thermodynamics of outer-shell solvation and the outer-shell contribution to the reorganization energy for electron transfer has frequently been noted (71,117,118). Indeed, theoretical models of solvation have recently been developed which take into account the spatial dispersion of the surrounding solvent structure (71,117,118). In principle, these models allow the various short-range vibrational and reorientational motions of the solvent to be treated, although they still do not consider the existence of specific interactions between the coordinated ligands and the nearest-neighbor solvent molecules. interactions are indicated from the redox thermodynamic measurements to be important for the present reactants (Chapter V).

CHAPTER VII

DETERMINATION OF REACTION MECHANISMS FOR Co(III)- and Cr(III)- AMINE COMPLEXES AT THE Hg/NONAQUEOUS INTERFACES

A. INTRODUCTION

It was noted in Chapter I that variations in the solvent medium can influence the rates of electron-transfer processes by changing the reaction mechanism. In order to interpret electrochemical kinetic parameters and to treat them theoretically, it is necessary to identify the reaction mechanisms. As noted in Chapter I two different pathways for the electron-transfer can be considered. (1) "outer-sphere" (0.S.) and (ii) "inner-sphere" (I.S.). Electron transfer during O.S. reactions takes place with the reactant center located at the so-called "outer Helmholtz plane" (o.H.p.) which is the plane of closest approach for reactants whose coordination spheres do not penetrate the layer of solvent molecules that are specifically adsorbed on the electrode surface. In this case only weak, nonbonding interactions occur between the reactant and the electrode in the transition state (12). During electrode reactions that proceed by I.S. pathways, one (or more) of the ligands in the reactant's primary coordination sphere penetrates the OHp and is attached to the electrode surface in the transition state (12).

In this chapter electroreduction kinetics of various $Co^{III}(NH_3)_5X$ and $Cr^{III}(NH_3)_5X$ (where $X = NH_3$, F^- , Cl^- ,

Br, SO_4^2 , NO_3 , N_3 and NCS) complexes studied at Hg/DMSO, Hg/DMF, Hg/Formamide and Hg/PC interfaces are reported.

B. METHOD FOR DISTINCTION BETWEEN I.S. AND O.S. MECHANISMS

The primary method developed for distinguishing between I.S. and O.S. electrode reactions for cationic reactants is based on the response of the reaction rate to changes in specific ionic adsorption of the supporting electrolyte (12). This method has successfully been used in aqueous media for mechanism diagnosis of the reduction of Co^{III} and Cr^{III} complexes at mercury (9,13) and solid electrode surfaces (14). The method consists of measuring the reaction rate of a complex at a given electrode potential, first in the absence and then in the presence of an anion which is known to be specifically adsorbed on the electrode surface and which cannot act as a bridging ligand between the reactant and electrode surface (12). If the complex of interest reacts by an I.S. pathway, the transition state will be formed at the "inner Helmholtz plane (iHp) and the presence of an anion which is strongly adsorbed on the electrode will lead to a competition for adsorption sites which should raise the energy of the transition state and produce lower reaction rate (12).

By contrast, if an O.S. reaction pathway is involved,

the addition of a strongly adsorbing species should produce negative changes in the average potential at the oHp. This will lead to large rate enhancements as a consequence of more favorable electrostatic interactions for cationic reactants (12).

C. RESULTS

The electroreduction kinetics of various Co^{III}(NH₃)₅X and Cr^{III}(NH₃)₅X complexes were studied as a function of electrode potential in four different nonaqueous media. These substitutionally inert complexes were selected because they can be reduced via relatively slow one-electron reactions, allowing their rates to be measured quantitatively. Moreover, these systems are reduced irreversibly at the dropping mercury electrode (d.m.e.); the back oxidation rates are negligible, which allows d.c. and normal pulse polarography to be used to monitor the electrode kinetics. (The absence of anodic back-reactions for these reactants were confirmed by cyclic voltammograms obtained at a hanging mercury drop electrode.)

1. Co(III)-amine Reactants

In order to identify the reduction mechanism as either inner- or outer-sphere, the reduction rates of each Co(III)-amine complexes were examined both in the absence and in

the presence of anionic specific adsorption of the supporting electrolyte. Since anion specific adsorption seems to be negligible for LiClO_4 under the experimental conditions employed for the nonaqueous solvents used here (100,106, 119), it was used as the main component of the supporting electrolyte. For mechanism diagnosis, a mixed supporting electrolyte with the general form of (0.1-a) $\underline{\text{M}}$ $\underline{\text{LiClO}}_4$ + $\underline{\text{aM}}$ MX with a = 0.01, 0.02, 0.03 $\underline{\text{M}}$ and X = Cl⁻, $\underline{\text{Br}}$, I⁻ and SCN⁻ was used. Electrocapillary and differential capacity measurements have shown that these anions are specifically adsorbed at the Hg/formamide (120), Hg/DMSO (100a), Hg/DMF (119b, 121) and Hg/PC (122) interfaces.

Tables 19 and 20 summarize the apparent (experimental) rate constants k_{app} for the reduction of cobalt complexes measured at (or extrapolated to) -350 mV vs. normal calomel reference electrode (NCE) both in the presence and absence of added SCN at a constant total ionic strength in DMSO and DMF. Also listed in Tables 19 and 20 are the apparent cathodic transfer coefficients α_{app} obtained from the experimental Tafel plots for reduction of each complex in 0.1 M LiClOh.

Table 21 summarizes k_{app} for the reduction of cobalt complexes measured at (or extrapolated to) -350 mV vs. NCE in 0.1 M LiClO4 and 0.08 M LiClO4 + 0.02 M LiCl as supporting electrolyte in formamide. In addition values of α_{app} measured in 0.1 M LiClO4 for each reactant are

Table 19. Experimental Rate Constants and Transfer Coefficients for Electroreduction of Various Co(III)-amine Complexes at Hg/DMSO at 25°C.

Complex	α _{app} a	kapp	k-350 ^c app	k <mark>-</mark> 350 ^d app
Co(NH ₃) ³⁺	1.0	2.4×10^{-6}		9.1 x 10 ⁻⁶
Co(NH ₃) ₅ F ²⁺	0.65	1.9×10^{-6}		5.0×10^{-6}
Co(NH ₃) ₅ NO ₃ ²⁺	0.74	5.9×10^{-4}	1.6×10^{-3}	2.2 x 10 ⁻³
Co(NH ₃) ₅ NCS ²⁺	0.76	2.0×10^{-4}	3.9×10^{-4}	4.9×10^{-4}
Co(NH ₃) ₅ N ₃ ²⁺	0.66	5.9 x 10 ⁻⁵	1.4×10^{-4}	1.8×10^{-4}
Co(NH ₃) ₅ C1 ²⁺	0.78	2.8	1.3	
Co(NH ₃) ₅ SO ₄ +	0.40	1.1×10^{-5}		2.7×10^{-5}

^aApparent cathodic transfer coefficient in 0.1 \underline{M} LiClO₄ obtained from $\alpha_{app} = -(\frac{2.3 \text{ RT}}{F})(\frac{\partial \log k_{app}}{\partial E})_{11}$

^bApparent rate constant evaluated at -350 mV vs. NCE in 0.1 $\underline{\text{M}}$ LiClO₄.

CApparent rate constant evaluated at -350 mV vs. NCE in 0.02 M NaSCN + 0.08 M LiClO₁₁ electrolyte.

 $^{^{}d}$ Apparent rate constant evaluated at -350 mV vs NCE in 0.03 $\underline{\text{M}}$ NaSCN + 0.7 $\underline{\text{M}}$ LiClO $_{4}$ electrolyte.

Table 20. Experimental Rate Constants and Transfer Coefficients for Electroreduction of Various Co(III)-amine Complexes at Hg/DMF at 25°C.

Complex	α _{app} a	k-350 ^b	k-350 ^c app
Co(NH ₃) ₆ 3+	0.9	1.5 x 10 ⁻⁴	5.0 x 10 ⁻⁴
Co(NH ₃) ₅ F ²⁺	0.7	4.0×10^{-5}	7.9×10^{-5}
Co(NH ₃) ₅ NO ₃ ²⁺	0.66	5.2 x 10 ⁻³	
Co(NH ₃) ₅ NCS ²⁺	0.57	3.8×10^{-3}	7.2×10^{-3}
Co(NH ₃) ₅ N ₃ ²⁺	0.52	1.2×10^{-3}	2.6×10^{-3}
Co(NH ₃) ₅ C1 ²⁺		∿1.6 x 10 ⁻¹	

^aApparent cathodic transfer coefficient in 0.1 \underline{M} LiClO₄.

^bApparent rate constant evaluated at -350 mV vs NCE in 0.1 M LiClO_{μ}.

^cApparent rate constant evaluated at -350 mV vs NCE in 0.02 $\underline{\text{M}}$ NaSCN + 0.08 $\underline{\text{M}}$ LiClO₄ electrolyte.

Table 21. Experimental Rate Constants and Transfer Coefficients for Electroreduction of Various Co(III)amine Complexes at Hg/Formamide at 25°C.

Complex	α app	k ^{-350b} app	k ^{-350°} app
Co(NH ₃) ³⁺	0.95	4.0 x 10 ⁻⁶	1.5 x 10 ⁻⁵
Co(NH ₃) ₅ F ²⁺	0.76	8.9×10^{-6}	2.8×10^{-5}
Co(NH ₃) ₅ NO ₃ ²⁺	0.63	3.6×10^{-3}	5.7×10^{-3}
Co(NH ₃) ₅ NCS ²⁺	0.62	1.0×10^{-2}	1.7×10^{-2}
Co(NH ₃) ₅ N ₃ ²⁺	0.47	9.1 x 10 ⁻⁴	1.5 x 10 ⁻³

^aApparent cathodic transfer coefficient in 0.1 \underline{M} LiClO₄.

^bApparent rate constant evaluated at -350 mV vs NCE in 0.1 <u>M</u> LiClO₄.

^cApparent rate constant evaluated at -350 mV vs NCE in 0.02 \underline{M} LiCl + 0.08 \underline{M} LiClO $_{\mu}$ electrolyte.

also listed in Table 21.

Experimental rate constants k_{app} for the reduction of cobalt complexes in 0.1 M LiClO $_{4}$ in propylene carbonate are given in Table 22 along with their transfer coefficients α_{app} . No accurate measurements could be done in propylene carbonate using mixed electrolyte. This was due to insolubility of the cobalt complexes in the presence of small amounts of halide ions.

The reduction of most cobalt-amine complexes in 0.1 $\underline{\text{M}}$ LiClO₄ in four nonaqueous solvents employed here were found to yield normal polarographic waves. Polarographic waves for $\text{Co(NH}_3)_5\text{Cl}^{2+}$ reduction exhibited small anodic currents just prior to the cathodic waves both in DMSO and PC. In propylene carbonate and formamide small anodic currents were observed for the reduction of $\text{Co(NH}_3)_5\text{NCS}^{2+}$ at the bottom of the polarographic waves. Electroreduction measurements of $\text{Co(NH}_3)_5\text{SO}_4^+$ were precluded in DMF and PC due to its low solubility.

In DMF rate constants for cobalt-amine complexes were not possible to measure in the presence of halide anions. This was mainly because of anion-induced mercury dissolution and the appearance of maxima in the presence of Brand I and also insolubility of complexes in the presence of Cl anions. In DMSO the reduction of most Co(III) complexes in the presence of Cl, Br, and I could only be monitored by the use of shorter drop times, (0.5 sec) and analyzing the top middle portion of the polarograms.

Table 22. Experimental Rate Constants and Transfer Coefficients for Electroreduction of Various Co(III)-amine Complexes at Hg/PC at 25°C.

Complex	α app	k ^{-125^b app}	
Co(NH ₃) ³⁺	0.65	1.4 x 10 ⁻⁵	
Co(NH ₃) ₅ F ²⁺	0.67	$\sim 7.9 \times 10^{-7}$	
Co(NH ₃) ₅ NO ₃ ²⁺	∿0.38	2.2×10^{-3}	
Co(NH ₃) ₅ NCS ²⁺	0.59	4.5×10^{-3}	
Co(NH ₃) ₅ N ₃ ²⁺	0.38	1.7×10^{-3}	
Co(NH ₃) ₅ C1 ²⁺	0.54	2.5 x 10 ⁻²	

^aApparent cathodic transfer coefficient in 0.1 $\underline{\text{M}}$ LiClO₄.

^bApparent rate constant evaluated at -125 mV vs NCE in 0.1 \underline{M} LiClO₄.

2. <u>Cr(III)-amine Reactants</u>

Table 23 summarizes the apparent rate constants along with the values of $\alpha_{\rm app}$ for reduction of each Cr(III) complex measured at a convenient potential vs. NCE in 0.1 M LiClO4 in three solvents, DMSO, DMF and formamide. Electro-reduction kinetic measurements for the chromium complexes in PC were precluded. This was because of the lack of reproducible polarograms and undefined limiting currents.

Since the Cr(III)-amine complexes are reduced at very negative potentials at which even iodide (which is one of the strongest adsorbing anions) does not seem to be especially adsorbed, no mechanism diagnosis could be obtained when rate constants in pure and in mixed supporting electrolytes were compared. Indeed, significant rate enhancements due to addition of I could only be observed for complexes which exhibited more positive reduction potentials like $Cr(NH_3)_5Br^{2+}$. For other Cr(III)-amine complexes almost no variation in rate constants were observed in the presence and in the absence of added iodide.

D. DISCUSSION

Inspection of the data presented in Tables 19-21 indicates that except for $\text{Co(NH}_3)_5\text{Cl}^{2+}$ reduction (Table 19), reaction rates of all other Co(III) amine reactants that were examined here are markedly accelerated at a given

Experimental Rate Constants and Transfer Coefficients for Electroreduction of Various Cr(III)-amine Complexes at Hg/DMSO, Hg/DMF and Hg/Formamide Interfaces at 25°C. Table 23.

	Q	DMSO		DMF	For	Formamide
Complex	a app	k_1200 ^b app	a app	k_1100 ^b app	a _{app}	k_1000 ^b app
Cr(NH ₃)3+	0.48	1.6×10^{-3}	0.73	2.2×10^{-3}	0.82	2.9×10^{-3}
$\operatorname{cr}(\operatorname{NH}_3)_{5^{\mathrm{F}^{2+}}}$	0.63	8.7 x 10 ⁻⁶	19.0	7.2×10^{-6}	0.67	5.0 x 10 ⁻⁶
Cr(NH ₃) ₅ NCS ²⁺	99.0	1.4 x 10 ⁻⁴	0.61	1.1×10^{-4}	0.65	5.1×10^{-4}
$Cr(NH_3)_5N_3^{2+}$	0.51	5.0×10^{-5}	0.54	1.4 x 10 ⁻⁴	0.50	2.5×10^{-4}
$cr(NH_3)_5c1^{2+}$	0.58	2.7×10^{-4}	0.56	$2. \times 10^{-4}$	0.72	2.7×10^{-3}
Cr(NH ₃) ₅ Br ²⁺	0.48	5.7×10^{-3}	0.59	$4. \times 10^{-3}$	0.54	2.5×10^{-2}

 a Apparent cathodic transfer coefficient in 0.1 $\underline{\text{M}}$ LiClO $_{\mu}$ in each solvent.

 $^{^{}m D}_{
m App}$ arent rate constant evaluated at quoted potential in mV vs. NCE in 0.1 ${
m M}$ LiClO $_{
m l}$ in each solvent.

electrode potential by the addition of adsorbed non-reacting anions.

Figure 11 shows rate-potential data for the reduction of $\text{Co(NH}_3)_5\text{F}^{2+}$ in the presence and absence of added iodide in DMSO. It is seen that the addition of iodide results in a significant rate enhancement which becomes gradually less pronounced at more negative potentials as adsorption of iodide diminishes.

In Figure 12 rate-potential data for the reduction of $\text{Co(NH}_3)_5\text{NO}_3^{2+}$ in the presence and absence of added NCS-in DMSO are shown. Essentially similar responses to NCS-adsorption are also exhibited by all Co(III)-amine complexes (except for $\text{Co(NH}_3)_5\text{Cl}^{2+}$) in DMSO and DMF. The only difference being that quantitatively larger enhancements result with tripositive $\text{Co(NH}_3)_6^{3+}$ while smaller rate enhancements are obtained with the less highly charged $\text{Co(NH}_3)_5\text{SO}_4^{4+}$.

This behavior is in qualitative agreement with that expected for an outer-sphere electrode reaction mechanism with a cationic complex whose concentration at the electrode surface is increased by the greater electrostatic attraction it experiences when anions are adsorbed on the electrode surface.

These observations therefore indicate that all the cobalt complexes studied here (except $\text{Co(NH}_3)_5\text{Cl}^{2+}$) are apparently reduced via outer-sphere pathways. In the case of $\text{Co(NH}_3)_5\text{Cl}^{2+}$ addition of NCS⁻ in DMSO results in a

Figure 11. Comparison of the effect of specific iodide adsorption upon rate-potential plots for the electroreduction of $Co(NH_3)_5F^{2+}$ in mixed $LiClO_4 + LiI$ supporting electrolytes in DMSO. Symbols are experimental points in (0.1-X) M $LiClO_4 + XM$ LiI with X = O (\blacksquare), 0.01 (\bigcirc), 0.03 (\triangle).

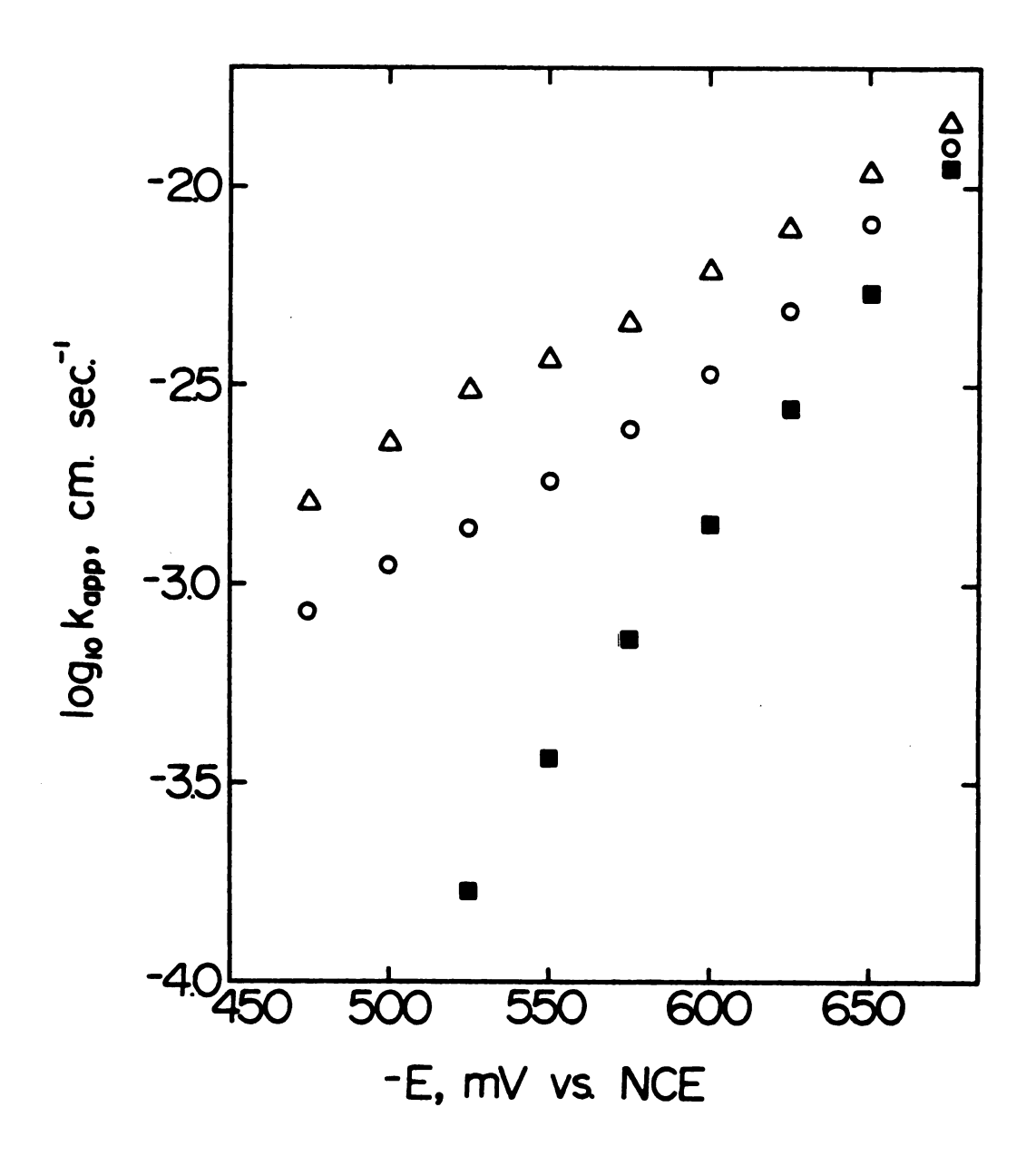


Figure 11

Figure 12. Comparison of the effect of specific NCS-adsorption upon rate-potential plots for the electroreduction of $Co(NH_3)_5NO_3^{2+}$ in mixed LiClO₄ + NaNCS supporting electrolytes in DMSO. Symbols are experimental points in (0.1-X) M LiClO₄ + XM NaNCS with X = 0 (\blacksquare), 0.01 (\bigcirc), 0.03 (\triangle).

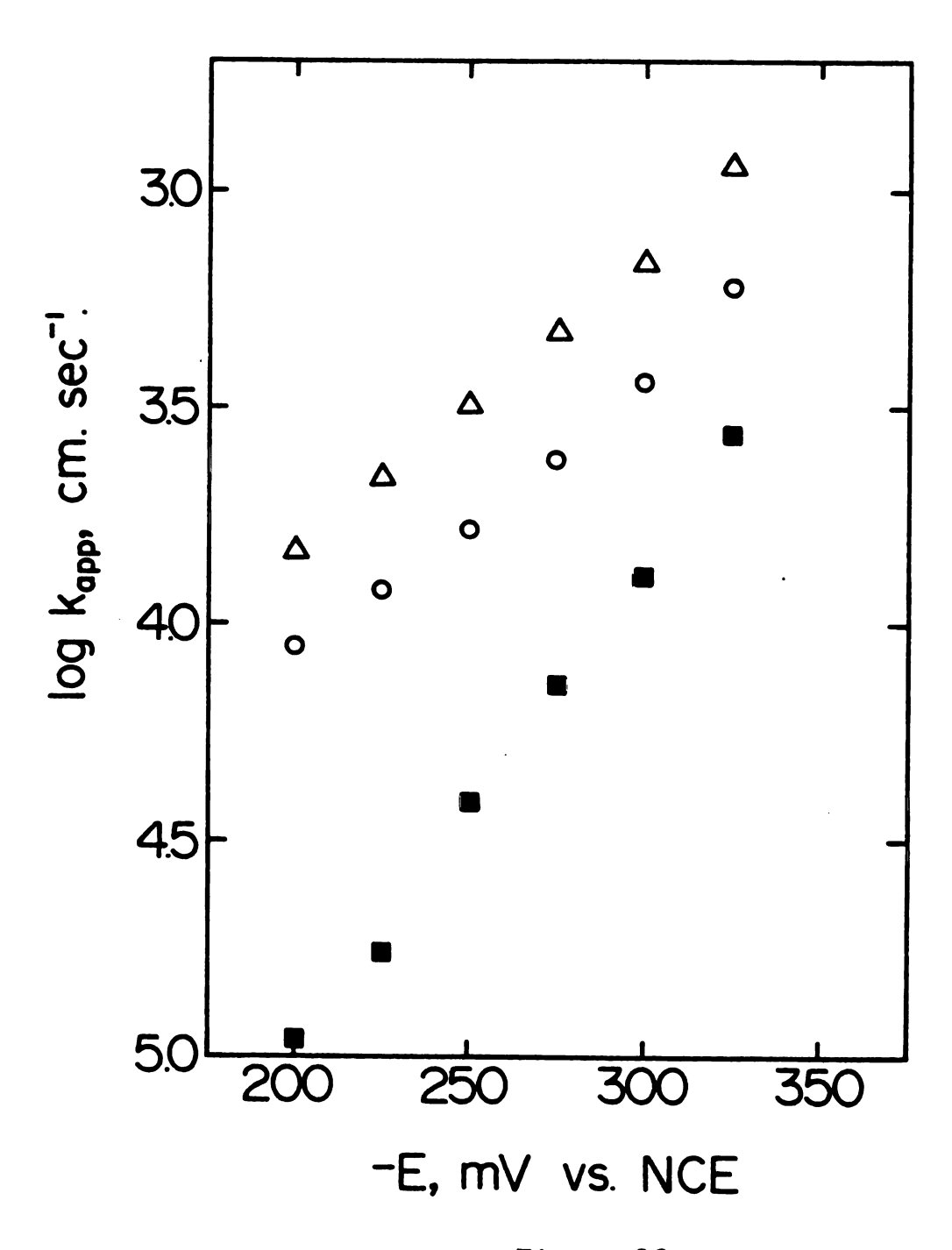


Figure 12

slight decrease in reaction rate (Table 19) instead of the marked increase observed with the other cobalt complexes. The most probable explanation for this behavior is that an inner-sphere pathway is followed by this complex with the coordinated chloride anion attached to the electrode surface in the transition state.

Measurements at the ${\rm Hg/H_{2O}}$ interface (13) have shown that ${\rm Co(NH_3)_5^{3+}}$, ${\rm Co(NH_3)_5^{F}}^{2+}$ and ${\rm Co(NH_3)_5^{SO}_4^{+}}$ are almost certainly reduced via 0.S. pathways since they lack coordinated ligands that significantly specifically adsorbed in the potential region where the kinetics were monitored. Of the various pentaammine cobalt complexes studied in Reference 13 at the ${\rm Hg/H_2O}$ interface only ${\rm Co(NH_3)_5NCS}^{2+}$ was found to reduce via a pure inner-sphere mechanism. (Although reduction of ${\rm Co(NH_3)_5Cl}^{2+}$ at the ${\rm Hg/H_2O}$ was too fast to be measured accurately (13), it is very possible that this reactant is also reduced via I.S. mechanism due to strong adsorption of ${\rm Cl}^-$ at the mercury surface.) Complexes of ${\rm Co(NH_3)_5NO_3^{2+}}$ and ${\rm Co(NH_3)_5N_3^{2+}}$ were found to reduce via mixed 0.S. and I.S. mechanisms (13).

Although no mechanism diagnosis could be obtained for reduction of Cr(III)-ammine complexes at the Hg/non-aqueous interfaces studied here (except for $Cr(NH_3)_5Br^{2+}$ which was found to reduce via O.S. mechanism), it is very probable that all of these Cr(III) complexes are reduced via O.S. pathways. The reasons for the last

statement are: (i) these Cr(III) complexes are reduced at very negative potentials at which the anion specific adsorption are very weak. (ii) In addition, among Cr(III)-amine complexes studied in aqueous media (9) at the mercury electrode, only Cr(NH₃)₅NCS²⁺ and Cr(NH₃)₅Br²⁺ were found to reduce with dominating anion-bridged (I.S.) pathways. Since in the present work it was found that even Cr(NH₃)₅Br²⁺ with a traditionally good heterogeneous bridging ligand, Br⁻, is not reducing via I.S. mechanism, therefore one can conclude that all Cr^{III}(NH₃)₅X complexes studied here are reduced via outer-sphere mechanisms.

The inability of mercury/nonaqueous interfaces to induce I.S. mechanisms is understandable since anion adsorption is known to be somewhat weaker in most non-aqueous media, compared to aqueous media (123). Apparently this is due to the fact that nonaqueous solvents compared to water are more strongly adsorbed on the mercury electrodes (119b). Therefore, there is a competition between anions and solvent molecules to adsorb on the electrode surface. This effect is probably more pronounced when the anion in the coordination sphere of the reactant which has less freedom wants to act as a bridging ligand between the electrode and the metal ion center.

CHAPTER VIII

CONCLUSIONS AND SUGGESTIONS FOR FURTHER WORK

A. CONCLUSIONS

The results obtained in the present work demonstrate that the chemical nature of the solvent can play an important role both in the thermodynamics and kinetics of electron transfer, even when the solvent is excluded from the reactant's coordination sphere.

The large values of reaction entropy ΔS_{rc}^{o} for all $exttt{M}(exttt{III})/(exttt{II})$ redox couples in the nonaqueous solvents compared to the corresponding values in aqueous media, are due to the greater enhancement of solvent polarization in the vicinity of the complex for nonaqueous solvents. observations can be explained by the unusually high degree of internal order exhibited by liquid water. The large changes in $\Delta S_{\mbox{\scriptsize rc}}^{\mbox{\scriptsize o}}$ when the solvent is varied are primarily determined by the relative ability of the tripositive M(III) complex compared to the corresponding M(II) species to disturb the bulk solvent structure and reorientate solvent molecules within its vicinity. The values of ΔS_{rc}^{o} for each redox couple were found to increase as the extent of internal order of the bulk solvent decreased (Figures 2, 7 and 9). Large differences in ΔS_{rc}^{o} in a given solvent were observed for couples having different coordinated ligands. Thus M(III)/(II) amine and ethylenediamine couples gave values of ΔS_{rc}^{o} that were ~ 15 e.u. larger in a given solvent than for the corresponding polypyridine couples (see Tables 6 and 8). The different ΔS_{rc}^{o} values for analogous Co and Cr, Fe, and Ru couples in a given solvent indicate that the electronic structures of the metal redox center can also have a significant effect on the reaction entropy. The high-spin Co(III)/(II) couples exhibited values of $\Delta S_{\mathbf{rc}}^{\mathbf{o}}$ that were ~ 20 e.u. larger than for the low-spin Ru(III)/(II), Fe(III)/(II), and Cr(III)/(II) couples containing the same ligands (Tables 6 and 8). It would appear from these results that in a given solvent two redox couples will have comparable reaction entropies when they have the same coordination sphere and when the electronic structures of the two central metal ions are similar. For example, similar values of ΔS_{rc}^{o} for $Cr(bpy)_{3}^{3+/2+}$ and $Fe(bpy)_3^{3+/2+}$ couples in water, propylene carbonate and acetonitrile can be mentioned (see Table 6).

The variations in ΔS_{rc}^{o} for the ferricinium/ferrocene redox couple between water and a number of nonaqueous solvents provide a major contribution to the apparent breakdown of the ferrocene assumption for estimating free energies of single ion transfer. This is simply because of the greater tendency of solvent dipoles to be polarized by the ferricinium cation compared with the ferrocene molecule.

Small negative values of $\Delta(\Delta G_{rc}^o)^{s-w}$, [free energy of transfer for a redox couple from water to a given nonaqueous

solvent], for couples containing aromatic ligands were typically obtained. These are due to partial compensation of the entropic terms by the corresponding enthalpic components. The resulting values of $\Delta(\Delta G_{rc}^{o})^{S-W}$ for cationic complexes containing ammine and ethylenediamine and anionic redox couples were found to vary considerably (ca. -4 to 14 Kcal mol⁻¹) with the nature of the nonaqueous solvent. These behavioral differences (between polypyridine and ammine couples) are due to the strong donor-acceptor interactions between the nearest-neighbor solvent molecules (as donors) and the acidic amine hydrogens (as acceptors). The correlation obtained between the values of $\Delta(\Delta G_{rc}^{o})^{S-W}$ for the ammine couples and the basicity of the solvent as determined by the Donor Number are shown in Figure 4. For anionic redox couples, such as $Fe(EDTA)^{-/2-}$, the solvent molecules are acting as an acceptor toward the molecule of EDTA; therefore the values of ΔG_{rc}^{o}) s-w decrease with an increasing solvent Acceptor Number (see Figure 8). A useful generalization that might be made from the results in this work is the apparent insensitivity of $\Delta(\Delta G_{rc}^{o})^{S-W}$ to the electronic structure of the central metal ion. For example, Ru(en) $\frac{3+}{2}$ and Co(en) $\frac{3+}{2}$ in both DMSO and DMF (Table 9), and $Fe(EDTA)^{-/2}$ and $Co(EDTA)^{-/2}$ in methanol (Table 12) gave comparable values of $\Delta(\Delta G_{rc}^{o})^{S-W}$. Therefore, for redox couples for which measurements of $E_{\mathbf{f}}$ are impractical [e.g., $Co(NH_3)_6^{3+/2+}$], the values of ΔE_f

between pair of solvents could be predicted with some confidence using $\Delta(\Delta G_{\text{rc}}^{\circ})^{\text{S-W}}$ values of analog Ru(III)/(II) couple.

Studies of reaction mechanisms at the mercury/nonaqueous interfaces for reduction of various Co(III)- and Cr(III)- amine complexes indicate that the outer-sphere mechanism is the usual pathway for electron transfer. This is due to the fact that specifically adsorbed anions are not strongly adsorbed at the mercury/nonaqueous interfaces. The lack of adsorption at the mercury electrode prevents formation of anion bridge (between the electrode and metal ion) during the transition state which is necessary for innersphere pathways.

The double-layer corrected rate constants obtained for the reduction of Co(III)-amine and Co(III)-ethylenediamine complexes were found to be smaller in all nonaqueous solvents compared with water. These rate changes indicate that there are large increases in the outer-shell component of the intrinsic free energy barrier to electron transfer $(\Delta G_1^{\not=})_{OS}$ when water is replaced by nonaqueous, particularly aprotic, solvents. Such solvent dependencies of $(\Delta G_1^{\not=})_{OS}$ are much larger, and in even qualitative disagreement with the predictions of conventional dielectric continuum model (Table 17). These discrepancies between theory and experiment are probably due to the fact that this model does not consider any specific short-range interactions. Indeed,

a roughly linear correlation that was observed between the experimental solvent dependence of ΔG_1^{\neq} for $Co(en)_3^{3+/2+}$ and the corresponding values of ΔS_{rc}° (Figure 10) suggests that there is a contribution to ΔG_1^{\neq} arising from the short-range reorganization of solvent molecules. Another factor that might be responsible for the observed differences between theory and experiment is the electron tunneling probability within the transition state. This could be significantly smaller in some nonaqueous solvents as a result of the probable increase in the distance between the reacting molecules and the electrode surface. Therefor, this could be responsible for the smaller rate constants observed in nonaqueous media.

The results obtained in the present work are important because they provide the first clear-cut demonstration that the dielectric continuum model can provide a seriously inadequate account of the influence of the outer-shell solvent upon the electrochemical kinetics as well as the thermodynamics of simple inorganic redox reactions. In addition, they illustrate the important influence of short-range solvent-solute interactions upon the redox thermodynamics and electrode kinetics of these redox couples.

B. SUGGESTIONS FOR FURTHER WORK

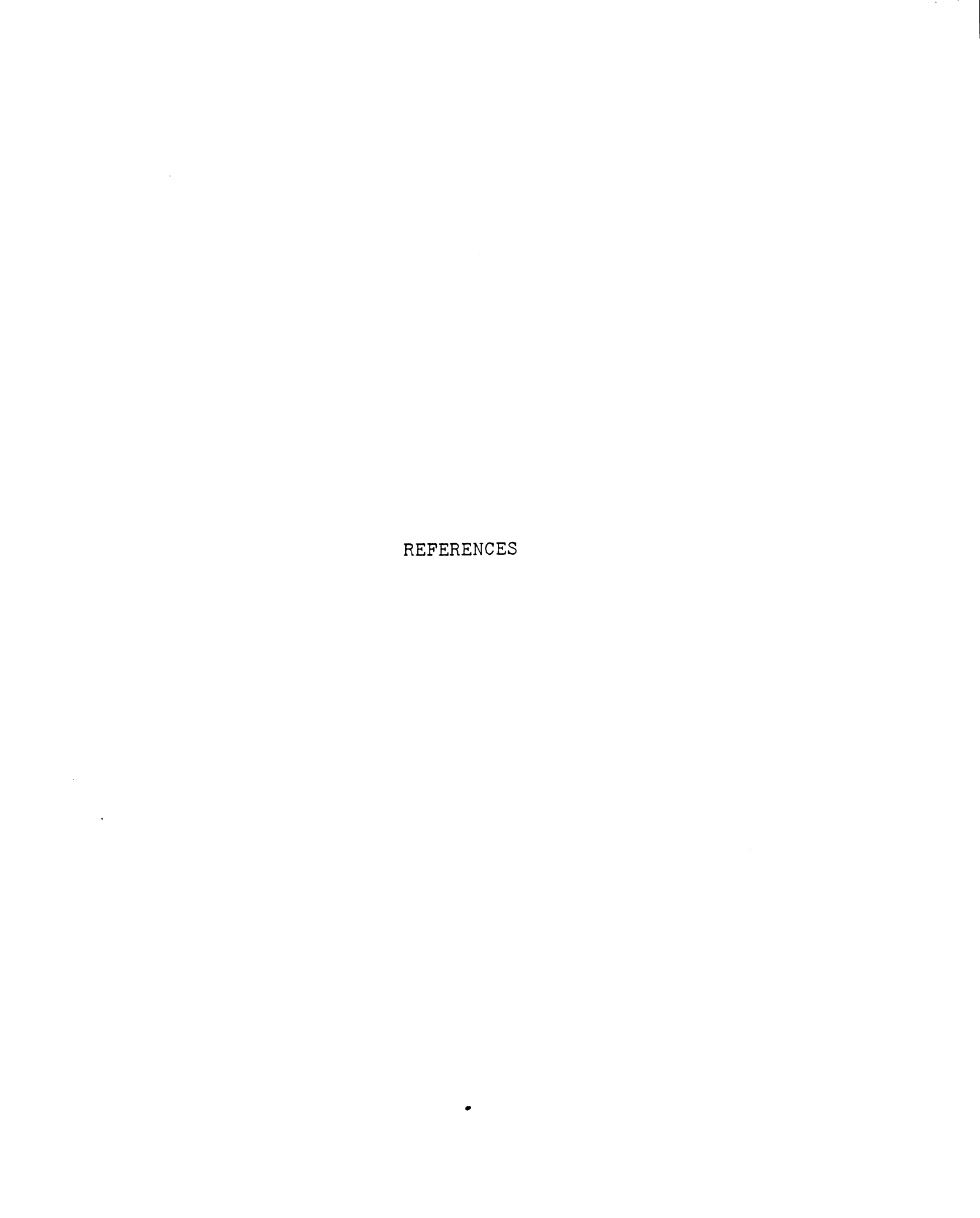
The conclusions reached in the previous section regarding the factors responsible for the discrepancies observed between the dielectric continuum theory and experimental values are somewhat clouded by the uncertainty to what extent these reactivity differences between the various solvents are due to variations in the efficiency of electron tunneling rather than in the free energy of activation for electron transfer. Further studies with suitable systems are required to distinguish between these two factors. In principle, such distinction could be made by careful studies of the temperature dependence of the electrochemical rate constants. One possible experiment which seems to be useful involves the employment of a binary mixed solvent in which a strongly adsorbing nonaqueous solvent with small solvation ability (of the bulk reactant) is added to water. Employment of such a system should allow one to separate the contributions to the measured solvent effects upon electrochemical kinetics from solvation of the bulk reactant and the transition state which is formed in the interfacial region. Thermodynamic measurements (i.e., $\Delta S_{\textbf{rc}}^{\textbf{o}}$ and $\textbf{E}_{\textbf{f}})$ can assist us in finding that whether there is any change in the bulk solvation of the redox couple in mixed solvent and pure aqueous media. The corresponding changes in the interfacial solvent environment can be

obtained by double-layer capacitance measurements. Finding the suitable binary mixed solvent (i.e., with a nonaqueous solvent that is strongly adsorbed to the electrode but does not change the bulk structure), electrode kinetics of various reactants such as $Co(en)_3^{3+/2+}$ can be measured. If the rate constants in this mixed solvent are substantially smaller than that in pure water, then it is very possible that the rate decreases observed in pure nonaqueous solvents for Co(III)-amine and ethylenediamine complexes (Chapter VI) are also, mainly due to decreases in the electron tunneling probability through the thicker nonaqueous solvent layer compared to water. These and similar studies would be worthy of examination in order to find out to what extent the intrinsic barrier $\Delta G_i^{\not\equiv}$ is sensitive to the nature of the solvent and how the reactant-solvent interactions may influence ΔG_{i}^{\neq} .

Of the redox couples studied in Chapter V, some were found to be unsuitable for kinetic measurements at mercury electrodes. This is due to the fact that their formal potentials are more positive than the anodic limit of mercury. It is possible to investigate the electrode reduction kinetics of these couples $[Co(bpy)_3^{3+/2+}, Fe(bpy)_3^{3+/2+}, and Co(phen)_3^{3+/2+}]$ at solid metal electrodes such as Pt, Au and Ag on account of the wide potential ranges available on these metals in contact with nonaqueous media. In addition, it would be interesting to examine the

effects of varying the nature of the electrode metal upon the electrode kinetics of various Co(III)-amine, $Co(en)_3^{3+/2+}$ and $Co(EDTA)^{-/2-}$ complexes in different nonaqueous solvents. Such studies and their comparison with the data obtained for the corresponding complexes at the mercury/nonaqueous interfaces should provide some useful information regarding the effect of the electrode upon the rate and mechanism of electron transfer in solvents other than water.

In order to get some meaningful results at the solid electrode surfaces in nonaqueous solvents and compare them with the corresponding data at mercury electrodes, it is necessary that the experimental rate constants be corrected for the double-layer effects. For this purpose, information about the metal charge density q^m as a function of electrode potential E is required. Although a few such data are available at mercury/nonaqueous interfaces, the corresponding data at solid electrodes are very scarce. Such data for interfaces of interest can be obtained using double-layer capacitance measurements.



REFERENCES

- J. N. Gaur and K. Zutsh, J. Electroanal. Chem., <u>11</u>, 390 (1966).
- 2. J. N. Gaur and N. K. Goswumi, Electrochim. Acta., 12, 1489 (1967).
- 3. T. Biegler, E. R. Gonzalez and R. Parsons, Coll. Czech. Chem. Comm., 36, 414 (1971).
- 4. G. J. Hills and L. M. Peter, J. Electroanal. Chem., 50, 87 (1974).
- G. J. Hills and L. M. Peter, J. Electroanal. Chem., 50, 1975 (1974).
- 6. N. Tanaka, Electrochim. Acta., 21, 701 (1976).
- 7. S. Fronaeus and C. L. Johansson, J. Electroanal. Chem., 80, 283 (1977).
- 8. For example, see H. Taube, "Electron Transfer Reactions of Complex Ions in Solution", Academic Press, N. Y., 1970.
- 9. M. J. Weaver and T. L. Satterberg, J. Phys. Chem., 81, 1772 (1977).
- (a) R. A. Marcus, J. Chem. Phys., 43, 679 (1965);
 (b) R. A. Marcus, J. Phys. Chem., 72, 891 (1968).
- M. J. Weaver and F. C. Anson, J. Electroanal. Chem., 58, 95 (1975).
- M. J. Weaver and F. C. Anson, J. Am. Chem. Soc., 97, 4403 (1975); Inorg. Chem., 15, 1871 (1976).
- 13. T. L. Satterberg and M. J. Weaver, J. Phys. Chem. 82, 1784 (1978).
- 14. K. L. Guyer, S. W. Barr, R. J. Cave and M. J. Weaver in S. Bruckenstein, J. D. E. MsIntyrc, B. Miller, E. Yeager (eds.), Proc. 3rd Symp. on Electrode Processes 1979, Electrochem. Soc. Prinston, 1980, p. 380.

- 15. W. J. Moore, "Physical Chemistry", Fourth Edition, Prentice-Hall, 1972, p. 232.
- 16. G. N. Lewis and M. Randall, "Thermodynamics", Second Edition, McGraw-Hill, New York, 1961, p. 399.
- 17. C. M. Criss and M. Salomon, in "Physical Chemistry of Organic Solvent Systems", A. K. Covington and T. Dickinson (Editors), Plenum Press, New York, 1973, Chapter 2.
- 18. C. M. Criss, R. P. Held, and E. Luksha, J. Phys. Chem., 72, 2970 (1968).
- 19. W. M. Latimer and W. L. Jolly, J. Am. Chem. Soc., 75, 4147 (1953).
- 20. C. M. Criss, J. Phys. Chem., 78, 1000 (1974).
- 21. E. L. Yee, R. J. Cave, K. L. Guyer, P. D. Tyma, and M. J. Weaver, J. Am. Chem. Soc., 101, 1131 (1979).
- 22. E. L. Yee, Ph.D. Thesis, Michigan State University (1980).
- 23. N. Sutin, M. J. Weaver and E. L. Yee, Inorg. Chem., 19, 1096 (1980).
- 24. E. L. Yee and M. J. Weaver, Inorg. Chem., 19, 1077 (1980).
- 25. M. P. Youngblood and D. W. Margerum, Inorg. Chem., 19, 3068 (1980).
- 26. B. Kratochvil and J. Knoeck, J. Phys. Chem., <u>70</u>, 944 (1966).
- 27. B. R. Baker and B. D. Mehta, Inorg. Chem. $\frac{4}{9}$, 848 (1965).
- 28. F. H. Burstall and R. S. Nyholm, J. Chem. Soc., 3570 (1952).
- 29. H. J. Schugar, A. T. Hubbard, F. C. Anson, and H. B. Gray, J. Am. Chem. Soc., 91, 71 (1969).
- 30. F. P. Dwyer, E. C. Gyarfas and D. P. Mellor, J. Phys. Chem., <u>59</u>, 296 (1955).
- 31. V. P. Pfeiffer and B. Werdelmann, Z. Anorg. Chem., <u>261</u>, 197 (1950).

- 32. I. M. Kolthoff and F. G. Thomas, J. Phys. Chem., $\underline{69}$, 3049 (1965).
- 33. H. S. Lim, D. J. Barclay and F. B. Anson, Inorg. Chem., 11, 1460 (1972).
- 34. F. Basolo and R. K. Neumann, Inorg. Synth., $\frac{4}{2}$, 171 (1946).
- 35. L. L. Poe and R. B. Jordan, Inorg. Chem., 7, 527 (1968).
- 36. G. Brauer, Ed., "Handbook of Preparative Inorganic Chemistry", Vol. 2, 2nd ed., Academic Press, N. Y., 1965, p. 1531.
- 37. W. G. Palmer in "Experimental Inorganic Chemistry", Cambridge University Press, London, 1969, p. 535.
- 38. R. L. Carlin and J. O. Edwards, J. Inorg. Nucl. Chem., 6, 217 (1958).
- 39. V. M. Linhard and H. Flygare, Z. Anorg. Chem., 262, 340 (1950).
- 40. J. B. Work, Inorg. Synth., 2, 221 (1953).
- 41. M. Mori, Inorg. Synth., <u>5</u>, 132 (1954).
- 42. A. E. Ogard and H. Taube, J. Am. Chem. Soc., 80, 1084 (1958).
- 43. D. L. Gay and G. C. Lalor, J. Chem. Soc. A, 1179 (1966).
- 44. M. Linhard and W. Berthold, Z. Anorg. Chem., 279, 173 (1955).
- 45. (a) I. I. Creaser, J. MacB. Harrowfield, A. J. Herlt, A. M. Sargeson, J. Springborg, R. J. Geue, and M. R. Snow, J. Am. Chem. Soc., 99, 3181 (1977); (b) A. M. Sargeson, Chemistry in BrItain, 15, 23 (1979).
- 46. R. Parsons, Trans. Far. Soc., 47, 1332 (1951).
- 47. P. Delahay, "Double Layer and Electrode Kinetics", Interscience, New York, 1965, Chapter 7.
- 48. For a recent review, see O. Popovych in "Treatise in Analytical Chemistry", I. M. Kolthoff, P. J. Elving (eds.), Part I, Vol. I, 2nd edition, Wiley, New York, 1978, p. 711 et seq.

- 49. H. M. Koepp, H. Wendt and H. Strehlow, Z. Elektrochem. <u>64</u>, 483 (1960).
- 50. J. F. Coetzee and W. K. Istove, Anal. Chem., $\underline{52}$, 53 (1980).
- 51. J. F. Coetzee and J. J. Campion, J. Am. Chem. Soc., 89, 2513 (1967).
- 52. I. M. Kolthoff and M. K. Chantooni, Jr., J. Phys. Chem., 76, 2024 (1972).
- 53. J. W. Diggle and A. J. Parker, Electrochim. Acta, 18, 975 (1973).
- 54. M. Alfenaar, J. Phys. Chem., 79, 2200 (1975).
- 55. R. Alexander, A. J. Parker, J. H. Sharp and W. E. Waghorne, J. Am. Chem. Soc., 94, 1148 (1972).
- 56. R. Alexander and A. J. Parker, J. Am. Chem. Soc., 89, 5549 (1967).
- 57. B. G. Cox, G. R. Hedwig, A. J. Parker and D. W. Watts, Aust. J. Chem., 27, 477 (1974).
- 58. E. Grunwald and B. J. Berkowitz, J. Am. Chem. Soc., 73, 4939 (1951).
- 59. O. Popovych, Anal. Chem., 38, 558 (1966).
- 60. O. Popovych, Anal. Chem., 46, 2009 (1974).
- 61. S. Villermax, V. Baudot and J. J. Delpuech, Bull. Soc. Chim. Fr., 1781 (1972).
- 62. J. I. Kim, J. Phys. Chem., 82, 191 (1978).
- 63. M. Abraham and A. Nasehzadeh, Can. J. Chem., <u>57</u>, 2004 (1979).
- 64. For a general review, see J. N. Agar, Adv. Electro-chem. Eng., 3, 31 (1963).
- 65. For example see (a) E. D. Eastman, J. Am. Chem. Soc., 50, 292 (1928); (b) A. J. deBethune, T. S. Licht and N. Swendeman, J. Electrochem. Soc., 106, 616 (1959); A. J. deBethune, ibid, 197, 829 (1960); (c) G. Milazzo and M. Sotto, Z. Phys. Chem. (Frankfurt am Main), 52, 293 (1967); G. Milazzo, M. Sotto and C. Devillez, ibid., 54, 1 (1967).

- 66. D. T. Sawyer and J. L. Roberts, Jr., "Experimental Electrochemistry for Chemists", Wiley, New York, 1974, Chapter 7.
- 67. R. S. Nicholson, Anal. Chem., 37, 1351 (1965).
- 68. R. S. Nicholson and I. Shain, Anal. Chem., 36, 706 (1964).
- 69. M. Born, Z. Phys. 1, 45 (1920).
- 70. See for example, R. M. Noyes, J. Am. Chem. Soc. 84, 513 (1962).
- 71. For a recent review, see P. P. Schmidt, "Electro-chemistry A Specialist Periodical Report", The Chemical Society London, Vol. 5, 1975, Chapter 2; Vol. 6, 1977, Chapter 4.
- 72. R. A. Marcus in "Special Topics in Electrochemistry", P. A. Rock (ed.), Elsevier, N. Y., 1977, p. 161.
- 73. G. M. Brown, and N. Sutin, J. Am. Chem. Soc., 101, 883 (1979).
- 74. M. J. Weaver, P. D. Tyma and S. M. Nettles, J. Electroanal. Chem., 114, 53 (1980).
- 75. M. J. Weaver, J. Electroanal. Chem., 93, 231 (1978).
- 76. M. J. Weaver, Inorg. Chem., 18, 402 (1979).
- 77. N. Sutin, Acc. Chem. Res., 1, 225 (1968).
- 78. W. L. Reynolds and R. W. Lumry, "Mechanisms of Electron Transfer", Ronald Press, New York, 1966.
- 79. D. T. Sawyer and J. L. Roberts, Jr., "Experimental Electrochemistry for Chemists", Wiley, New York, 1974 Chapter 4.
- 80. J. O'M. Bockris and A. K. N. Reddy, "Modern Electro-chemistry", Vol. 1, Plenum Press, N. Y., 1977, Chapter 2.
- 81. V. Gutmann, "The Donor-Acceptor Approach to Molecular Interactions", Plenum, N. Y., 1978, Chapter 2.
- 82. U. Mayer, A. Kotocova and V. Gutmann, J. Electroanal. Chem., 103, 409 (1979).

- 83. P. Prins, A. R. Korsuragen, and A. G. T. G. Kotbeek, J. Organometallic Chem., 39, 335 (1972); A. Horsfield, A. Wassermann, J. Chem. Soc., Dalton, 187 (1972).
- 84. D. R. Stranks, Disc. Far. Soc., 29, 73 (1960).
- 85. For example, see A. G. Sykes, Adv. Inorg. Chem. Radiochem., 10, 153 (1967); M. Chou, C. Creutz, and N. Sutin, J. Am. Chem. Soc., 99, 5615 (1977).
- 86. H. C. Stynes, J. A. Ibers, Inorg. Chem., 10, 2304 (1971).
- 87. $Co(sep)^{3+/2+} = (S^1) (1,3,6,8,10,13,16,19-octa-azabicyclo-[6.6.6]eicosane) cobalt(III)/(II).$
- 88. R. G. Wilkins and R. Yelin, J. Am. Chem. Soc., <u>89</u>, 5496 (1967).
- 89. V. Gutmann, G. Gritzner and K. Danksagmuller, Inorg. Chim. Acta., 17, 81 (1976).
- 90. G. Gritzner, K. Danksagmuller and V. Gutmann, J. Electroanal. Chem., 72, 177 (1976).
- 91. G. Gritzner, K. Danksagmuller and V. Gutmann, J. Electroanal. Chem., 90, 203 (1978).
- 92. A. Messina and G. Gritzner, J. Electroanal. Chem., 101, 201 (1979).
- 93. M. H. Abraham and J. Liszi, J. Chem. Soc. Far. Trans I, 74, 1604 (1978), and references listed therein.
- 94. (a) R. R. Dogonadze, A. A. Kornyshev, J. Chem. Soc. Far. Trans II, 70, 1121 (1974); see also Yu. I. Kharkats, A. A. Kornyshev, M. A. Vorotyntsev, ibid, 72, 361 (1976); (b) M. H. Abraham and J. Liszi, J. Chem. Soc. Far. Trans I, 74, 2171 (1978).
- 95. For example, see R. Lumry and S. Rajender, Biopolymers, 9, 1125 (1970).
- 96. P. George, G. I. H. Hanania and D. H. Irvine, J. Chem. Soc., 2548 (1959); quoted by J. Lin, W. G. Breck, Can. J. Chem. 43, 766 (1965).
- 97. U. Mayer, A. Kotocova, V. Gutmann, W. Gerger, J. Electroanal. Chem., 100, 875 (1979); A. Kotocova, U. Mayer, Coll. Czech. Chem. Comm., 45, 335 (1980).

- 98. J. Koutecky, Collect. Czech. Chem. Commun., $\underline{18}$, 597 (1953); J. Weber and J. Koutecky, ibid., $\underline{20}$, 980 (1955).
- 99. K. B. Oldham and E. P. Parry, Anal. Chem., 40, 65 (1968).
- 100. For example see (a) R. Payne, J. Am. Chem. Soc., 89, 489 (1967); (b) W. R. Fawcett and R. O. Loutfy, J. Electroanal. Chem., 39, 185 (1972).
- 101. L. M. Baugh and R. Parsons, J. Electroanal. Chem., 40, 407 (1972).
- 102. P. D. Tyma and M. J. Weaver, J. Electroanal. Chem., 111, 195 (1980).
- 103. Reference 47, Chapter 3.
- 104. For a simplified derivation of Equation (7), see Reference 72.
- 105. J. M. Hale, in "Reactions of Molecules at Electrodes", N. S. Hush (ed.), Wiley, N. Y., 1971, p. 229.
- 106. R. Payne, J. Phys. Chem. <u>73</u>, 3598 (1969).
- 107. A. H. Narten and H. A. Levy, J. Chem. Phys., <u>55</u>, 2263 (1971).
- 108. For example, see B. Chance, D. C. DeVault, H. Frauen-felder, R. A. Marcus, J. R. Schrieffer, and N. Sutin (eds.), "Tunneling in Biological Systems", Academic Press, New York, 1979.
- 109. M. D. Newton, In Proc. Int. Symp. on Atomic Molecular and Solid State Theory, Flagler Beach, Fla., 1980, in press.
- 110. S. U. M. Khan, P. Wright and O'M. Bockris, Sov. Electrochem. 13, 774 (1977).
- 111. M. J. Weaver, Israel J. Chem., 18, 35 (1979).
- 112. For example, see W. J. Albery, "Electrode Kinetics", Clarendon Press, Oxford, 1975, Chapter 4.
- 113. M-S. Chan and A. C. Wahl, J. Phys. Chem., 82, 2542 (1978).
- 114. R. C. Young, F. R. Keene and T. J. Meyer, J. Am. Chem. Soc., <u>99</u>, 2468 (1977).

- 115. Equation (89) in Reference 10a.
- 116. E. S. Young, M-S. Chan and A. C. Wahl, J. Phys. Chem., 84, 3094 (1980).
- 117. R. R. Dogonadze and A. A. Kornyshev, Phys. Stat. Solid; (b), 53, 439 (1972); 55, 843 (1973); J. Chem. Soc. Far. Trans. II 70, 1121 (1974).
- 118. R. R. Dogonadze, A. M. Kuznetsov and T. A. Maragishvili, Electrochim. Acta, 25, 1 (1980).
- 119. (a) T. Biegler and R. Parsons, J. Electroanal. Chem. 21, App 4 (1969); (b) Ya. Doilido, R. V. Ivanova and B. B. Damaskin, Elektrokhimiya 6, 3 (1970).
- 120. For example see (a) R. Payne, J. Chem. Phys., 42, 3371 (1965); (b) R. Payne, J. Electroanal. Chem., 41, 145 (1973).
- 121. (a) B. B. Damaskin, I. M. Ganzhina and R. V. Ivanova, Elektrokhimiya, 6, 1540 (1970); (b) I. M. Ganzhina, B. B. Damaskin and R. V. Ivanova, Elektrokhimiya, 6, 709 (1970).
- 122. V. A. Kuznetsov, N. G. Vasil'kevich and B. B. Damaskin, Elektrokhimiya, 6, 1339 (1970).
- 123. R. Payne in "Advances in Electrochemistry and Electrochemical Engineering", P. Delahay, C. W. Tobias (eds.) Interscience, N. Y., Vol. 7, 1970. p. 1; R. Payne, in "Physical Chemistry of Organic Solvent Systems", A. K. Covington, T. Dickinson (eds.) Plenum, 1973, Chapter 7.

